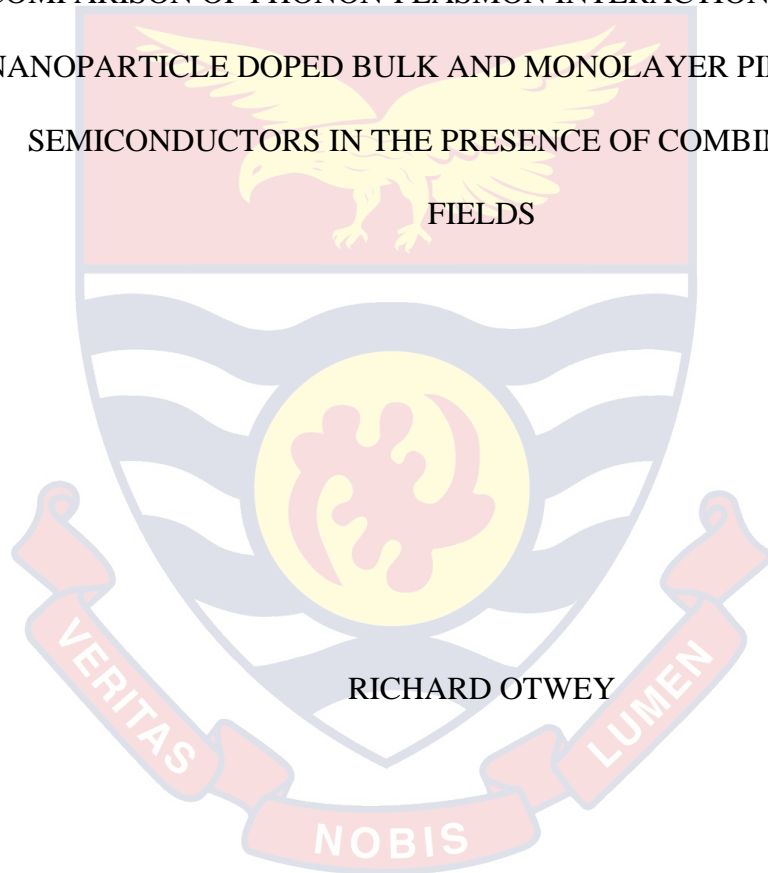UNIVERSITY OF CAPE COAST

COMPARISON OF PHONON-PLASMON INTERACTION IN SELECTED

NANOPARTICLE DOPED BULK AND MONOLAYER PIEZOELECTRIC

SEMICONDUCTORS IN THE PRESENCE OF COMBINED DC-AC

FIELDS

RICHARD OTWEY

2020
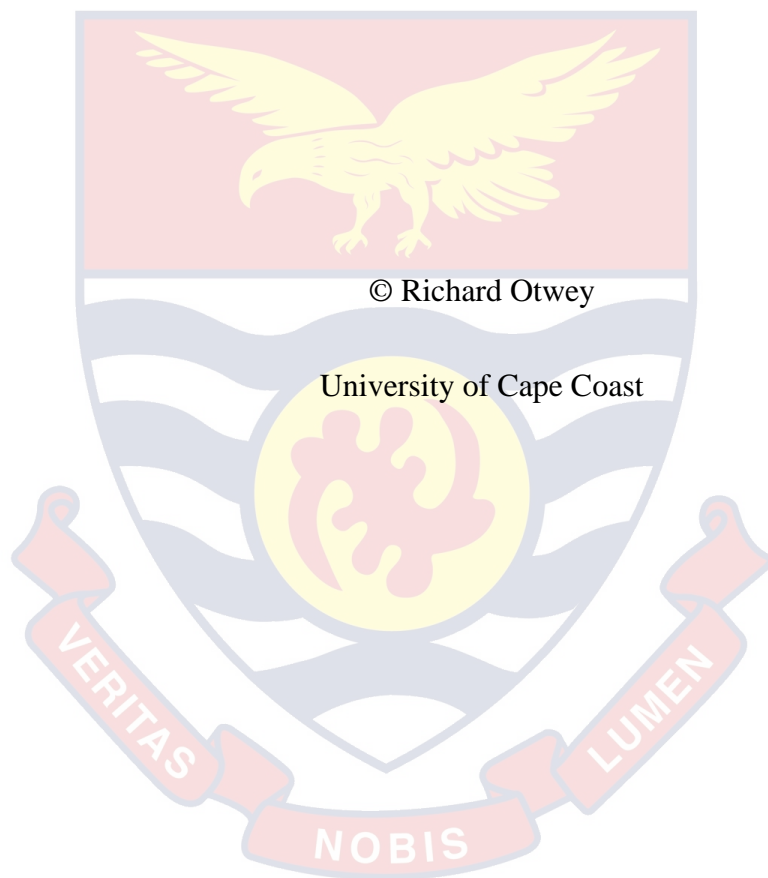
© Richard Otwey

University of Cape Coast

UNIVERSITY OF CAPE COAST

COMPARISON OF PHONON-PLASMON INTERACTION IN SELECTED

NANOPARTICLE DOPED BULK AND MONOLAYER PIEZOELECTRIC

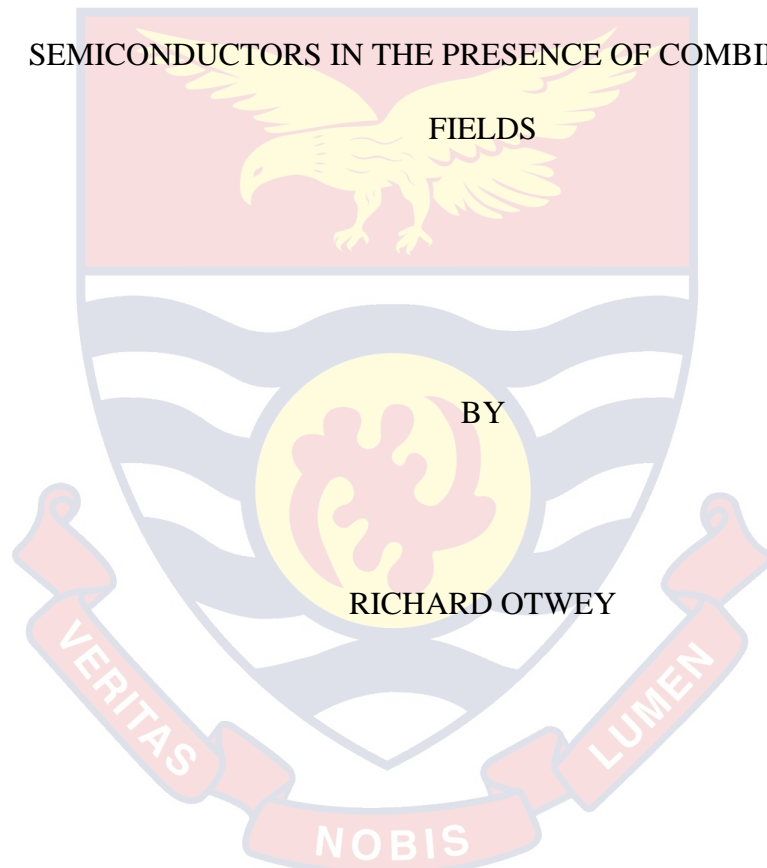SEMICONDUCTORS IN THE PRESENCE OF COMBINED DC-AC

FIELDS

BY

RICHARD OTWEY

Thesis submitted to the Department of Physics of the School of Physical
Sciences, College of Agriculture and Natural Sciences, University of Cape
Coast, in partial fulfillment of the requirements for the award of Master of
Philosophy degree in Physics

OCTOBER, 2020

DECLARATION

Candidate's Declaration

I hereby declare that this thesis is the result of my own original research and that no part of it has been presented for another degree in this university or elsewhere.

Candidate's Signature:……………………   Date:…………………..

Name: Richard Otwey

Supervisor's Declaration

We hereby declare that the preparation and presentation of the thesis were supervised in accordance with the guidelines on supervision of thesis laid down by the University of Cape Coast.

Principal Supervisor's Signature:…………… Date:………………………

Name: Dr. Raymond Edziah

Co-Supervisor's Signature:………………… Date…………………………

Name: Dr. Baah Sefa-Ntiri

ABSTRACT

As semiconductor plasma medium experiences the spread of an acoustic wave, the wave reacts with several basic excitations. An example of such excitations is plasmon. In such a reaction in the presence of certain physical conditions, there is a lost or gain of energy in the acoustic wave. Monolayer materials have offered several distinctive material concepts and properties that differ dramatically from their bulk counterparts. This work analytically studied longitudinal phonon-plasmon interaction in bulk (CdS) and monolayer (MoS_2) semiconductors doped with nanoparticle cluster using fields of combined direct current-alternating current (dc-ac) and fields of commensurate frequencies. The theoretical formulation made use of the hydrodynamic model of plasma and macroscopic model of piezoelectric media to derive an expression for the acoustic gain (α). Variation of the acoustic gain with velocity ratio, behavior of the acoustic gain per unit length $\left(\alpha\omega / v_s \right)$ with frequency and variation of the acoustic gain with carrier density (n_{0e}) were explored graphically and investigated. The results show that velocity ratio (i.e. the ratio of electrons drift velocity to sound velocity) is greatest for this monolayer material whenever it is subjected to both combined dc-ac fields and fields of commensurate frequencies. This variation also increases with increasing levels of nanoparticle (NP) cluster. Therefore, NP doped monolayer piezoelectric semiconductors will be better candidates for the fabrication of high speed sensors and transducers.

KEY WORDS

Amplification

Cadmium sulphide (CdS)

Molybdenum disulphide (MoS_2)

Nanoparticles (NPs)

Phonon-plasmon interaction

Piezoelectric semiconductors (PSCs)

ACKNOWLEDGEMENTS

My sincerest gratitude goes to the Almighty God for his unending mercies and support throughout my life and in the execution of this thesis. I am very grateful to Mr. Emmanuel Oloboi Quaye who encouraged and urged me to pursue my graduate program in spite of all the odds.

My profound appreciation goes to my supervisors, Dr. Raymond Edziah and Dr. Baah Sefa-Ntiri whose direction, criticisms and advice nurtured this work into fruition. I also take this opportunity to show appreciation to the Head of Department and all Lectures in the Department of Physics for their support, advice and guidance throughout my stay in this university.

Finally, I am again grateful to my family and friends for their support, especially, my wife Barbara Otwey, my children Ama Adzepa Otwey and Esi Botemaa Otwey.
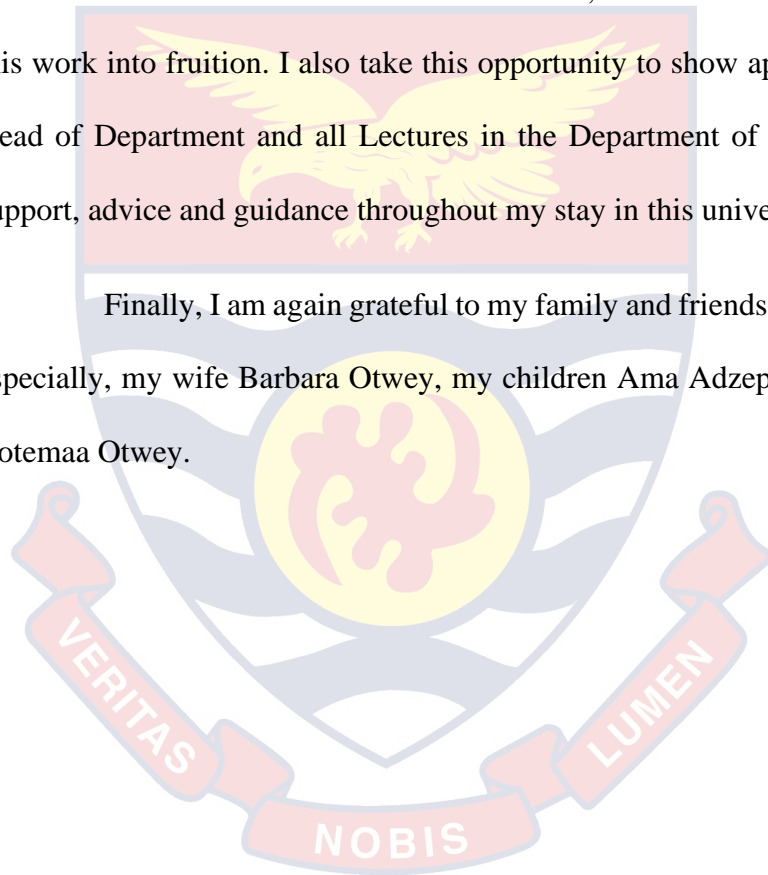
DEDICATION

In memory of my parents, Mr. Robert Benjamin Otwey and Miss Vida

Amoah.

TABLE OF CONTENTS

LIST OF FIGURES

the presence of commensurate fields using $l = 0.001$, $l = 0.008$

and without NP cluster $(l = 0.001)$ for:(i) CdS and

(ii) $\text{Mo}S_2$ at $\omega = 5 \times 10^{12} \, s^{-1}$ and $\dfrac{v_0}{v_s} = 1.25$.   49

LIST OF ABBREVIATIONS

ac	Alternating Current
AlN	Aluminium Nitride
dc	Direct Current
GaN	Gallium Nitride
LA	Longitudinal Acoustic
LO	Longitudinal Optical
m	Mass
MoS_2	Molybdenum Disulphide
NC	Nanoparticle Cluster
NP	Nanoparticle
NPs	Nanoparticles
PSCs	Piezoelectric Semiconductors
TA	Transverse Acoustic
TO	Transverse Optical
UV	Ultraviolet
v_0	Drift Velocity
v_s	Sound Velocity

CHAPTER ONE

INTRODUCTION

Chapter one presents a background of this research work. It also highlights information on problem statement, the research significance, the objectives, delimitations and the limitations of the research and finally the organization of the study.

Background to the Study

As semiconductor plasma medium experiences the spread of an acoustic wave, the wave reacts with several basic excitations. An example of such excitations is plasmon. In such a reaction in the presence of certain physical conditions, there is a loss or gain of energy in the acoustic wave. The process whereby the acoustic wave loses energy is termed as attenuation and then amplification when it gains energy. The use of a dc electric field in a piezoelectric semiconductor has led to the realization of acoustic amplification. Most research scientists have studied in this area and used several ways of amplifying acoustic in several kinds of semiconductors.

Nanoparticles

Nanoparticles (NPs) are particles whose dimensions ranges between 1 and 100 nanometers and surrounded by an interfacial layer. The integral part of nanoscale matter is known as the interfacial layer which affect fundamentally its characteristics or features. The interfacial layer comprises of ionic, inorganic and organic molecules (Laurent et al., 2008). Nanoparticles can be made from gold, silver, copper , silica, titanium dioxide, liposomes, hydrogel and many others (Masserini, 2013). Nanoparticles are grouped into different classes based

1

on their features, sizes or shapes. The different groups comprise of fullerenes, metal NPs, ceramic NPs, and polymeric NPs. The special physical and chemical characteristics of nanoparticles are as a result of their greater surface area and nanoscale size (Sigmund *et al*., 2006; Mansha *et al*., 2017). Nanoparticles have principal parameters such as shape, size, and the morphological sub-structure. Nanoparticles are in the form of mostly solid or liquid phase in air, mostly solid in liquids or two liquid phases. In the existence of chemical agents also termed as surfactants, the surface and the interfacial characteristics undergo changes. The outer layer of the particle can undergo changes through the conservation of a charge of the particle as a result of indirect stabilization of the agents against aggregation. In the case of historical growth and the lifetime of a nanoparticle, complicated compositions, with complicated materials which are made up of two or more different substances physically combined are adsorbed, and expected.

In nanoscale, particle-particle interactions are generated as a result of weak Van der Waals forces, stronger polar and electrostatic interactions or covalent interactions. Based on the viscosity and polarizability of the fluid, particle aggregation is found by the interparticle interaction (Willets & Van Duyne, 2007). Piezoelectric semiconductors can be doped with NPs. As a result of phonon-plasmon interactions in nanoparticles doped piezoelectric semiconductors, the nanoparticles physical and chemical features can help in constructing high performance plasmonic devices and technologies. They also contribute to the reduction of the upper limit of the acoustic gain. The interaction of light with nanoparticles have been revealed to rely on the size, thereby giving dissimilar colours because of visible region absorption.

2

Nanoparticles have the condition or quality of being reactive, the ability to absorb energy and practically deform without fracturing. They also show distinctive features which rely on their special size, structure and shape. Because of the above features, NPs serve as better nominees in the activities of industries and various homes. Examples are; making a visual representation of materials using an electromagnetic beam, software developed for medical purposes, evaluation of renewable energy sources and health and safety monitoring (Dreaden et al., 2012; Eustis and El-Sayed, 2006; Saeed and Khan, 2016).

Phonons

Phonons are definite discrete units or quanta of vibrational mechanical energy or a phonon is a quantum of energy of the independent oscillators in an ensemble (Schwabl, 2008). They can also be defined as the vibration of the atomic lattice. Phonons exist with discrete amounts of energy: they lose or accept energy in accordance with the Planck relation: $\Delta E = h v$, where ΔE is the change in energy, h is Planck's constant and v is frequency of vibration. Phonons behave similarly as particles or waves, just as electrons can. The smallest lattice point of solids having at least two atoms have two categories of phonons: acoustic phonons and optical phonons (Simon, 2013). Acoustic phonons are the coherent motion of atoms of the lattice from their equilibrium positions. Transverse and longitudinal acoustic phonons are mostly represented as TA and LA phonons, respectively. The motion of atoms in the lattice (out-of-phase) whereby one atom moves to the left, and the other to the right are referred as optical phonons. They are often denoted as LO and TO phonons, as longitudinal and transverse optical phonons respectively: the splitting between LO and TO frequencies is accurately briefed by the Lyddane-Sachs-Teller

3

relation. They belong to a group of particles in quantum statistics called Bosons (Misra, 2010; Kittel, 2004; Fetter & Walecka, 2003).

Some of the novel applications of phonons are the design of metamaterials with the aim of controlling dissipative heat effects and also insulating, diffusion or absorbing sound waves in a super enhanced way (Schwabl, 2008).

Plasmons

A plasmon is a quantum of plasma oscillation. A plasmon can be regarded as a quasiparticle since it arises from the quantization of plasma oscillations, just like phonons are the vibration of the atomic lattice. Thus, plasmons are collective (a discrete number) oscillations of the free electron gas density. Plasmons can be classified into two groups. These are surface plasmons and volume plasmons. Plasmons that are confined to surfaces and that strongly interact with light leading to a polariton are referred to as surface plasmons. Volume or bulk plasmons are the quanta of energy of volume plasma oscillations (Cottam & Tilley, 1989; Raether, 1980). Volume or bulk plasmons have higher energy than surface plasmons (Barnes, Deurrex & Ebesen, 2003).

Piezoelectric Semiconductors

Piezoelectric semiconductors (PSCs) are semiconductors without center of symmetry and when they undergo mechanical deformations, they produce electric charges, and vice versa, when electric fields are applied to them, they are mechanically strained. In piezoelectric semiconductors, the electric fields that accompany an elastic wave produce electronic currents and space charge which modify the attenuation and wave velocity.

Piezoelectricity is an important property of non-centro symmetric crystals that allows the conversion of mechanical strain into electric field. The linear electromechanical interaction or reaction between the mechanical and electrical states within crystalline materials without inversion symmetry produces piezoelectric effect. The piezoelectric effect is a reversible process: materials generating the piezoelectric effect (the internal generation of electrical charge resulting from applied mechanical force) also show a reverse effect of piezoelectricity, the internal generation of a mechanical strain obtained from electrical field that is applied. The deformation of the static structure of lead zirconate by about 0.1% of its original dimension produces piezoelectricity that can be measured. However, these crystals will alter about 0.1% of their static dimension by the external application of the field to the material (Manbanchi & Cobbold, 2011).

A number of usual applications, such as the production and detection of sound, piezoelectric inkjet printing, generation of high voltages, electronic frequency generation, and ultrafine focusing of optical assemblies make use of piezoelectricity. Also, it serves as the basis for a lot of scientific instrumental techniques with atomic resolution.

A few widely used PSCs have a crystal class of 6 mm and are of n-type with electronic conduction (Hickernell, 2005). The piezoelectric semiconductors of crystal class 6 mm which are mostly utilized include Zinc Oxide (ZnO), Cadmium Sulphide (CdS), and Cadmium Selenide (CdSe) (Hickernell, 2005) serve as typical examples of n-type semiconductors because of their native defects. Considering a lot of components used in controlling electrical currents, the use of semiconductors which are piezoelectric are

normally considered to be the elementary ones because they exhibit special features.

Many devices obtained from acoustic waves are revealed to be manufactured from piezoelectric semiconductors. In a process that creates growth or positive change in science, engineering and technology conducted at the nanoscale that ranges from 1 to 100 nm, several devices with at least one dimension in the nanoscale are been manufactured from nanowires from ZnO (Hu, Zeng & Yang, 2007). A change in electric polarization have been found in ZnO and CdS semiconductors. For example; hardness, strength, elasticity, etc. of piezoelectric semiconductors are already investigated. Based on the investigations of the unique reaction between forces that feature some direct contact between two objects and a particle that is free to move, carrying an electric charge of PSCs, many modern single devices which are based on piezoelectric semiconductors with an electrical and mechanical components are reported, which comprises of devices that generate or sense ultrasound energy and those based on piezoelectricity (Hickernell, 2005). The strongest piezoelectric semiconductor materials are from wurtzite family of crystal structure such as ZnO, GaN, InN, and AlN.

PSCs have widely been applied in various smart structures, and electromechanical devices and systems. The properties stemming from piezoelectric-semiconducting coupling in nanowires have inspired the development of many devices yielding a new field called piezotronics that has attached interests for various applications and research (Johar, Hassan, Waseem, & Ryu, 2018). Due to the fact that piezoelectric semiconductors can be utilized in changing mechanical energy to electrical energy and also since

6

they are semiconductors, they can be used as junction device for performing diode and transistor type functions. These properties influence them to be strong candidates for use in electromechanically coupled sensors, and transducers. Piezoelectric semiconducting coupled property of PSC is used in the fabrication of novel and unique electronic devices and components by introducing the concepts of piezotronics (Zhao, Li, Yan & Fan, 2016).

Statement of the Problem

A number of research works have been done on piezoelectric semiconductors doped with nanoparticles using dc and ac fields (Ghosh & Dubey, 2017). However, no study has been reported on phonon-plasmon interaction in piezoelectric semiconductors doped with nanoparticles using combined dc-ac fields and fields with commensurate frequencies. Hence a research on this sort is looked at under this study.

Objectives of the Study

The main objective of the study is to analytically study phonon-plasmon interaction in piezoelectric plasma medium doped with a nanoparticle using combined dc-ac fields and fields with commensurate frequencies with respect to material and field parameters.

The specific objectives are to:

(i) understand the physics of phonon-plasmon interactions in nanoparticle

doped PSCs by analytically deriving an expression for the acoustic gain.

(ii) investigate the variations of acoustic gain with the physical parameters of

the material media using codes developed in MATLAB.

7

Significance of the study

From the study, results obtained will assist in the provision of the necessary additional theoretical basis for the phonon-plasmon interaction in doped piezoelectric semiconductors in order to promote the understanding of the physics of phonon-plasmon interactions in such media.

Based on the nature of the variation of the gain with the piezoelectric materials, possible practical applications will be suggested.

Delimitations

The scope of the study will cover analytical derivation of expressions for the gain using combined dc-ac and commensurate fields. The work will also compare the variations of acoustic gain with wave frequency, carrier density and velocity ratio. Typical values of parameters of n-CdS, and MoS_2 semiconductor plasma will be adopted to calculate the gain using the analytic derivations acquired.

Limitations

The limitations of this work are as follows:

(i)The study would have considered different piezoelectric semiconductors doped with same nanoparticles but due to time constraint and computational limitation, only few were considered under study.

(ii) A piezoelectric semiconductor doped with nanoparticles of different dimensions could have been considered but due to lack of time this has not been considered in this study.

(iii) Phonon-plasmon interactions in nanoparticles doped piezoelectric semiconductor could have been modelled computationally but due to time limitation this was not carried out under study.

Organization of the study

This work comprises of five sections: Chapter one deals with the background to the study with a short introduction that presents the problem under study, why the problem is important, how the study relates to previous work, and the practical and theoretical implications of the study. This chapter also points out existing knowledge gaps, controversies to be resolved, what previous research in the area has not been resolved, and so forth. The chapter also stated the reason of conducting this work as well as it objectives. The relevance of the work is also stated. It also covers the scope and the constraints or hindrances of the work. The second section deals with a recap of what the study is about. It also covers the key concepts or theories around which the study is built. Chapter three covers the theoretical formulation; the designed procedures used in obtaining the results in the research. Chapter four presents the results or the findings from the research. It also addresses the endings and then interprets the investigations by linking them to previous findings. The fifth section covers the conclusions and the recommendations of the study.

Chapter Summary

This chapter outlines the background of the study. It also provides information on problem statement, the significance of the study, the objectives, delimitation and limitations of the research. The concept of phonons, plasmons, nanoparticles and piezoelectric semiconductors are highlighted.

CHAPTER TWO

LITERATURE REVIEW

Introduction

This chapter reviews previous works that are related to the study. The concept of piezoelectric semiconductors is analyzed and reviewed. In addition, phonons in piezoelectric semiconductors, general interactions in piezoelectric semiconductors, and acoustic wave amplification in piezoelectric semiconductors. Optical and electrical properties of nanoparticles are also reviewed.

Piezoelectric Semiconductors

Piezoelectric semiconductors (PSCs) are semiconductors without center of symmetry (Elloh, 2001) and when they undergo mechanical deformations, they produce electric charges, and vice versa, when electric fields are applied to them, they are mechanically strained (Willatzen & Christensen, 2014). In piezoelectric semiconductors, the electric fields that accompany an elastic wave generate electronic currents and space charge which modify the attenuation and wave velocity.

Piezoelectric semiconductors that exhibit elementary features are narrated using phenomenological theory of linear vicoelastic behavior (Hickernell, 2005). This theory has been used to examine the problem of inclusion for piezoelectric semiconductor composites, the electromechanical energy conversion in these materials, the fracture of piezoelectric semiconducting materials, vibrations of piezoelectric semiconductor plates, and ensures the growth of theories of semiconductor shells and plates that are

piezoelectric and restricted in one or more directions. Also with large mechanical destructions, the complete general nonlinear theories for piezoelectric semiconductors in the presence of strong electrical fields have been developed by scientists (Hu, Zeng & Yang, 2007). In piezoelectric semiconductors, several scattering mechanisms occur which includes ionized impurity scattering, polar and nonpolar optical phonon scatterings, acoustic phonon scattering, carrier-carrier scattering, piezoelectric scattering and alloy scattering among others which determine the variation of mobility with temperature, carrier concentration, and in some cases the compensation ratio (Hickernell, 2005).

For an increase in acoustic wave and also by the transport of an acoustic charge as a result of the motion of carriers under the influence of electrical field accompanying an acoustic wave, piezoelectric semiconductors serve as better candidates for designing piezoelectric devices (Ghosh and Muley, 2016). Piezoelectric semiconductors serve as better nominees in changing mechanical energy into electrical energy or electrical energy into mechanical energy as a result of interaction between acoustic phonons and plasmons by means of piezoelectricity. Currently, piezoelectric semiconductors are playing an important role in fast growth of wireless electrical devices because of their ability in providing power to very minute or small electrical devices with decreased power expectation (Ghosh and Muley, 2016).

Phonons in piezoelectric semiconductors

Phonons are quanta of energy or quasiparticles associated with a compressional wave such as sound or a vibration of a crystal lattice. Phonons can also be defined as units of vibrational energy that arise from oscillating

atoms within a crystal (Schwabl, 2008). Practically, phonons exist in all features of materials such as the limitation of electrical conductivity by acoustic and optical phonons. The interaction of light with piezoelectric semiconductors is enhanced by optical phonons, meanwhile acoustic phonons serve as carriers of heat in materials that do not conduct electricity and also play a vital role in those that can conduct electricity partially.

Lattice vibrations have basic theory dates back to the 1930's and is still considered today to be the reference theory in this field. It is well known that optical transitions between bound states of defects in piezoelectric semiconductors usually involve the absorption or emission of phonons (Krauth, 2006; Kittel, 2004). At very less temperatures, optical phonon scattering in a piezoelectric semiconductor is suppressed, scattering by acoustic phonons can be expected to become an important limiting factor for the mobility of the two-dimensional electron gas confined to the atomic layer of an extrinsic two-dimensional piezoelectric semiconductor (Krauth, 2006; Kittel, 2004). Longitudinal optical phonon generation in direct-gap polar piezoelectric semiconductors by electrons is more intense because electrons accelerated in electric field can lose all their kinetic energy giving birth to the phonons (Simon, 2013).

The elasticity model (Krauth, 2006; Kittel, 2004) has been adopted in establishing features or characteristics of phonons in piezoelectric semiconductors such as nanofilms made from GaN. Based on the relation of piezoelectric constituent in nanofilms made from GaN, the expression of dispersion of phonons has been determined. The speed of propagation of acoustic phonons, the number of electron states per unit volume per unit energy

(phonon density) and the ability of phonons to show conductivity properties have also been found because of the role played by piezoelectricity. Piezoelectricity in piezoelectric semiconductor nanofilms such as those made from GaN beneficially alters the features or characteristics of phonon such as the phonon speed of propagation and proportion of states that are to be occupied by the phonons at each energy, leading to differences in the ability of nanofilms made from GaN to conduct heat. Phonons transport heat in semiconductors; thus, the investigation of phonon properties and phonon thermal conductivity in semiconductor nanostructures becomes essential (Xu, 2016).

A convenient tool for the dynamic manipulation of optical phonons in piezoelectric semiconductors is provided by surface acoustic waves which are mechanical waves of deformations on a surface popularly generated when a high frequency signal is applied to electrodes on a piezoelectric surface, using an interdigitated transducer (Hutson & White, 1962).

A number of interesting phenomena associated with phonon instability have been noted in piezoelectric semiconductors. Typical experimental features include the amplification of the injected supersonic wave and the nonohmic-current behaviors such as the current saturation in the steady state or the various types of oscillatory current (Yamada, 1968).

Plasmons in piezoelectric semiconductors

A plasmon is a quantum of plasma oscillation. The plasmon can be considered as a quasiparticle since it arises from the quantization of plasma oscillations, just like phonons are quantization of mechanical vibrations (Maier, 2007). However, in the presence of oscillation frequencies of the electric field

13

of light (optical frequencies), the quanta of plasma oscillations can interact with an elementary particle such as photon in the production of other quasiparticles known as surface plasmon-polariton. A lot of features of plasmons are established by Maxwell's equations (Raether, 1980). Materials made from plasmons quickly alter at the optical frequency with respect to their optical features. There is a negative permittivity in the case of frequencies that are lesser than the resonance frequency of plasmons. Some structures and devices that behave extraordinarily as field enhancement and sub-diffraction mode confinement are influenced by a negative permittivity. In sensing and photonic circuits, the devices and structures are better applied. However, irrespective of capability and desire, the limitations of applied devices made from plasmons are as a result of light which could have generated an electron-hole pair, but does not (Feng *et al*, 2015). Collective excitations in classical plasmas were first examined by Langmuir. The pioneering theoretical investigations on their quantum counterparts were carried out by Bohm and Pines (Bohm & Pines, 1951). Experimental evidence for the existence of plasmons as a well-defined collective mode of the outermost shell electrons of metals comes from characteristic energy-loss experiments (Atwater, 2007; Ekmel, 2006). The collective oscillation of free electrons in a piezoelectric semiconductor may involve surface charge density called surface plasmons or volume charge density called volume or bulk plasmons. Surface plasmons are those plasmons that are confined to surfaces and interact strongly with light resulting in a polariton. They occur at the interface of a material showing positive real part of their relative permittivity, i.e. dielectric constant, and a material that have a

14

negative real part of permittivity at the given light frequency, typically a heavily doped piezoelectric semiconductor (Barnes, Dereux & Ebbesen, 2003).

Plasmons play a significant role in the optical properties of piezoelectric semiconductors. Light of requencies above the plasma frequency is transmitted by a material because the electrons in the material cannot respond fast enough to screen it. Semiconductors that exhibit piezoelectricity have outermost shell electron frequency of plasmons normally found within a region of deep ultraviolet (UV), the visible range also shows the transformation between electronic bands, in which particular colors are soaked up, resulting in the production of the distinct colours (Atwater, 2007; Ozbay, 2006). Piezoelectric semiconductors that are doped with or have impurities of nanoparticles establishes a frequency of plasmon located within regions of mid-infrared and near-infrared.

General Interactions in Piezoelectric Semiconductors

The interactions between collective excitations of free electrons and holes with the lattice vibrations is one of the fundamental interaction processes in piezoelectric semiconductors. Hutson & White,1962 have explained plasma waves with respect to the restraining of vibrational motion. The loss of energy in lattice waves results in the establishment of plasma frequency in a collisionless boundary. The existence of resonance between vibrations of applied optics of the plasma and the lattice waves with very small temperature is as a result of frequency not much greater than the frequency of plasma. There exist also an intense interaction between electrons that show conductivity properties and acoustic waves spreading through some areas in piezoelectric semiconductors such as CdS. The exchange mechanism of energy has greatly

15

been non-linear, and thus inclusion of many collinear acoustic waves into the piezoelectric semiconductors result in new signals at the frequencies of the combination (summation and difference). Through experimentation, the authenticity of such analysis method has been examined and confirmed, and the explanation of such mechanism of reaction in considering the non-linear cross term found in the equation of current-density is determined to be developed. (Dompreh, Mensah, Abukari, Sam & Edziah, 2015).

Interactions between charge carriers and phonons also occur in piezoelectric semiconductors. Piezoelectric semiconductors depict three types of charge carrier-phonon reactions. One type of these interactions is due to dilation associated with the lattice acoustic waves, which decreases the energy of the edges of band and such dilations are presented in terms of potential deformation. This is the commonest type of charge carrier-phonon reaction located within semiconductors showing piezoelectricity. The second type is the charge carrier-phonon reaction that happens in semiconductors with polarity whereby a strain attached with acoustic phonons can produce a macroscopic electric polarization known as the effect of piezoelectricity. The interaction coordinate could denote the destruction in the electrovalent or ionic regime because of the electric potential fields of piezoelectricity. The third interaction can be applied to piezoelectric semiconductors with polarity. The charge carrier-acoustic phonon reaction as a result of piezoelectric interaction possess non-zero role played by both longitudinal and acoustic phonons respectively. The piezoelectric charge carrier-phonon reaction has not led to a great focus from semiconductors that are piezoelectric (Misra, 2010 ; Kittel, 2004 ; Fetter & Walecka, 2003).

Phonons can affect electrons through their reactions. These reactions play a vital role on the optical and transport features of electrons found within piezoelectric semiconductors. Optical phonons are considered in the production of "internal strain" and their coupling with electrons can be narrated by optical-phonon deformation potentials. Piezoelectric semiconductors that have polarity, both high acoustic and optical phonons wavelength could produce electrical fields by means of charges attached with the ions in motion. These fields can couple intensively with electrons, resulting in Frohlich interaction for optical phonons and piezoelectric electron-phonon interactions for acoustic phonons (Talwar, Vandevyer, Kunc & Zigone, 1981).

Electrical Properties of Nanoparticles

Electrical conductivity is an important property for technological applications of nanoparticles that has failed to be widely investigated. Conventional descriptions such as the Maxwell model do not account for surface charge effects that play an important role in electrical conductivity, particularly at higher nanoparticle volume fractions (Laurent et al., 2010). In nanoparticles, especially metal nanoparticles, the dc electrical conductivity is much affected by the microstructure, and this is a consequence of large area to bulk ratio of the individual grains. The length scale of the microstructure is compared to the electrons mean-free-path that have conductivity property, making the grain boundaries an importance source of scattering of the conduction electrons. The grain boundary scattering has an effect briefed as conduction electrons tunneling through the grain boundaries or limits, modelled as potential barriers associated with a probability of transmission (Masserini, 2013).

17

Optical Properties of Nanoparticles

Nanoparticles are fascinating objects whose features are normally different from those of the bulk material. They are small minuscule pieces of atoms or molecules whose size lie between bulk materials and individual atoms (Ghosh & Dubey, 2016). Optical properties of nanoparticles play an important role in either the type of application in which nanoparticles may be utilized or the type of the nanoparticle which may be used for a desired outcome. Several kinds of optical features produced by nanoparticles from bulk material are because of confinement of electron, and the characteristics of collective excitations together with the features of collective electronic excitations like frequency of resonance are altered. (Kelly, Coronado, Zhao & Schatz, 2003). Some nanoparticles exhibit very different optical properties such as colour compared with bulk materials (Dreaden et al., 2012 ; Eustis and El-Sayed, 2006 ; Saeed and Khan, 2016). Complicating factors in getting concept of the nanoparticle optical properties, consist of a supporting substrate, a solvent layer on top of the particles, and particles that are much nearer together that their electromagnetic interaction alters their spectra (Kelly, Coronado, Zhao & Schatz, 2003).

Nanoparticles' interaction with light depends strongly on the size, shape and composition of the particles, as well as on the composition of the medium in which particles are found. If nanoparticles are supplied by light, they produce radiation through scattering as a result of oscillatory motion of their electrons. Some of the linear optical properties of composites containing metal nanoparticles such as extinction, absorption and scattering matrix elements have been known both through analytical and numerical approaches (Kociak et al,

18

2014). Strongly scattering nanoparticles have been utilized in improving contrast in microscopy of dark-field and optical tomography of coherence(Park, 2014).

The nanoparticle optical properties are unveiled with electrons by two types of spectroscopies: loss of energy by electron spectroscopy and cathodoluminescence spectroscopy. Electrons with high speed nearer to a nanoparticle can exhibit some movement of energy as a result of Coulombic reaction. If the amount of energy loss by electron is measured, then this gives an idea of the extinction properties of the nanoparticle. Thus, the amount of energy loss by the electron could be found by means of energy loss by electron spectroscopy, and considered as spectroscopy of extinction at the nanometer scale. Similarly, there should be a release of energy moved to the nanoparticle and luckily when there is an occurrence of transfer of photons within regions of the infrared, visible or ultraviolet, then through cathodoluminescence spectroscopy there could be a way out to illumination features or characteristics.

Amplification of acoustic waves in piezoelectric semiconductors

An acoustic wave can be thought of as a sound and a vibrational wave. This wave travels with a velocity that takes care of variations within the direction of interfacial waves and depicts an impedance that also manages the bouncing or reflection of wave and amplitudes of transmission at interfaces (Steele & Vural, 1969).

When an acoustic wave spread through a crystal with piezoelectricity an electrical field normally accompanies it. For a crystal that is not a semiconductor, the electrical field generates current and charges in space

resulting in dispersion and loss of acoustic (Hutson & White, 1962). A travelling acoustic wave and mobile charges react in piezoelectric materials in a process called the acoustoelectric effect (Weinreich et al., 1959). An acoustic wave travelling in a piezoelectric semiconductor could undergo amplification through the application of an initial of dc electric field which is biased (White, 1962). Acoustoelectric effect and acoustoelectric amplification of acoustic waves have resulted in the manufacture of a lot of acoustoelectric devices (Busse & Miller, 1981). Semiconductors with the property of piezoelectricity, and acoustoelectric effect that have an elementary of fundamental character are briefed using a linear phenomenological theory (Hutson & White, 1962). The acoustoelectric amplification in piezoelectric semiconductors shows that the attenuation of an acoustic wave crosses over to its amplification as the drift velocity becomes greater than the acoustic wave velocity. In other words, acousto electric amplification occurs most effectively in piezoelectric semiconductors when charge carriers drift in the presence of an applied electrical field with a speed greater than that of the acoustic wave, thus there is an energy transfer to lesser speed phonons (Ghosh & Dubey, 2016).

Furthermore, acoustic wave absorption/amplification in graphenes, rectangular quantum wires, and quantum dots have all received attention (Dompreh *et al*., 2015).

The acoustic waves amplification in a crystal of photoconductive CdS upon using an external electric field. The energy transfer was analytically treated for interaction of electrons-acoustic waves under the influence of a field having an electrical property with the material considered as a free electron gas (Hutson & White, 1962).

20

Chapter Summary

The chapter reviews previous works that are related to the study. It also analyzes and reviews the concept of phonons in piezoelectric semiconductors and general interactions in piezoelectric semiconductors. Finally, optical and electrical properties of nanoparticles are also reviewed

21

CHAPTER THREE

METHODOLOGY

Introduction

This section provides the theoretical basis of the study. It outlines the use of the hydrodynamic model of plasma together with other relevant equations to derive an expression for the acoustic gain in the presence of alternating and direct current fields and fields of commensurate frequencies.

Theoretical Formulation

The displacements of the lattice are obtained from solids been elastic and which experiences stress. For a unit cell of a crystal, $\vec{u}$ is chosen as a vector which is also taken to be the displacement in describing the equations that govern the motion of such displacements. The relationship between $\vec{u}$ and the Cstress tensor T according to the equations of Newton[Steele &Vural, 1969] is given by

$$\rho \frac{\partial^2 \vec{u}_i}{\partial t^2} = \frac{\partial T_{ij}}{\partial z_j} \tag{1}$$

where ρ represents the medium density while T_{ij} also denote the second-rank stress tensor components. When piezoelectricity is equal to zero ($\beta = 0$), the relationship between T and the second-rank-stress tensor S through the fourth-rank elastic tensor C is given as

$$T_{ij} = C_{ijkl}S_{ij} \tag{2}$$

as shown in Figure 1.

22
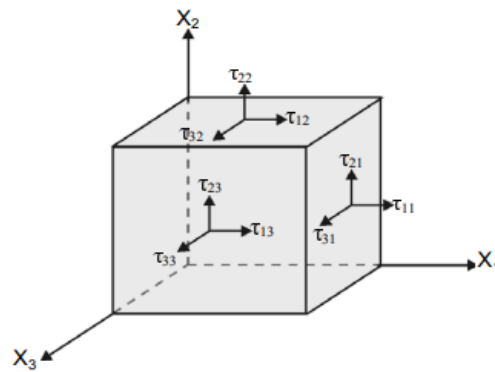
Figure 1: Shear stresses on an infinitesimal cube whose surfaces are parallel to the coordinate system.

Here, X_1, X_2 and X_3 are the axes of the infinitesimal cube and τ_{ij} is the stress tensor.

Equation (2) shows the Hooke's law expressed in terms of stress and strain. The elements of S which are diagonal and also known as linear strains are defined as

$$S_{ii} = \frac{\partial \vec{u}_i}{\partial z_i} \tag{3}$$

The crystal can exhibit piezoelectricity when it lattice point contains more than one atom. In such a material, the elastic and electrical variables show a relationship that makes use of the piezoelectric tensor β as a third-rank tensor.

The basic equations of state describing the piezoelectric crystal are given as

$$T_{ij} = C_{ijkl} S_{kl} - \beta_{ijm} E_m \tag{4}$$

23

$$D_n = \varepsilon_{mn} E_m + \beta_{nij} S_{ij} \qquad\qquad (5)$$

Where ε_{mn} denote the lattice dielectric tensor, D_n represents the electric displacement tensor and E_m stands for electric field tensor.

In the analytical description of the phonon-plasmon reaction in a piezoelectric semiconductor plasma which has undergone doping, an expression known as dispersion relation is derived using the motion equation of lattice and hydrodynamical quantum model of plasma. A semiconductor plasma exhibiting piezoelectricity doped with nanoparticles (NPs) having density number N, density of electrons n_{on} with r as radius, was considered to be present within the host medium. The medium is acted upon by an external dc electric field $\vec{E}_0 = \left(E_0 \hat{z} \right)$ due to which electrons of the medium get drifted by velocity, $\vec{v}_0 = \left(v_0 \hat{z} \right)$. A shear sound wave is considered to be propagating along the z - direction in the medium. The medium is assumed to be piezoelectric having cubic symmetry. The role of the physical interactions under study has not been changed due to the simplification of the tensor components by these assumptions.

The displacement lattice $\vec{u}$ is taken in the $x-$ direction as $<100>$ crystal lattice axis. This approach is geometrically appropriate for many piezo-compound semiconductors of III-V class. In this study, all perturbations are assumed to vary as $\exp\left[i \left(\omega t - kz \right) \right]$, in which ω and k are respectively frequency and wave number and also all amplitude terms are assumed to be unity with their respective units for simplicity. Based on these considerations,

24

only longitudinal piezoelectric fields need to be considered and the problem at hand has essentially been reduced to one-dimensional one. Therefore, equation (1) becomes:

$$\rho \frac{\partial^2 \vec{u}_x}{\partial t^2} = \frac{\partial T}{\partial z} \qquad (6)$$

Also (2), (3), (4) and (5) are respectively

$$T = CS \qquad (7)$$

$$S = \frac{\partial \vec{u}_x}{\partial z} \qquad (8)$$

$$T = CS - \beta E \qquad (9)$$

$$D = \varepsilon E + \beta S \qquad (10)$$

From equation (6), the relation between $\vec{u}$ and stress tensor T is given as:

$$\rho \frac{\partial^2 \vec{u}_x}{\partial t^2} = \frac{\partial T}{\partial z} \qquad (11)$$

Substituting equation (8) into equation (9), the stress tensor T becomes:

$$T = C \frac{\partial \vec{u}_x}{\partial z} - \beta E \qquad (12)$$

Differentiating the stress tensor T with respect to z in equation (12) gives:

$$\frac{\partial T}{\partial z} = C \frac{\partial^2 \vec{u}_x}{\partial z^2} - \beta \frac{\partial E_z}{\partial z} \qquad (13)$$

25

Substituting equation (13) into equation (11):

$$\rho\frac{\partial^2 \vec{u}_x}{\partial t^2} = C\frac{\partial^2 \vec{u}_x}{\partial z^2} - \beta\frac{\partial E_z}{\partial z} \qquad (14)$$

(Refer to Appendix A).

In a piezoelectric elastic medium, the equation of wave may be obtained as :

$$\left(-\rho\omega^2 + Ck^2\right)u_x = ik\beta\vec{E}_Z \qquad (15)$$

(Refer to Appendix B).

using equation (14) and other related equations.

Here, β is piezoelectric constant $\vec{E}_Z$ is applied electric field, ρ is mass density, C is elastic stiffness constant. In absence of piezoelectricity, $\beta = 0$, then equation (15) reduces to $V_s = \sqrt{C/\rho}$ as sound velocity (Refer to Appendix C). Whereas, when $\beta \neq 0$, i.e. in the presence of piezoelectricity, the sound mode is interacted with movement of electrons via applied electrical field $\vec{E}_Z$. Following the procedure of (Steele & Vural, 1969), the electric displacement component of sound wave is obtained as:

$$\vec{D}_Z = \varepsilon\vec{E}_Z\left[1 + \frac{\beta^2 k^2}{\varepsilon\left(-\rho\omega^2 + Ck^2\right)}\right] \qquad (16)$$

(Refer to Appendix D)

As the motion of free electrons in piezo-semiconductor plasma is governed by hydrodynamical model, the velocity of free electrons of the

26

medium (in the absence of NP cluster (where NP cluster are small minuscule pieces of nanoparticles)) may be defined by solving momentum transfer equation under the quasi-static limit $k^2 c_L^2 << \omega^2$ as (Ghosh & Dubey, 2016):

$$v_z = \frac{i\left(e/m\right)\vec{E}_Z}{F\left(\omega,k\right)} \tag{17}$$

Here, m represents the electronic mass and

$F\left(\omega,k\right) = \left[\omega - kv_0 - i\nu - \frac{D\nu k^2}{\left(\omega - kv_0\right)}\right]$ in which ν is the transfer collision

frequency of momentum and D is the diffusion coefficient. Using equation $\left(17\right)$ in the expression for conduction current density, $\vec{J}_Z = -n_{0e}ev_Z$

$$\vec{J}_Z = -\frac{i\varepsilon\omega_{pe}^2 \vec{E}_Z}{F\left(\omega,k\right)} \tag{18}$$

(Refer to Appendix E)

where $\omega_{pe} = \sqrt{\frac{n_{0e}e^2}{m\varepsilon}}$ is electron plasma frequency, n_{0e} is carrier density of the medium and ε is the permittivity of the medium. The displacement $\vec{\Delta}$ of the motion of electrons within the nanoparticle cloud can be described by equation of motion:

$$\frac{d^2\vec{\Delta}}{dt^2} + \frac{\omega_{pn}^2\vec{\Delta}}{3} = -\frac{e\vec{E}_Z}{m} \tag{19}$$

27

Here, $\omega_{pn} = \sqrt{e^2 n_{0n}/m}$ is the frequency of electron plasma found in the cluster

of nanoparticle while n_{0n} is the electron density. On solving the above equation

(19), the velocity of electron cloud may be obtained as

$$v_{np} = \frac{i\omega\left(e/m\right)\vec{E}_z}{X} \qquad (20)$$

(Refer to Appendix F)

where $X = \left(\omega^2 - \dfrac{\omega_{pn}^2}{3}\right)$. Substituting equation (20) into the current density

expression for electron cloud of nanoparticle cluster, $\vec{J}_{np} = -\dfrac{4\pi}{3} r^3 N n_{0n} e v_{np}$

gives

$$\vec{J}_{np} = -i\frac{4\pi}{3}\varepsilon l\frac{\omega\omega_{pn}^2}{X}\vec{E}_z \qquad (21)$$

where $l = Nr^3$ is a dimensionless physical parameter of a nanoparticle cluster

and r is the radius.

Using equations (18) and (21), the resultant current density $\vec{J} = \vec{J}_z + \vec{J}_{np}$ is

obtained as:

$$\vec{J} = -i\varepsilon\vec{E}_z\left[\frac{\omega_{pe}^2}{F\left(\omega,k\right)} + \frac{4\pi}{3}l\frac{\omega\omega_{pn}^2}{X}\right] \qquad (22)$$

From Maxwell's equation

$$\vec{\nabla}\cdot\vec{D} = \rho \qquad (23)$$

28

where ρ is the charge density.

$$\rho = -en \qquad (24)$$

Substituting (24) into (23)

$$\vec{\nabla} \cdot \vec{D} = -en \qquad (25)$$

Recalling the continuity equation

$$\vec{\nabla} \cdot \vec{J} = -\frac{\partial \rho}{\partial t} \qquad (26)$$

the one-dimensional continuity equation is given as:

$$\frac{\partial \vec{J}}{\partial z} = e \frac{\partial n}{\partial t} \qquad (27)$$

Combining equation (22), with the continuity equation (equation 27), the space-charge density is obtained as:

$$n^{'} = \frac{ik\varepsilon \vec{E}_Z}{e(\omega - kv_0)} \left[\frac{\omega_{pe}^2}{F(\omega,k)} + \frac{4\pi}{3} l \frac{\omega \omega_{pn}^2}{X} \right] \qquad (28)$$

(Refer to Appendix G)

which on using in Maxwell's equation $\vec{\nabla} \cdot \vec{D} = -en^{'}$, modifies the electric displacement of free electrons of the medium due to nanoparticle cluster and may be expressed as:

$$\vec{D}_Z = \frac{\varepsilon \vec{E}_Z}{(\omega - kv_0)} \left[\frac{\omega_{pe}^2}{F(\omega,k)} + \frac{4\pi}{3} l \frac{\omega \omega_{pn}^2}{X} \right] \qquad (29)$$

(Refer to Appendix H)

29

Using equations (16) and (29), the desired dispersion relation is given as:

$$\left(\omega^2 - k^2 v_s^2\right)\left[1 - \left(\frac{1}{\omega - k v_0}\right)\left\{\frac{\omega_{pe}^2}{F(\omega,k)} + \frac{4\pi}{3}l\frac{\omega\omega_{pn}^2}{X}\right\}\right] = K^2 k^2 v_s^2 \qquad (30)$$

(Refer to Appendix I)

where $K = \dfrac{\beta^2}{C\varepsilon}$ is a non-dimensional electromechanical coupling coefficient.

For no piezoelectricity, $\beta = 0$, and equation (30) yields:

$$\left(\omega^2 - k^2 v_s^2\right)\left[1 - \left(\frac{1}{\omega - k v_0}\right)\left\{\frac{\omega_{pe}^2}{F(\omega,k)} + \frac{4\pi}{3}l\frac{\omega\omega_{pn}^2}{X}\right\}\right] = 0 \qquad (31)$$

This implies that,

$$\left(\omega^2 - k^2 v_s^2\right) = 0 \qquad (32)$$

and

$$\left[1 - \frac{1}{\omega - k v_0}\left\{\frac{\omega_{pe}^2}{F(\omega,k)} + \frac{4\pi}{3}l\frac{\omega\omega_{pn}^2}{X}\right\}\right] = 0 \qquad (33)$$

(Refer to Appendix I)

Equations (32) and (33) represent the usual sound mode propagating through an elastic medium and the electrokinetic mode modified due to the presence of a nanoparticle cluster within the host material.

Using the collision dominated regime[$\omega \ll \nu$ and $kv_0 \ll \nu$] with the standard approximation $\dfrac{kv_s}{\omega} = 1 + i\alpha$, the expression for acoustic gain per radian $\alpha(\alpha \ll 1)$ is obtained by simplifying the dispersion relation (30) as:

$$\alpha = \frac{\dfrac{1}{2}K^2 \gamma X^2 \dfrac{\omega_R}{\omega}}{\left(\dfrac{\omega_R}{\omega}\right)^2 \left[X + \dfrac{\omega^2}{\omega_D \omega_R}\left(X + \dfrac{4\pi}{3}l\dfrac{\omega_{pn}^2}{\gamma}\right)\right]^2 + \left[\gamma X + \dfrac{4\pi}{3}l\omega_{pn}^2\right]^2} \tag{34}$$

(Refer to Appendix I)

where $\omega_D = \dfrac{v_S^2}{D}$ is the diffusion frequency, $\omega_R = \dfrac{\omega_{pe}^2}{\nu}$ is the relaxation frequency and $\gamma = \dfrac{v_0}{v_s} - 1$. Since $\alpha > 0$ is the necessary condition for sound wave to be amplified, it is clear from equation (34) that acoustic gain will be obtained only if $\gamma > 0$ or $\dfrac{v_0}{v_s} > 1$.

The above analysis reveals that in the presence of nanoparticle cluster in a piezoelectric medium, the maximum value of the acoustic gain per unit length $\left(\alpha\omega\big/v_s\right)$ is attained at resonance point defined by $\omega^2 = \omega_R \omega_D + \dfrac{4\pi}{3}l\omega_{pn}^2$ whereas in the absence of nanoparticle cluster it is achieved at $\omega^2 = \omega_R \omega_D$. This infers that in the presence of a nanoparticle cluster, the maximum acoustic gain points get shifted to higher frequency, and the amount of shift is proportional to ω_{pn}^2 and the parameter l.

31

In the case of combined dc-ac fields, $E(t) = E_0 + E_1 \cos \omega t$, where E_0

is the constant dc field and E_1 is the amplitude of ac field, and ω is the wave

frequency. Hence, equations (16) and (29) respectively become

$$\vec{D}_Z = \varepsilon \left(E_0 + E_1 \cos \omega t \right) \left[1 + \frac{\beta^2 k^2}{\varepsilon \left(-\rho \omega^2 + C k^2 \right)} \right] \tag{35}$$

$$\vec{D}_Z = \frac{\varepsilon \left(E_0 + E_1 \cos \omega t \right)}{\left(\omega - k v_0 \right)} \left[\frac{\omega_{pe}^2}{F(\omega,k)} + \frac{4\pi}{3} l \frac{\omega \omega_{pn}^2}{X} \right] \tag{36}$$

Equating equations (35) and (36) the desired dispersion relation becomes

$$\left(\omega^2 - k^2 v_s^2 \right) \left[\left(E_0 + E_1 \cos \omega t \right) - \frac{\left(E_0 + E_1 \cos \omega t \right)}{\left(\omega - k v_0 \right)} \left\{ \frac{\omega_{pe}^2}{F(\omega,k)} + \frac{4\pi}{3} l \frac{\omega \omega_{pn}^2}{X} \right\} \right] = \left(E_0 + E_1 \cos \omega t \right) K^2 k^2 v_s^2$$

$$\tag{37}$$

(Refer to Appendix J)

For collision dominated limit $[\omega \ll \nu$ and $kv_0 \ll \nu]$ and with the same standard

approximation as shown above, the expression for acoustic gain per radian

$\alpha(\alpha \ll 1)$ using combined dc-ac fields becomes:

$$\alpha = \frac{\frac{1}{2} K^2 \gamma X^2 \frac{\omega_R}{\omega} \left(E_0 + E_1 \cos \omega t \right)}{\left(\frac{\omega_R}{\omega} \right)^2 \left[\left(E_0 + E_1 \cos \omega t \right) X + \frac{\omega^2 \left(E_0 + E_1 \cos \omega t \right)}{\omega_R \omega_D} \left(X + \frac{4\pi}{3} l \frac{\omega_{pn}^2}{\gamma} \right) \right]^2 +}$$

32

$$\overline{\left[\left(\gamma\left(E_0+E_1\cos\omega t\right)X+\left(E_0+E_1\cos\omega t\right)\frac{4\pi}{3}l\omega_{pn}^2\right)\right]^2} \tag{38}$$

(Refer to Appendix J)

Similarly, in the presence of commensurate fields,

$E(t)=E_1\cos\omega_1 t+E_2\cos\left(\omega_2 t+\theta\right)$, where E_1 and E_2 are fields amplitudes, ω_1

and ω_2 are the commensurate frequencies $\left(\omega_1\approx\omega_2\right)$ and θ is the phase

difference between the two fields, the gain becomes

$$\alpha=\frac{\frac{1}{2}K^2\gamma X^2\frac{\omega_R}{\omega}\left(E_1\cos\omega_1 t+E_2\cos\left(\omega_2 t+\theta\right)\right)}{\left(\frac{\omega_R}{\omega}\right)^2\left[\left(E_1\cos\omega_1 t+E_2\cos\left(\omega_2 t+\theta\right)\right)X+\frac{\omega^2\left(E_1\cos\omega_1 t+E_2\cos\left(\omega_2 t+\theta\right)\right)}{\omega_R\omega_D}\left(X+\frac{4\pi}{3}l\frac{\omega_{pn}^2}{\gamma}\right)\right]^2}\times$$

$$\overline{\left[\left(E_1\cos\omega_1 t+E_2\cos\left(\omega_2 t+\theta\right)\right)\frac{4\pi}{3}l\omega_{pn}^2+\gamma\left(E_1\cos\omega_1 t+E_2\cos\left(\omega_2 t+\theta\right)\right)X\right]^2}$$

$$\tag{39}$$

(Refer to Appendix K)

Chapter Summary

This chapter outlines the relevant theory of a piezoelectric semiconductor plasma doped with nanoparticle cluster that shows a phonon-plasmon reaction. The theoretical formulation makes use of the hydrodynamic model of plasma together with other relevant equations to "derive an expression for the acoustic gain in the presence of dc-ac fields and fields of commensurate frequencies".

CHAPTER FOUR

RESULTS AND DISCUSSION

Introduction

The results of phonon-plasmon interaction in piezoelectric semiconductors doped with a nanoparticle cluster using combined dc-ac fields and fields of commensurate frequencies are discussed in this chapter. It also highlights the results of the study graphically using MATLAB codes generated and shows various plots of the variations of the acoustic gain with field parameters.

The study theoretically examined phonon-plasmon interaction in piezoelectric semiconductors doped with nanoparticle cluster (NC) using dc-ac fields and commensurate fields. The hydrodynamic model of plasma was employed to study the motion of electrons in the system and the relevant equations were solved analytically to obtain an expression for the acoustic gain as a function of some physical parameters of the medium. To visualize the results of the study graphically, two piezoelectric semiconductors, cadmium sulphide (CdS) and molybdenum disulphide (MoS_2) have been chosen.

Monolayer materials such as MoS_2 consist of more than one atomic element, where one Mo plane is sandwiched by two S planes, which makes their lattice dynamics more complex than that in bulk material (CdS) including the symmetry and frequency trends varying with thickness. Furthermore, in comparison to their bulk counterpart, monolayer materials show very distinctive physical properties in lattice dynamics and electronic structure. The unit cell of monolayer MoS_2 consists of two S-Mo-S units with total of 6 atoms suggesting

34

that there are 18 phonon modes (3 acoustic and 15 optical modes) more than that in the bulk material (Ghosh & Pal, 2007).

To visualize the theoretical results obtained, nanoparticle doped CdS and MoS$_2$ were considered at room temperature (300K) with the following physical parameters as listed below.

(i) Cadmium Sulphide

$$\varepsilon_L = 9.35, \ \mu = 0.035 m^2 V^{-1} s^{-1}, \ m_e = 0.17 m_0, \ \rho = 4820 kgm^{-3}, \ \beta = 0.21 \frac{C}{m^2}$$

(ii) Molybdenum disulphide

$$\varepsilon_L = 2.5, \qquad \mu = 0.041 m^2 V^{-1} s^{-1}, \qquad m_e = 0.16185 m_0, \qquad \rho = 5060 kgm^{-3},$$

$$\beta = 0.0156 \frac{C}{m^2}$$

Interaction in the presence of combined dc-ac fields

Figure 2 shows the variation of the acoustic gain (α) with velocity ratio $\left(\dfrac{v_0}{v_s} \right)$ at $\omega = 15 \times 10^{12} \, s^{-1}$ and $n_{0e} = 10^{26} \, m^{-3}$ using combined dc-ac fields for nanoparticle doped MoS$_2$ and CdS.
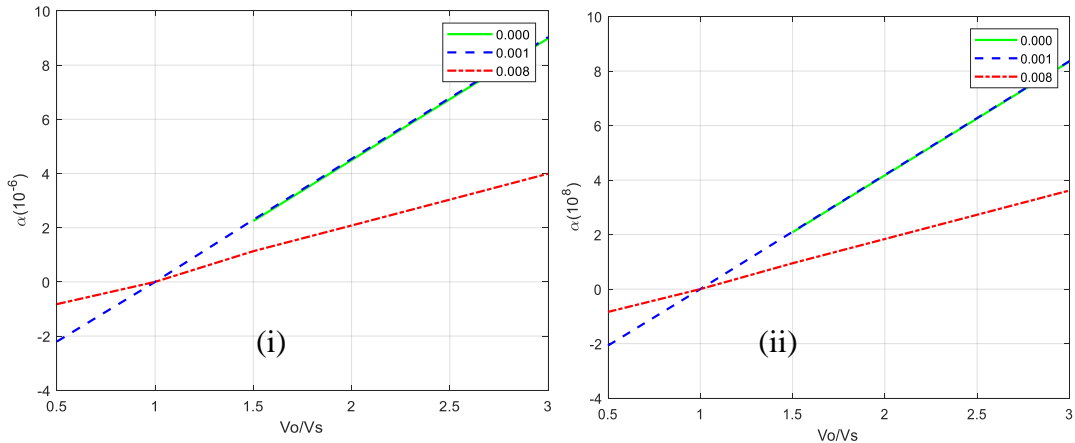
Figure 2: Variation of acoustic gain (α) with velocity ratio $\left(\dfrac{v_0}{v_s}\right)$ using

combined dc-ac fields for $l = 0.001$, $l = 0.008$ and without NP

cluster ($l = 0.000$) for:(i) CdS and (ii) $\text{Mo}S_2$ at $\omega = 5 \times 10^{12}\, s^{-1}$ and

$n_{0e} = 10^{26}\, m^{-3}$ (using equation (38)).

From Figure 2, the acoustic gain (equation (38)) increases as the velocity ratio increases in both (i) and (ii). This is due to enhanced amplification of the acoustic waves in both materials which results in more gain. In general, the acoustic gain is largely independent on l as depicted in (i) and (ii). At $\dfrac{v_0}{v_s} < 1$, there is attenuation of the acoustic waves while for $\dfrac{v_0}{v_s} > 1$, the acoustic waves are amplified in both materials. However, the order of magnitude of the acoustic gain in (ii) is greater than that in (i). This is as a result of increased acoustic gain in the monolayer material than in the bulk caused by enhanced interaction in $\text{Mo}S_2$ than CdS due to the low dimension.

36

When the ac field is turned off, the variation of acoustic gain with velocity ratio for CdS in this study is the same as that obtained by Ghosh *et al* [Ghosh & Dubey, 2016] as shown in Figure 3(i). Figure 3(ii) represents the variation of the dc induced gain versus velocity ratio for the monolayer material. Therefore, comparing Figures 2 and 3, it is clear that in the case of purely dc field, the acoustic gain in CdS is largely independent on l while that for the combined dc-ac fields is l dependent. Moreover, in terms of the order of magnitude of the acoustic gain, CdS shows or has the same range of values when both dc and combined dc-ac fields are used for the same values of nanoparticle cluster.   For purely dc field in the case of MoS_2, it is also largely independent on l while in the case of combined dc-ac fields, it is largely dependent on l. However, the order of magnitude of the acoustic gain under purely dc field is the same as that for the combined dc-ac fields.
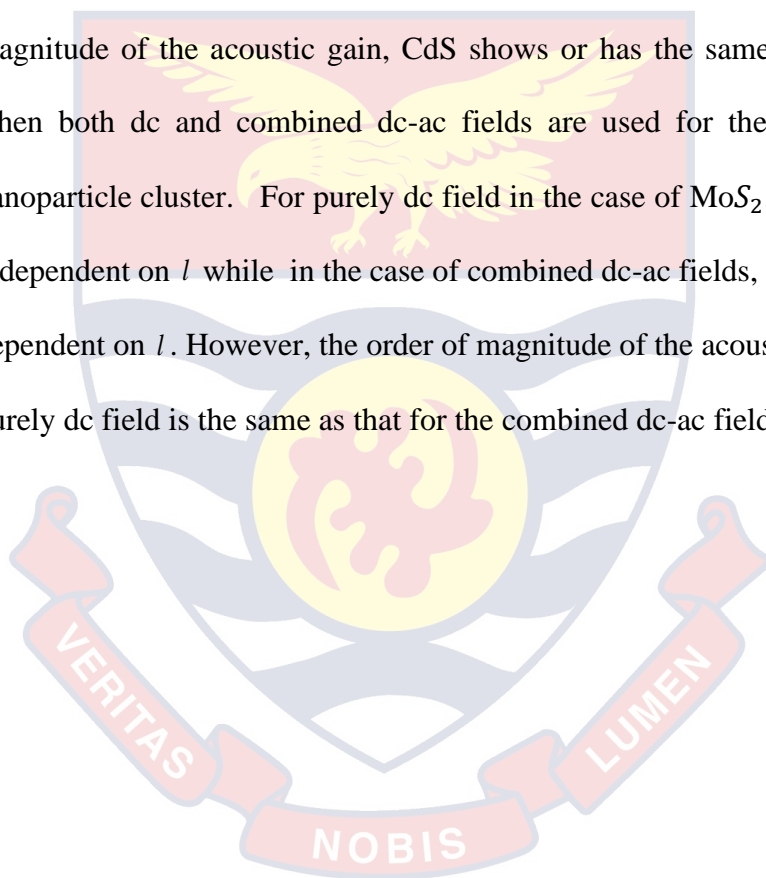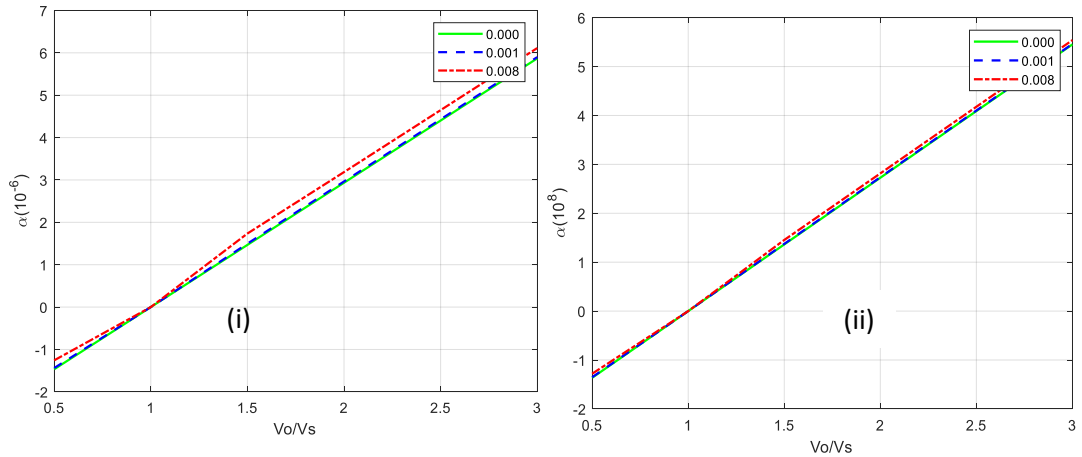
Figure 3: Variation of acoustic gain (α) with velocity ratio $\left(\dfrac{v_0}{v_s}\right)$ in the presence of a dc field using $l = 0.001$, $l = 0.008$ and without NP cluster ($l = 0.000$) for:(i) CdS and (ii) MoS_2 at $\omega = 5 \times 10^{12}\, s^{-1}$ and $n_{0e} = 10^{26}\, m^{-3}$ (using equation (34)).

Figure 4 displays the behavior of the acoustic gain per unit length $\left(\alpha\omega\big/v_s\right)$ with wave frequency (ω) at $\dfrac{v_0}{v_s} = 1.25$ and $n_{0e} = 10^{26} m^{-3}$ using combined dc-ac fields for nanoparticle doped MoS_2 and CdS.
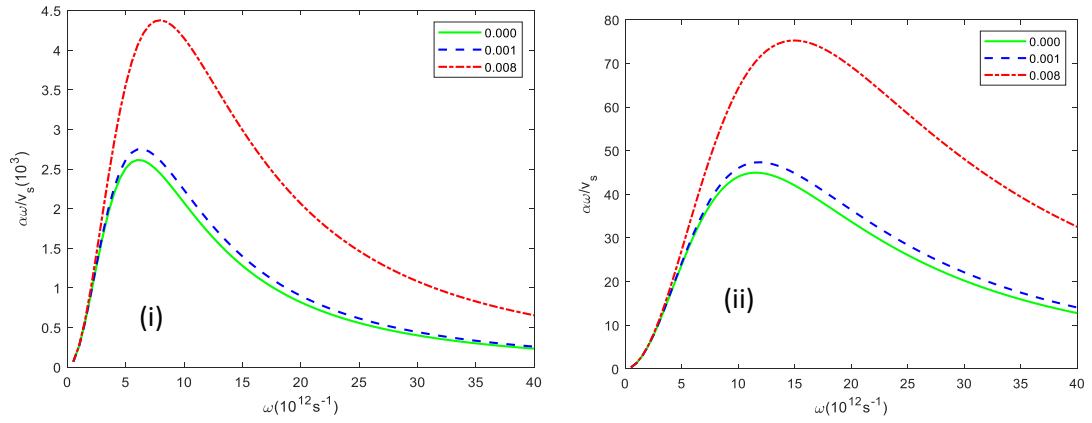
Figure 4: Acoustic gain per unit length $\left(\dfrac{\alpha\omega}{v_s}\right)$ variation with wave frequency (ω) using combined dc-ac fields for $l = 0.001$, $l = 0.008$ and without NP cluster $(l = 0.000)$ for: (i) CdS and (ii) MoS_2 at $n_{0e} = 10^{26}\, m^{-3}$ and $\dfrac{v_0}{v_s} = 1.25$ (using equation (38)).

From Figure 4, the acoustic gain per unit length initially (equation (38)) increases sharply with frequency and attains maxima in both (i) and (ii). With further increase in the wave frequency beyond the peak values, the acoustic gain per unit length experiences exponential decrease for both materials. The initial increment is caused by pronounced amplification of the acoustic waves in the materials and the exponential decrease is as a result of attenuation of the acoustic waves in these materials. Also, as l increases the peak values of the acoustic gain per unit length increase in both (i) and (ii) due to more amplification of the acoustic waves in the materials. For example, for $l = 0.008$, (i) (CdS) has maximum value of the acoustic gain per unit length than (ii) (MoS_2). Moreover, (i) has greater value of the acoustic gain per unit

39

length than (ii). This is also because the acoustic wave amplified is enhanced in CdS than in MoS_2.

In the absence of the ac field, the behavior of acoustic gain per unit length with wave frequency for CdS in this study is the same as that achieved by Ghosh *et al* [Ghosh & Dubey, 2016] as shown in Figure 5(i). Also, Figure 5(ii) depicts the acoustic gain per unit length variation with wave frequency for the monolayer material in the presence of a purely dc field. In comparison, for the combined dc-ac fields, the order of magnitude of the acoustic gain per unit length for CdS is the same as that for the purely dc field. Moreover, MoS_2, has greater order of magnitude of the acoustic gain per unit length using the combined dc-ac fields than that for the purely dc field.
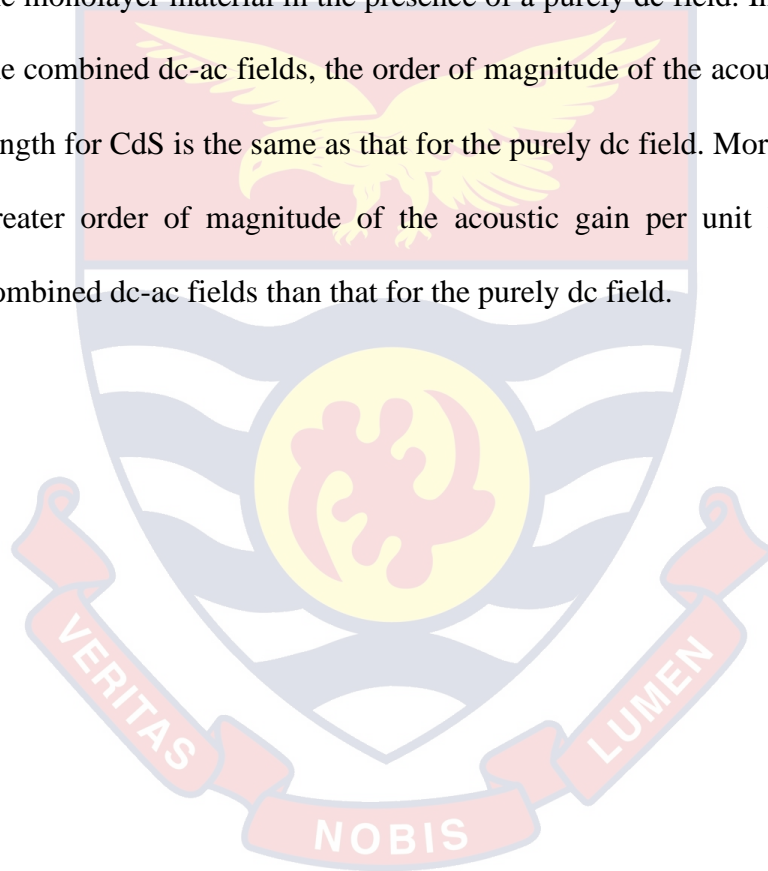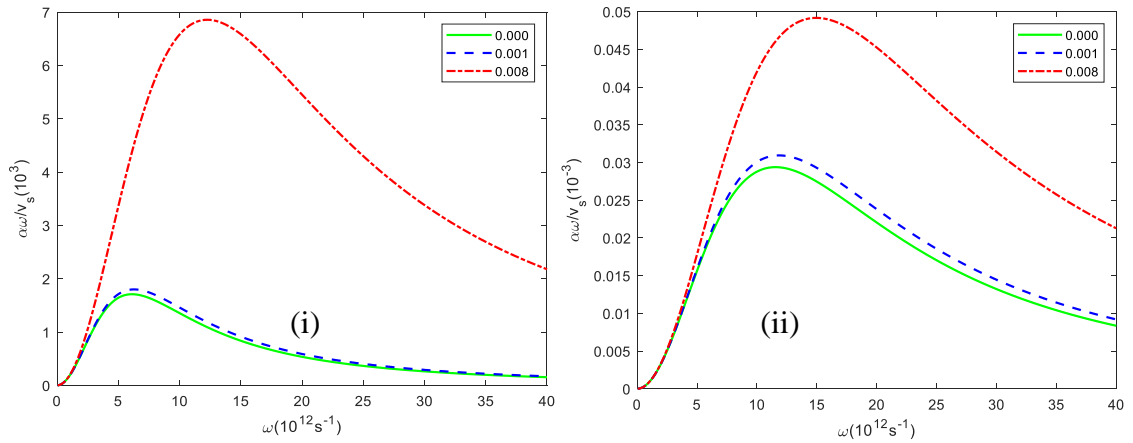
Figure 5: Acoustic gain per unit length $\left(\alpha\omega \middle/ v_s \right)$ variation with wave frequency (ω) under the influence of a dc field using $l = 0.001$, $l = 0.008$ and without NP cluster $(l = 0.000)$ for:(i) CdS and (ii) MoS_2 at $n_{0e} = 10^{26} m^{-3}$ and $\dfrac{v_0}{v_s} = 1.25$ (using equation (34)).

Figure 6 depicts the variation of the acoustic gain as a function of carrier density (n_{0e}) at $\omega = 5 \times 10^{12} s^{-1}$ and $\dfrac{v_0}{v_s} = 1.25$ using combined dc-ac fields for nanoparticle doped MoS_2 and CdS.

41
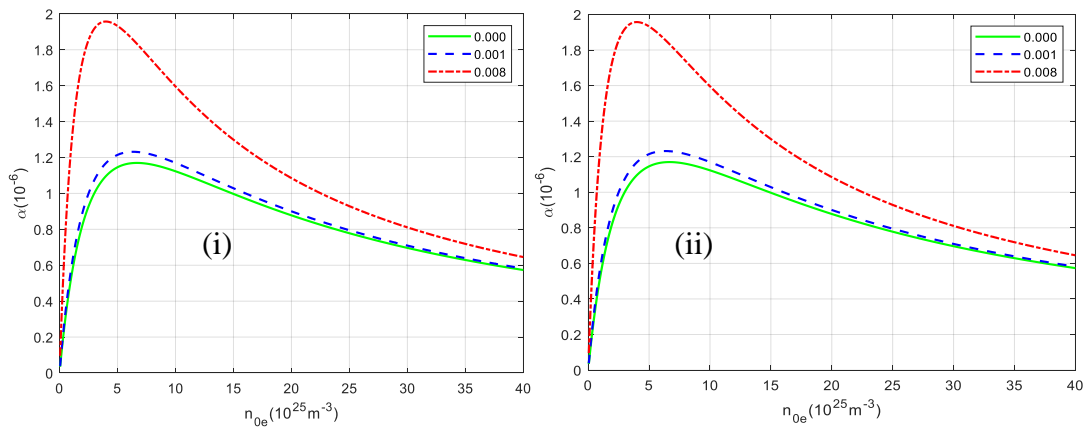
Figure 6: Variation of acoustic gain with carrier density of the medium using combined dc-ac fields for $l = 0.001$, $l = 0.008$ and without NP cluster $(l = 0.000)$ for:(i) CdS and (ii) MoS_2 at $\omega = 5 \times 10^{12}\, s^{-1}$ and $\frac{v_0}{v_s} = 1.25$ (using equation (38)).

It can be seen from Figure 6 that the acoustic gain (equation (38)) generally increases as the carrier density increases up to a maximum value. With further increase in the carrier density beyond the maximum values in (i) and (ii), the acoustic gain decreases and this is as a result of attenuation of the acoustic waves in both materials. As l increases, the peak values of the acoustic gain also increase in (i) and (ii). This is because of enhanced amplification of acoustic waves in both materials. Under the condition of $l = 0.008$, the maximum value of the acoustic gain in (ii) is equal to that in (i). The order of magnitude of the acoustic gain in the monolayer and bulk materials is the same.

If the ac source is turned off, the variation of acoustic gain with carrier density for CdS is the same as that shown by Ghosh *et al* [Ghosh & Dubey,

42

2016] as obtained in Figure 7(i). Again, Figure 7(ii) shows the dc induced variation of acoustic gain with carrier density for the monolayer material. Comparing the behaviour of CdS using applied combined dc-ac fields to the purely dc field, it can be clearly seen that CdS has the same order of magnitude of the acoustic gain for both fields. However, CdS has higher peaks of the acoustic gain in the case of the combined dc-ac fields than that for the purely dc field.

Comparing the response of the materials under combined dc-ac and purely dc fields, it is obvious that for the dc-ac case, MoS_2 has a lower order of magnitude of the acoustic gain as compared to that of the purely dc field case. Under the influence of the purely dc field, MoS_2 depicts higher order of peaks of the acoustic gain than that of the combined dc-ac fields for MoS_2 as compared to CdS.

43
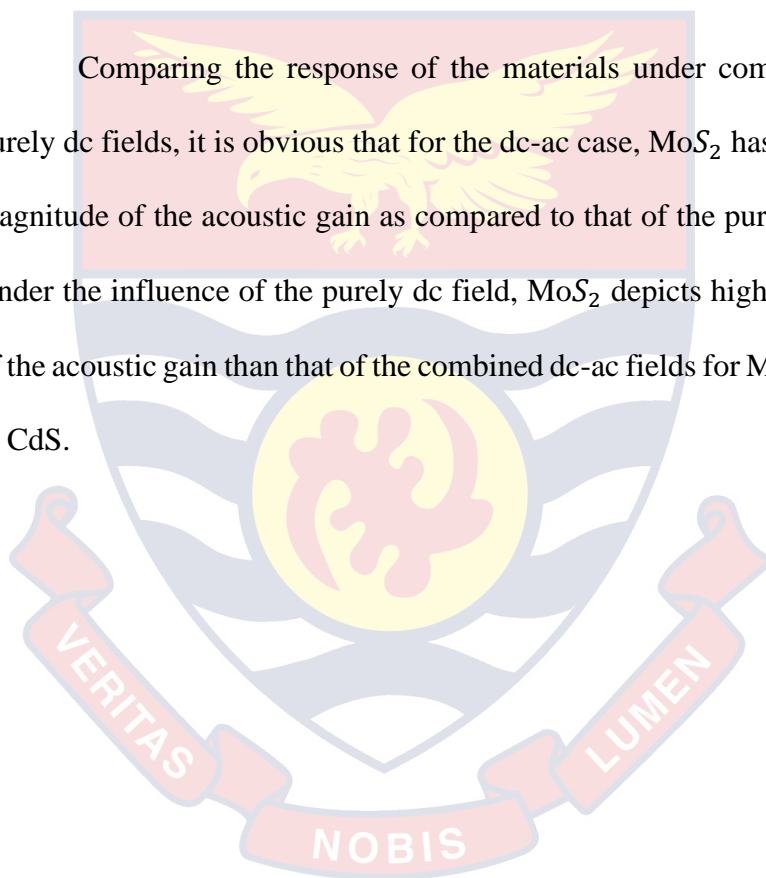
Figure 7: Variation of acoustic gain with carrier density of the medium in the presence of a dc field using $l = 0.001$, $l = 0.008$ and without NP cluster $(l = 0.000)$ for: (i) CdS and (ii) MoS$_2$ at $\omega = 5 \times 10^{12} \, s^{-1}$ and

$$\frac{v_0}{v_s} = 1.25 \, (\text{using equation} \, (34)).$$

Interaction in the presence of commensurate fields

Figure 8 displays the variation of acoustic gain with velocity ratio at $\omega = 5 \times 10^{12} \, s^{-1}$ and $n_{0e} = 10^{26} m^{-3}$ in the presence of commensurate fields for nanoparticle doped MoS$_2$ and CdS.

44

Figure 8: Variation of acoustic gain with velocity ratio in the presence of

commensurate fields using $l = 0.001$, $l = 0.008$ and without NP

cluster $(l = 0.000)$ for:(i) CdS and (ii) MoS_2 at $\omega = 5 \times 10^{12} s^{-1}$ and

$n_{0e} = 10^{26} m^{-3}$.

From Figure 8, the acoustic gain (equation (39)) generally increases as

the velocity ratio increases as shown in (i) and (ii). This behavior is due to

amplification of the acoustic waves in these materials. Also, as l increases the

acoustic gain increases for both materials. However, when $\frac{v_0}{v_s} < 1$, $\alpha < 0$ in both

(i) and (ii). This is because at velocity ratio less than unity, the acoustic wave

suffers attenuation. Moreover, the order of magnitude of the acoustic gain in (ii)

is far greater than that in (i) and this is as a result of more amplification of

acoustic waves in the monolayer than in the bulk material.

45

Comparably, for interaction in the presence of commensurate fields, the bulk material has a higher order of magnitude of the acoustic gain as compared to the case of purely dc and combined dc-ac fields. Again, considering acoustic gain as a function of velocity ratio in the case of combined dc-ac fields is largely independent on l while for the commensurate and purely dc fields, it is l dependent. However, for the monolayer material, the order of magnitude of the acoustic gain using combined dc-ac fields and purely dc field is greater than that for the commensurate fields. In addition, the acoustic gain for the combined dc-ac fields is largely independent on l while that of the purely dc and commensurate fields depends on l as shown in Figures 2 and 7.

Figure 9 depicts the variation of the gain per unit length as a function of wave frequency at $n_{0e} = 10^{26} \text{m}^{-3}$ for nanoparticle doped MoS$_2$ and CdS in the presence of commensurate fields.
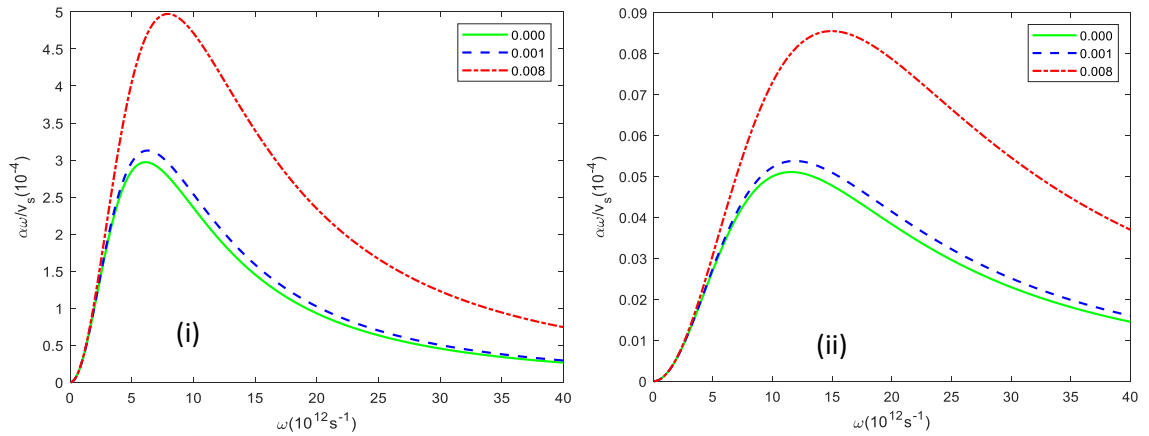
Figure 9: Acoustic gain per unit length variation with wave frequency in the presence of commensurate fields using $l = 0.001$, $l = 0.008$ and without NP cluster $(l = 0.000)$ for:(i) CdS and (ii) MoS_2 at $\frac{v_0}{v_s} = 1.25$ and $n_{0e} = 10^{26} m^{-3}$ (using equation (39)).

It is clearly seen that the acoustic gain per unit length (equation (39)) in Figure 9 initially increases and attains maxima in both (i) and (ii). With further increase in the wave frequency, the acoustic gain per unit length experiences exponential decrease. Here, initial increase in the acoustic gain per unit length is as a result of pronounced amplification of the acoustic waves in both materials and the exponential decrease is also due to the attenuation of acoustic waves in these materials. However, as l increases the peak values of the acoustic gain per unit length also increase in both (i) and (ii). This behavior is due to increased amplification of the acoustic waves in the bulk and monolayer materials with increasing l.

47

Moreover, the order of magnitude of the acoustic gain in (i) is greater than that in (ii). This is caused by enhanced amplification of the acoustic waves in the bulk material than in the monolayer one. For example in the case of $l = 0.008$, the peak value of the acoustic gain per unit length in (i) is greater than that in (ii).

In comparing the bulk material in the case of the combined dc-ac fields and the purely dc field, it is clearly seen that the order of magnitude of the acoustic gain of the bulk material is greater than that in the case of commensurate fields. In other words, the presence of purely dc and combined dc-ac fields depict higher acoustic gain per unit length than commensurate fields. Similarly, considering the monolayer material it is clear that in the case of the combined dc-ac fields the order of magnitude of the acoustic gain for this material is greater than that in the purely dc field and least also in the case of the commensurate fields. Moreover, comparing Figures 3, 4 and 8 it is obvious that both materials behave similarly with respect to their trends.

Figure 10 shows the variation of the acoustic gain as a function of carrier density at $\frac{v_0}{v_s} = 1.25$ and $\omega = 5 \times 10^{12} s^{-1}$ in the presence of fields of commensurate frequencies for nanoparticle doped MoS_2 and CdS.
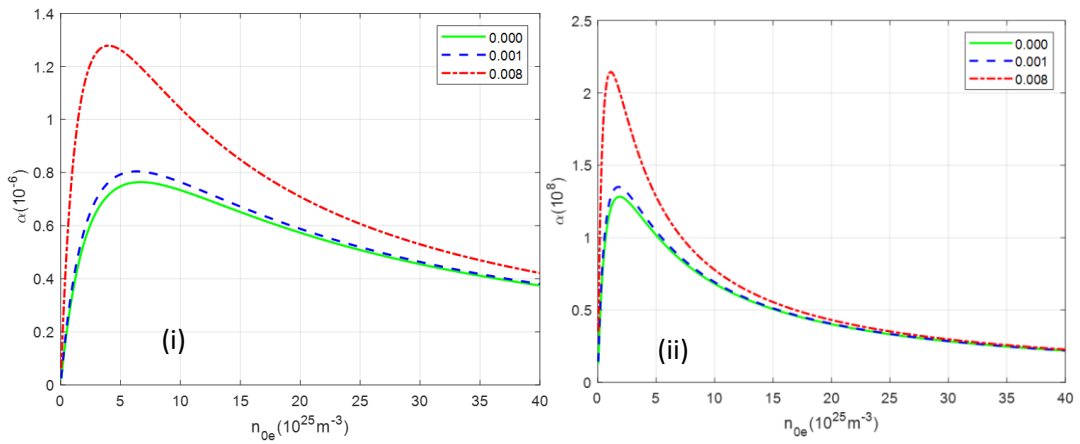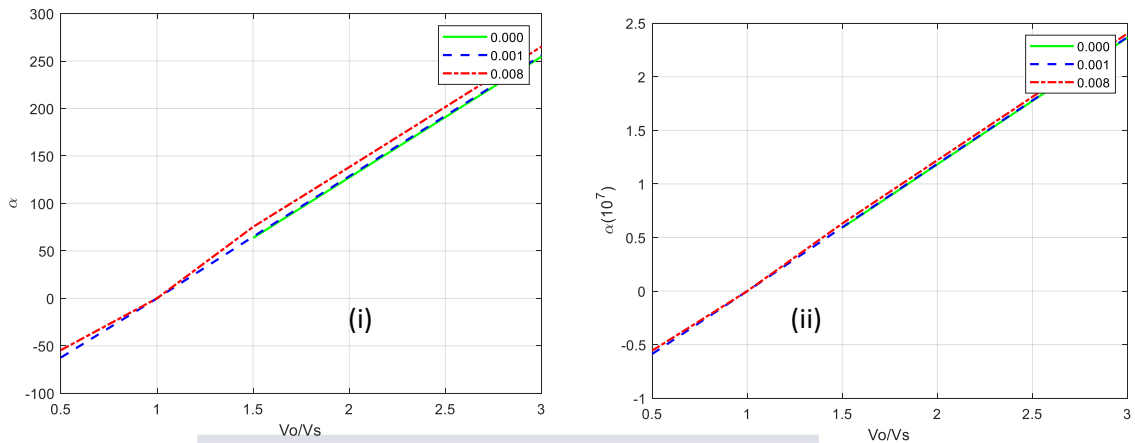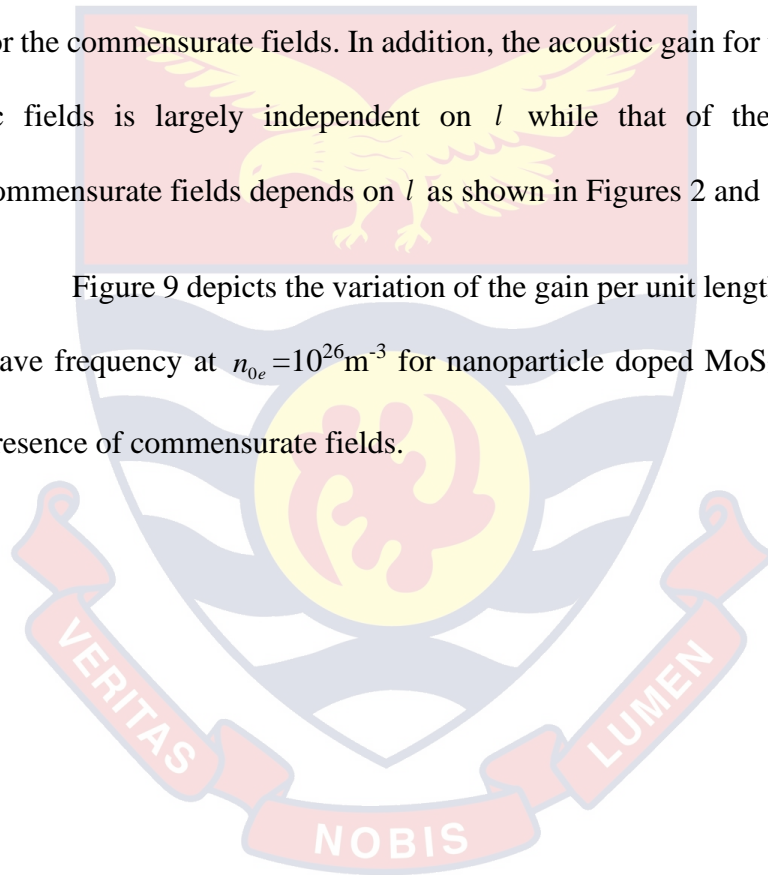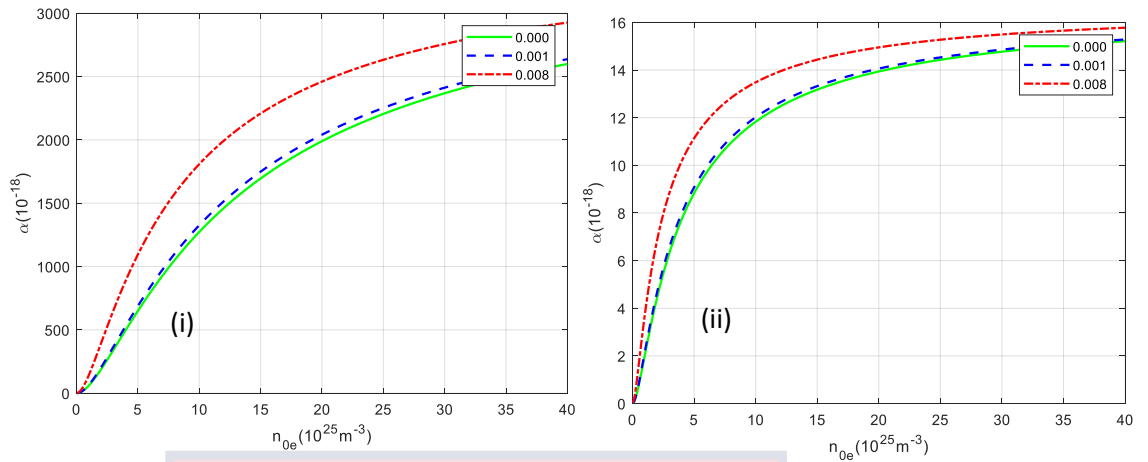
Figure 10: Variation of acoustic gain with carrier density of the medium in the presence of commensurate fields using $l = 0.001$, $l = 0.008$ and without NP cluster ($l = 0.001$) for: (i) CdS and (ii) MoS$_2$ at $\omega = 5 \times 10^{12} s^{-1}$ and $\frac{v_0}{v_s} = 1.25$ (using equation(39)).

From Figure 10, the acoustic gain (equation(39)) generally increases as the carrier density increases in both (i) and (ii). This is as a result of increased presence of nanoparticle cluster in both materials. As l increases, the acoustic gain also increases in both (i) and (ii) with the order of magnitude of the acoustic gain in (i) greater than that in (ii).

In using the combined dc-ac and the purely dc fields, the order of magnitude of the acoustic gain in the bulk material is largely greater than that in the presence of the commensurate fields. Again, in the presence of purely dc and combined dc-ac fields, further increase in carrier density decreases the acoustic gain. However, for the commensurate fields, increase of the carrier density increases the acoustic gain. On the other hand, for the monolayer

49

material using combined dc-ac fields, the order of magnitude of the acoustic gain is lesser than that in the purely dc case. For commensurate fields, the order of magnitude of the acoustic gain is the least as compared to the other two applied fields. Moreover, unlike Figure 9 it is clearly seen that Figures 5 and 6 depict a similar behavior in terms of their trends.

Chapter Summary

The chapter presents the results of phonon-plasmon interaction in bulk and monolayer piezoelectric semiconductors doped with nanoparticle cluster using combined dc-ac fields and fields with commensurate frequencies. Graphs showing the variation of acoustic gain with velocity ratio, acoustic gain per unit length with wave frequency and acoustic gain with carrier density were obtained. The figures were discussed with explanations provided for the observed trends. The chapter also compares the results of this work with those obtained by other researches in the presence of only a dc field.

Finally, it also compares the results obtained using fields of commensurate frequencies with those of purely dc and combined dc-ac fields.

CHAPTER FIVE

SUMMARY, CONCLUSIONS AND RECOMMENDATIONS

Introduction

This work employed the hydrodynamical model of plasma and macroscopic model of piezoelectric media to study the interaction of phonons and plasmons in bulk and monolayer piezoelectric semiconductors doped with nanoparticle cluster (NC) using combined dc-ac fields and fields of commensurate frequencies.

Summary

The study reviewed the relevant theory of phonon-plasmon interaction in piezoelectric semiconductor doped with a nanoparticle cluster. The theoretical formulation made use of the hydrodynamic model of plasma together with other equations to "derive an expression for the acoustic gain using combined dc-ac fields and fields of commensurate frequencies".

To visualize the results graphically, CdS and MoS_2 were considered as typical examples of piezoelectric semiconductors. Three cases of the variation of the acoustic gain as a function of the physical parameters of the media in the presence of combined dc-ac fields and commensurate fields were considered:

(i) The behavior of acoustic gain spectrum as a function of velocity ratio.

(ii) The acoustic gain per unit length as a function of wave frequency

(iii) The acoustic gain as a function of the carrier density of the media.

51

Conclusions

The results of the study suggest that NP doped bulk and monolayer piezoelectric semiconductors respond differently to different applied external fields. Thus, the variation of the acoustic gain with velocity ratio in the NP doped monolayer piezoelectric semiconductor has been found to have higher several orders of magnitude than that of the doped bulk material whenever such materials are subjected to the same combined dc-ac fields and fields of commensurate frequencies. The response of the monolayer material increases with increasing levels of NP cluster. Interestingly, when the ac component of the combined dc-ac fields is turned off, the results of this study agree perfectly with those obtained by other researchers. Therefore, NP doped piezoelectric semiconductors could be used as better candidates in the fabrication of high-performance sensors and transducers as opposed to similar devices manufactured from intrinsic semiconductors.

On the other hand, the acoustic gain per unit length of both materials vary equally with carrier frequency when both materials are subjected to combined dc-ac fields. However, in the absence of the ac field, the acoustic gain per unit length of the NP doped bulk material exceeds that of the monolayer by several orders of magnitude in agreement with results of other studies. Similarly, the NP doped bulk piezoelectric semiconductor shows more enhanced acoustic gain per unit length under the influence of fields of commensurate frequencies. These results suggest that bulk NP doped piezoelectric semiconductors are better candidates for device applications in which the acoustic gain per unit length is required. Finally, the study revealed that both NP doped bulk and monolayer piezoelectric

52

semiconductors show low level of acoustic gain with carrier density when subjected to fields of commensurate frequencies.

Recommendations

The following are some recommendations for further study:

(i)   Different piezoelectric semiconductors such as two-dimensional strained-induced (for example GaN and AlN) could be adopted for a similar study.

(ii)   A similar study could be carried out using the same materials under the influence of fields with combined magnetic and electrical properties.
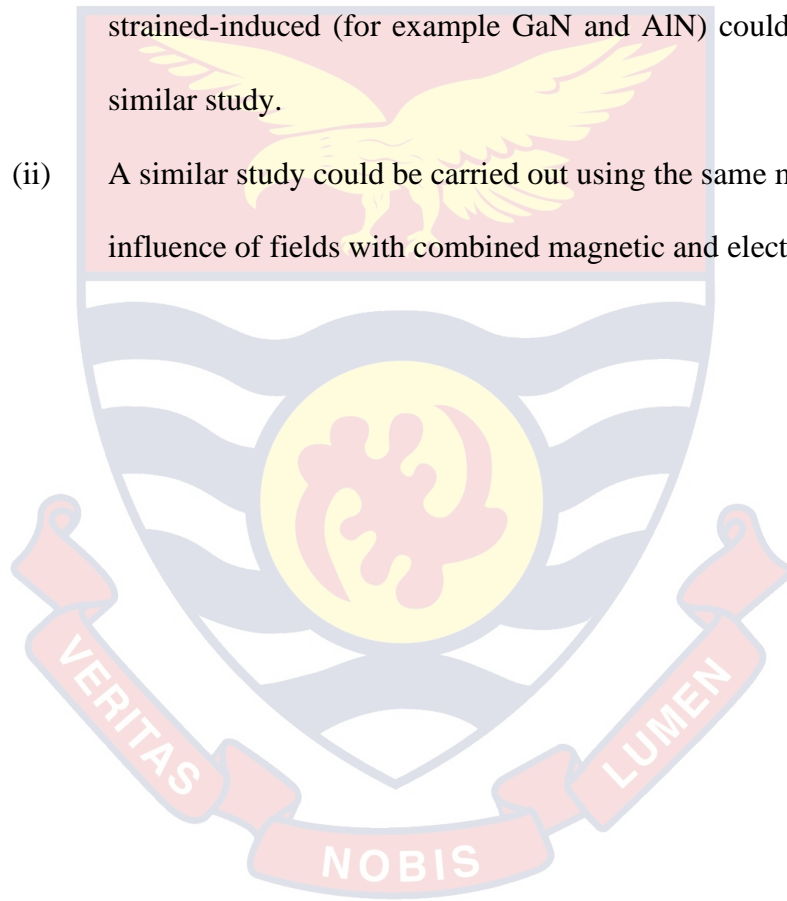
REFERENCES

Abukari, S. S., Adu, K. W., Mensah, S. Y., Mensah, N. G., Rabiu, M., Twum, A., & Dompreh, K. A. (2013). Rectification due to harmonic mixing of two coherent electromagnetic waves with commensurate frequencies in carbon nanotubes. *The European Physical Journal B*, *86*(3), 106.

Atwater, H. A. (2007). The promise of plasmonics. *Scientific American*, *296*(4), 56-63.

Barnes, W. L., Dereux, A., & Ebbesen, T. W. (2003). Surface plasmon subwavelength optics. *nature*, *424*(6950), 824-830.

Bohm, D., & Pines, D. (1951). A collective Description of Electron Interactions.I. Magnetic Interactions. *Phys. Rev., 82*, 625.

Busse, L. J., & Miller, J. G. (1981). Response characteristics of a finite aperture, phase insensitive ultrasonic receiver based upon the acoustoelectric effect. *The Journal of the Acoustical Society of America*, *70*(5), 1370-1376.

Cottam, M. G., & Tilley, D. R. (1989). *Introduction to surface and superlattice excitations*. CRC Press.

Dompreh, K.A., Mensah, N.G., Mensah, S.Y., Abukari, S.S., Sam, F. and Edziah, R. (2015). Hypersound Absorption of Acoustic Phonons in a Degenerate Carbon Nanotube. *Graphene, 4*, 62-74.

Dreaden, E. C., Alkilany, A. M., Huang, X., Murphy, C. J., & El-Sayed, M. A. (2012). The golden age: gold nanoparticles for biomedicine. *Chemical Society Reviews*, *41*(7), 2740-2779.

Dubey, P., & Ghosh, S. (2016). Modified longitudinal phonon-plasmon interactions in nanoparticle doped piezoelectric semiconductors. *Acta Acustica united with Acustica*, *102*(3), 436-440.

Elloh, V.W. (2001). *Propagation of ultrasound in a semiconductor in the presence of an electric field* (Master's thesis). University of Cape Coast, Cape Coast, Ghana.

Eustis, S., & El-Sayed, M. A. (2006). Why gold nanoparticles are more precious than pretty gold: noble metal surface plasmon resonance and its enhancement of the radiative and nonradiative properties of nanocrystals of different shapes.*Chemical society reviews*, *35*(3), 209-217.

Feng, K., Streyer, W., Islam, S. M., Verma, J., Jena, D., Wasserman, D., & Hoffman, A. J. (2015). Localized surface phonon polariton resonances in polar gallium nitride. *Applied Physics Letters*, *107*(8), 081108.

 Fetter, A. L., & Walecka, J. D. (2003). *Theoretical mechanics of particles and continua*. Courier Corporation.

Feynman, R. P. (1960). There's plenty of room at the bottom. *California Institute of Technology, Engineering and Science magazine*.

Feynman, R. P. (1963). Feynman Lecture on Physics. *Addison-Wesley Publishing Company,* 1, 3-10.

Ghosh, S. K., & Pal, T. (2007). Interparticle coupling effect on the surface plasmon resonance of gold nanoparticles: from theory to applications. *Chemical reviews*, *107*(11), 4797-4862.

Ghosh, S., & Dubey, P. (2017). Electron–electron two-stream instability in embedded assembly of nanoparticle (NP) cluster in n-GaAs. *Canadian Journal of Physics*, *95*(1), 95-101.

Ghosh, S., & Muley, A. (2016). Phonon-plasmon interactions in piezoelectric semiconductor quantum plasmas. *Physica B: Condensed Matter*, *503*, 75-80.

Hickernell, F. S. (2005). The piezoelectric semiconductor and acoustoelectronic device development in the sixties. *IEEE transactions on ultrasonics, ferroelectrics, and frequency control*, *52*(5), 737-745.

Hu, Y., Zeng, Y., & Yang, J. (2007). A mode III crack in a piezoelectric semiconductor of crystals with 6 mm symmetry. *International journal of solids and structures*, *44*(11-12), 3928-3938.

Hutson, A. R., & White, D. L. (1962). Elastic wave propagation in piezoelectric semiconductors. *Journal of Applied Physics*, *33*(1), 40-47.

Hutson, A. R., McFee, J. H., & White, D. L. (1961). Ultrasonic amplification in CdS. *Physical Review Letters*, *7*(6), 237.

Johar, M. A., Hassan, M. A., Waseem, A., Ha, J. S., Lee, J. K., & Ryu, S. W. (2018). Stable and high piezoelectric output of GaN nanowire-based lead-free piezoelectric nanogenerator by suppression of internal screening. *Nanomaterials*, *8*(6), 437.

Kelly, K. L., Coronado, E., Zhao, L. L., & Schatz, G. C. (2003). The optical properties of metal nanoparticles: the influence of size, shape, and dielectric environment. *Journal of Physical Chemistry B, 107*(3), 668-677.

Kittel, C. (2004). Introduction to solid state physics. *American Journal of Physics*, *35*(6), 547-548.

Kittel, C., & McEuen, P. (1995). *Introduction to solid state physics* (Vol. 8). New York: Wiley.

Kociak, M., Stéphan, O., Gloter, A., Zagonel, L. F., Tizei, L. H., Tencé, M., ... & Meuret, S. (2014). Seeing and measuring in colours: Electron microscopy and spectroscopies applied to nano-optics. *Comptes Rendus Physique*, *15*(2-3), 158-175.

Krauth. (2006). *Statistical mechanics: Rigorous results*. World Scientific.

Laurent, S., Forge, D., Port, M., Roch, A., Robic, C., Vander Elst, L., & Muller, R. N. (2008). Magnetic iron oxide nanoparticles: synthesis, stabilization, vectorization, physicochemical characterizations, and biological applications. *Chemical reviews*, *108*(6), 2064-2110.

Li, Y., Gao, Y., & Song, J. (2016). Recent advances on thermal analysis of stretchable electronics. *Theoretical and Applied Mechanics Letters*, *6*(1), 32-37.

Maier, S. A. (2007). *Plasmonics: fundamentals and applications*. Springer Science & Business Media.

Manbachi, A., & Cobbold, R. S. (2011). Development and application of piezoelectric materials for ultrasound generation and detection. *Ultrasound*, *19*(4), 187-196.

Mansha, M., Khan, I., Ullah, N., & Qurashi, A. (2017). Synthesis, characterization and visible-light-driven photoelectrochemical hydrogen evolution reaction of carbazole-containing conjugated polymers. *International Journal of Hydrogen Energy*, *42*(16), 10952-10961.

Masserini, M. (2013). Nanoparticles for brain drug delivery. *ISRN biochemistry*, *2013*, 1-18.

Misra, P. (2010). *Physics of condensed matter*. Academic Press.

Ozbay, E. (2006). Plasmonics: merging photonics and electronics at nanoscale dimensions. *science*, *311*(5758), 189-193.

Park, W. (2014). Optical interactions in plasmonic nanostructures. *Nano Convergence, I(1)*, 2.

Raether, H. (1980). *Excitation of plasmons and interband transitions by electrons* (Vol. 88). Springer.

Reather, H. (1988). Surface plasmons on smooth and rough surfaces and on gratings. *Springer tracts in modern physics*, *111*, 1-3.

Saeed, K., & Khan, I. (2016). Preparation and characterization of single-walled carbon nanotube/nylon 6, 6 nanocomposites. *Instrumentation Science & Technology*, *44*(4), 435-444.

Schwabl, F. (2008). *Advanced quantum mechanics* . Springer Science & Business Media.

Sigmund, W., Yuh, J., Park, H., Maneeratana, V., Pyrgiotakis, G., Daga, A., ... & Nino, J. C. (2006). Processing and structure relationships in electrospinning of ceramic fiber systems. *Journal of the American Ceramic Society*, *89*(2), 395-407.

Simon, S. H. (2013). *The Oxford solid state basics*. OUP Oxford.

Steele, M. C., & Vural, B. (1969). *Wave interactions in solid state plasmas*. Mc-Graw Hill.

Talwar, D. N., Vandevyver, M., Kunc, K., & Zigone, M. (1981). Lattice dynamics of zinc chalcogenides under compression: Phonon dispersion, mode Grüneisen, and thermal expansion. *Physical Review B*, *24*(2), 741.

Weinreich, G., Sanders Jr, T. M., & White, H. G. (1959). Acoustoelectric effect in n-type germanium. *Physical Review*, *114*(1), 33.

White, D. L. (1962). Amplification of ultrasonic waves in piezoelectric semiconductors. *Journal of Applied Physics*, *33*(8), 2547-2554.

Willatzen, M., & Christensen, J. (2014). Acoustic gain in piezoelectric semiconductors at ε-near-zero response. *Physical Review B, 89*(4), 041201.

Willets, K. A., & Van Duyne, R. P. (2007). Localized surface plasmon resonance spectroscopy and sensing. *Annu. Rev. Phys. Chem.*, *58*, 267-297.

Xu, Z. (2016). Heat transport in low-dimensional materials: A review and perspective. *Theoretical and Applied Mechanics Letters*, *6*(3), 113-121.

Yamada, K. (1968). Nonlinear Phonon Interaction in Piezoelectric Semiconductors and Effect on Current Saturation. *Physical Review*, *169*(3), 690.

Zhao, M., Li, Y., Yan, Y., & Fan, C. (2016). Singularity analysis of planar cracks in three-dimensional piezoelectric semiconductors via extended displacement discontinuity boundary integral equation method. *Engineering Analysis with Boundary Elements*, *67*, 115-125.

Zolyomi, V., Drummond, N. D., & Fal'Ko, V. I. (2013). Band structure and optical transitions in atomic layers of hexagonal gallium chalcogenides. *Physical Review B*, *87*(19), 195403.

APPENDICES

APPENDIX A

DERIVATION OF THE RELATION BETWEEN DISPLACEMENT AND STRESS TENSOR

The relation between displacement $\vec{u}$ and stress tensor T is given as:

$$\rho \frac{\partial^2 \vec{u}_x}{\partial t^2} = \frac{\partial T}{\partial z}$$

A1

The linear strain corresponding to diagonal element of S is defined as

$$S = \frac{\partial \vec{u}_x}{\partial z}$$

A2

The basic equation of state describing piezoelectric crystal is given as

$$T = CS - \beta E$$

A3

Substituting equation (A2) into equation (A3), the stress tensor T becomes:

$$T = C \frac{\partial \vec{u}_x}{\partial z} - \beta E$$

A4

Differentiating the stress tensor T with respect to z in equation (A4) gives:

$$\frac{\partial T}{\partial z} = C \frac{\partial^2 \vec{u}_x}{\partial z^2} - \beta \frac{\partial E_z}{\partial z}$$

A5

Substituting equation (A5) into equation (A1):

61

$$\rho \frac{\partial^2 \vec{u}_x}{\partial t^2} = C \frac{\partial^2 \vec{u}_x}{\partial z^2} - \beta \frac{\partial E_z}{\partial z} \qquad\qquad \text{A6}$$

APPENDIX B

DERIVATION OF THE EQUATION OF A WAVE IN A PIEZOELECTRIC

MEDIUM

Given the Newton's equation of lattice vibration as

$$\rho \frac{\partial^2 \vec{u}_x}{\partial t^2} = C \frac{\partial^2 \vec{u}_x}{\partial z^2} - \beta \frac{\partial \vec{E}_z}{\partial z}$$ B1

Since all perturbations are assumed to vary as $\exp\left[i(\omega t - kz)\right]$, it implies that

$$\vec{u}_x = \exp\left[i(\omega t - kz)\right]$$ B2

and

$$\vec{E}_z = \exp\left[i(\omega t - kz)\right]$$ B3

This implies that

$$\frac{\partial^2 \vec{u}_x}{\partial z^2} = -k^2 \vec{u}_x$$ B4

Similarly

$$\frac{\partial^2 \vec{u}_x}{\partial t^2} = -\omega^2 \vec{u}_x$$ B5

Substituting equations (B4) and (B5) into equation (A1) gives

63

$$\left(-\rho\omega^2 + Ck^2\right)\vec{u}_x = -\beta\frac{\partial\vec{E}_Z}{\partial z} \qquad\qquad\text{B6}$$

Differentiating equation (B3) with respect to z gives

$$\frac{\partial\vec{E}_Z}{\partial z} = -ik\vec{E}_Z \qquad\qquad\text{B7}$$

Substituting equation (B7) into equation (B6) gives

$$\left(-\rho\omega^2 + Ck^2\right)\vec{u}_x = ik\beta\vec{E}_Z \qquad\qquad\text{B8}$$

64

APPENDIX C

DERIVATION OF THE VELOCITY OF SOUND

The wave equation in an elastic piezoelectric medium is given as

$$\left(-\rho\omega^2 + Ck^2\right)\vec{u}_x = ik\beta\vec{E}_z \qquad \text{C1}$$

Here β is piezoelectric constant, E_z is applied electric field, ρ is mass density, and C is elastic stiffness constant.

In the absence of piezoelectricity, $\beta = 0$

$$\left(-\rho\omega^2 + Ck^2\right)\vec{u}_x = 0 \qquad \text{C2}$$

$$\frac{\omega^2}{k^2} = \frac{C}{\rho} \qquad \text{C3}$$

But

$$V_s^2 = \frac{\omega^2}{k^2}.$$

This implies that,

$$V_s^2 = \frac{C}{\rho} \qquad \text{C4}$$

$$V_s = \sqrt{\frac{C}{\rho}} \qquad \text{C5}$$

65

APPENDIX D

DERIVATION OF THE ELECTRIC DISPLACEMENT COMPONENT OF SOUND WAVE

In presence of piezoelectricity, when $\beta \neq 0$ and based on equation C1

$$\left(-\rho\omega^2 + Ck^2\right)\vec{u}_x = ik\beta\vec{E}_z \qquad \text{D1}$$

$$S_{31} = S_{13} = \frac{1}{2}\frac{\partial\vec{u}_x}{\partial z} \qquad \text{D2}$$

where S_{13} and S_{31} are the strain components in terms of lattice displacement

$$\vec{D}_z = \varepsilon\vec{E}_z + 2\beta S_{13} \qquad \text{D3}$$

Here, ε is the electric permittivity constant, $\vec{D}_z$ is the electric displacement component, S is the strain and β is the piezoelectric constant

Substituting D2 into D3

$$\vec{D}_z = \varepsilon\vec{E}_z + 2\beta\left(\frac{1}{2}\frac{\partial\vec{u}_x}{\partial z}\right) \qquad \text{D4}$$

$$\vec{D}_z = \varepsilon\vec{E}_z + \beta\frac{\partial\vec{u}_x}{\partial z} \qquad \text{D5}$$

$$\vec{u}_x = \frac{ik\beta\vec{E}_z}{\left(-\rho\omega^2 + Ck^2\right)} \qquad \text{D6}$$

But

$$E_z = E_z \exp i\left(\omega t - kz\right)$$

66

$$\vec{u}_x = \frac{ik\beta \exp i\left(\omega t - kz\right)}{\left(-\rho\omega^2 + Ck^2\right)}$$ D7

$$\frac{\partial \vec{u}_x}{\partial z} = \frac{k^2 \beta \vec{E}_z}{\left(-\rho\omega^2 + Ck^2\right)}$$ D8

$$\vec{D}_z = \varepsilon\vec{E}_z + \beta\left(\frac{k^2 \beta \vec{E}_z}{\left(-\rho\omega^2 + Ck^2\right)}\right)$$ D9

$$\vec{D}_z = \varepsilon\vec{E}_z\left(1 + \frac{\beta^2 k^2}{\varepsilon\left(-\rho\omega^2 + Ck^2\right)}\right)$$ D10

67
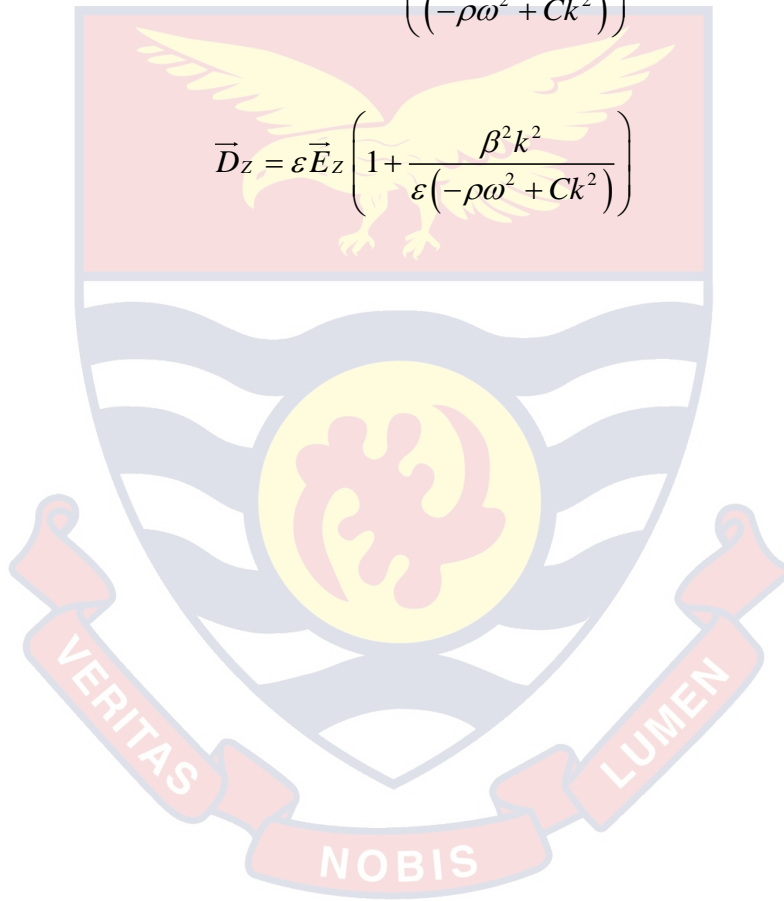
APPENDIX E

DERIVATION OF THE CONDUCTION CURRENT DENSITY

The velocity of free electrons of the piezoelectric semiconductor plasma medium is given as:

$$v_z = \frac{i\left(e/m\right)\vec{E}_z}{F(\omega,k)} \qquad \text{E1}$$

where $F(\omega,k) = \left[\omega - kv_0 - iv - \frac{Dvk^2}{(\omega - kv_0)}\right]$ in which v is the momentum transfer collision frequency and D is the diffusion coefficient.

The conduction current density is given as:

$$\vec{J}_Z = -n_{0e}ev_z \qquad \text{E2}$$

$$\vec{J}_Z = \frac{-n_{0e}e\left(ie/m\right)\vec{E}_z}{F(\omega,k)} \qquad \text{E3}$$

But

$$\omega_{pe} = \sqrt{\left(n_{0e}e^2/m\varepsilon\right)}$$

$$n_{0e}e^2/m = \varepsilon\omega_{pe}^2 \qquad \text{E4}$$

Substituting E4 into E3

$$\vec{J}_Z = -\frac{i\varepsilon\omega_{pe}^2\vec{E}_z}{F(\omega,k)} \qquad \text{E5}$$

where ω_{pe} is the electron plasma frequency and n_{0e} is the carrier density of the medium.

APPENDIX F

DERIVATION OF THE VELOCITY OF ELECTRON CLOUD

The motion of electrons presents within the nanoparticle cloud having displacement $\vec{\Delta}$ can be described by the equation of motion

$$\frac{d^2\vec{\Delta}}{dt^2} + \frac{\omega_{pn}^2 \vec{\Delta}}{3} = -\frac{e\vec{E}_z}{m} \qquad \text{F1}$$

Here, $\omega_{pn} = \sqrt{e^2 n_{0n} \big/ m}$ is plasma frequency of electrons present within the NP-cluster.

Since all perturbations vary are assumed to vary as $\exp\left[i\left(\omega t - kz\right)\right]$, then

$$\vec{\Delta} \sim \exp\left[i\left(\omega t - kz\right)\right] \qquad \text{F2}$$

Differentiating equation F2 with respect to t gives

$$\frac{d^2\vec{\Delta}}{dt^2} = -\omega^2 \vec{\Delta} \qquad \text{F3}$$

Substituting equation F3 into equation F1 gives

$$-\omega^2 \vec{\Delta} + \frac{\omega_{pn}^2}{3}\vec{\Delta} = -\frac{e}{m}\vec{E}_z \qquad \text{F4}$$

$$\vec{\Delta} = \frac{\left(e \big/ m\right)\vec{E}_z}{\left(\omega^2 - \dfrac{\omega_{pn}^2}{3}\right)} \qquad \text{F5}$$

Differentiating equation F5 with respect to t yields the velocity of the electron cloud as

$$v_{np} = \frac{\left(e/m\right)}{\left(\omega^2 - \dfrac{\omega_{pn}^2}{3}\right)} \frac{d\vec{E}_z}{dt}$$

F6

But

$$\vec{E}_z = \exp\left[i\left(\omega t - kz\right)\right]$$

By differentiating the expression of $\vec{E}_z$ with respect to t gives

$$\frac{d\vec{E}_z}{dt} = i\omega\exp\left[i\left(\omega t - kz\right)\right]$$

F7

$$\frac{d\vec{E}_z}{dt} = i\omega\vec{E}_z$$

F8

Substituting equation F8 into equation F6

$$v_{np} = \frac{i\omega\left(e/m\right)\vec{E}_z}{\left(\omega^2 - \dfrac{\omega_{pn}^2}{3}\right)}$$

F9

Let $X = \left(\omega^2 - \dfrac{\omega_{pn}^2}{3}\right)$, then the above equation yields

$$v_{np} = \frac{i\omega\left(e/m\right)\vec{E}_z}{X}$$

F10

70

APPENDIX G

DERIVATION OF THE SPACE CHARGE DENSITY

Recalling the continuity equation

$$\frac{\partial \vec{J}}{\partial z} = e \frac{\partial n}{\partial t} \qquad \text{G1}$$

But

$$\vec{J} = -i\varepsilon \vec{E}_Z \left[\frac{\omega_{pe}^2}{F(\omega,k)} + \frac{4\pi}{3} l \frac{\omega\omega_{pn}^2}{X} \right]$$

$$n = n_0 + n' \qquad \text{G2}$$

where n' is the space charge density and n_0 is the equilibrium electron density.

Substituting the resultant current density $\vec{J}$ into equation G1 yields

$$-i\varepsilon \left[\frac{\omega_{pe}^2}{F(\omega,k)} + \frac{4\pi}{3} l \frac{\omega\omega_{pn}^2}{X} \right] \frac{\partial \vec{E}_Z}{\partial z} = e \frac{\partial n'}{\partial t} \qquad \text{G3}$$

But

$$\vec{E}_Z = \exp\left[i(\omega t - kz) \right]$$

Differentiating equation $\vec{E}_Z$ with respect to z yields

$$\frac{\partial \vec{E}_Z}{\partial z} = -ik \vec{E}_Z \qquad \text{G4}$$

Substituting equation G4 into equation G3 gives

71

$$-\varepsilon k \vec{E}_Z \left[\frac{\omega_{pe}^2}{F(\omega,k)} + \frac{4\pi}{3} l \frac{\omega \omega_{pn}^2}{X} \right] = e \frac{\partial n'}{\partial t} \qquad \text{G5}$$

From equation G5

$$n' = \frac{-\varepsilon k}{e} \left[\frac{\omega_{pe}^2}{F(\omega,k)} + \frac{4\pi}{3} l \frac{\omega \omega_{pn}^2}{X} \right] \int \vec{E}_Z \partial t \qquad \text{G6}$$

But

$$\vec{E}_Z = \exp\left[i(\omega t - kz) \right] = \exp\left[it\left(\omega t - \frac{kz}{t} \right) \right]$$

But $v_0 = \frac{z}{t}$ is the drift velocity of electrons in the medium and hence, $\vec{E}_Z$ becomes

$$\vec{E}_Z = \exp\left[it(\omega t - kv_0) \right] \qquad \text{G7}$$

Therefore

$$\int \vec{E}_Z \partial t = \frac{\vec{E}_Z}{i(\omega - kv_0)} \qquad \text{G8}$$

Substituting equation G8 into equation G6 gives

$$n' = \frac{i\varepsilon k \vec{E}_Z}{e(\omega - kv_0)} \left[\frac{\omega_{pe}^2}{F(\omega,k)} + \frac{4\pi}{3} l \frac{\omega \omega_{pn}^2}{X} \right]. \qquad \text{G9}$$

APPENDIX H

DERIVATION OF VELOCITY OF FREE ELECTRONS OF A MEDIUM DUE TO

NANOPARTICLE CLUSTER

From Maxwell's equation

$$\vec{\nabla} \cdot \vec{D}_z = -en' \qquad \text{H1}$$

That is,

$$\frac{\partial \vec{D}_z}{\partial z} = -en' \qquad \text{H2}$$

$$\vec{D}_z = -e \int n' \partial z \qquad \text{H3}$$

From equation G9 in (Appendix G): $n' = \dfrac{i\varepsilon k \vec{E}_z}{e(\omega - kv_0)} \left[\dfrac{\omega_{pe}^2}{F(\omega,k)} + \dfrac{4\pi}{3} l \dfrac{\omega \omega_{pn}^2}{X} \right].$

Substituting n' into equation H3 and simplify to get

$$\vec{D}_z = -\frac{i\varepsilon k}{(\omega - kv_0)} \left[\frac{\omega_{pe}^2}{F(\omega,k)} + \frac{4\pi}{3} l \frac{\omega \omega_{pn}^2}{X} \right] \int \vec{E}_z \partial z \qquad \text{H4}$$

But

$$\int \vec{E}_z \partial z = -\frac{1}{ik} \exp\left[i(\omega t - kz) \right] = -\frac{1}{ik} \vec{E}_z \qquad \text{H5}$$

Substituting equation H5 into equation H4 gives

73

$$\vec{D}_Z = \frac{\varepsilon \vec{E}_Z}{\left(\omega - kv_0\right)}\left[\frac{\omega_{pe}^2}{F\left(\omega,k\right)} + \frac{4\pi}{3}l\frac{\omega\omega_{pn}^2}{X}\right]. \qquad\qquad \text{H6}$$

APPENDIX I

DERIVATION OF THE ACOUSTIC GAIN IN THE PRESENCE OF A DC FIELD

From equation (16)

$$\vec{D}_z = \varepsilon \vec{E}_z \left[1 + \frac{\beta^2 k^2}{\varepsilon\left(-\rho\omega^2 + Ck^2\right)} \right] \tag{I1}$$

and from equation (29)

$$\vec{D}_z = \frac{\varepsilon \vec{E}_z}{\omega - kv_0} \left[\frac{\omega_{pe}^2}{F(\omega,k)} + \frac{4\pi}{3} l \frac{\omega\omega_{pn}^2}{X} \right] \tag{I2}$$

I1 and I2 gives

$$\varepsilon \vec{E}_z \left[1 + \frac{\beta^2 k^2}{\varepsilon\left(-\rho\omega^2 + Ck^2\right)} \right] = \frac{\varepsilon \vec{E}_z}{\left(\omega - kv_0\right)} \left[\frac{\omega_{pe}^2}{F(\omega,k)} + \frac{4\pi}{3} l \frac{\omega\omega_{pn}^2}{X} \right] \tag{I3}$$

$$1 - \frac{1}{\left(\omega - kv_0\right)} \left[\frac{\omega_{pe}^2}{F(\omega,k)} + \frac{4\pi}{3} l \frac{\omega\omega_{pn}^2}{X} \right] = - \frac{\beta^2 k^2}{\varepsilon\left(-\rho\omega^2 + Ck^2\right)} \tag{I4}$$

Multiplying equation I4 by $\left(\omega^2 - k^2 v_s^2\right)$ gives

$$\left(\omega^2 - k^2 v_s^2\right)\left\{ 1 - \frac{1}{\left(\omega - kv_0\right)} \left[\frac{\omega_{pe}^2}{F(\omega,k)} + \frac{4\pi}{3} l \frac{\omega\omega_{pn}^2}{X} \right] \right\} = - \left[\frac{\beta^2 k^2}{\varepsilon\left(-\rho\omega^2 + Ck^2\right)} \right]\left(\omega^2 - k^2 v_s^2\right) \tag{I5}$$

$$\left(\omega^2 - k^2 v_s^2\right)\left\{ 1 - \frac{1}{\left(\omega - kv_0\right)} \left[\frac{\omega_{pe}^2}{F(\omega,k)} + \frac{4\pi}{3} l \frac{\omega\omega_{pn}^2}{X} \right] \right\} = - K^2 \left[\frac{k^2}{-\frac{1}{v_s^2}\left(\omega^2 - k^2 v_s^2\right)} \right]\left(\omega^2 - k^2 v_s^2\right) \tag{I6}$$

75

$$\left(\omega^2 - k^2 v_s^2\right)\left\{1 - \frac{1}{\left(\omega - kv_0\right)}\left[\frac{\omega_{pe}^2}{F\left(\omega,k\right)} + \frac{4\pi}{3}l\frac{\omega\omega_{pn}^2}{X}\right]\right\} = K^2 k^2 v_s^2 \qquad \text{I7}$$

For no piezoelectricity, $\beta = 0$ and $K = 0$

$$\left(\omega^2 - k^2 v_s^2\right)\left\{1 - \frac{1}{\left(\omega - kv_0\right)}\left[\frac{\omega_{pe}^2}{F\left(\omega,k\right)} + \frac{4\pi}{3}l\frac{\omega\omega_{pn}^2}{X}\right]\right\} = 0 \qquad \text{I8}$$

This implies that,

$$\left(\omega^2 - k^2 v_s^2\right) = 0 \qquad \text{I9}$$

and

$$\left\{1 - \frac{1}{\left(\omega - kv_0\right)}\left[\frac{\omega_{pe}^2}{F\left(\omega,k\right)} + \frac{4\pi}{3}l\frac{\omega\omega_{pn}^2}{X}\right]\right\} = 0 \qquad \text{I10}$$

But,

$$F\left(\omega,k\right) = \left[\omega - kv_0 - iv - \frac{Dvk^2}{\left(\omega - kv_0\right)}\right] \qquad \text{I11}$$
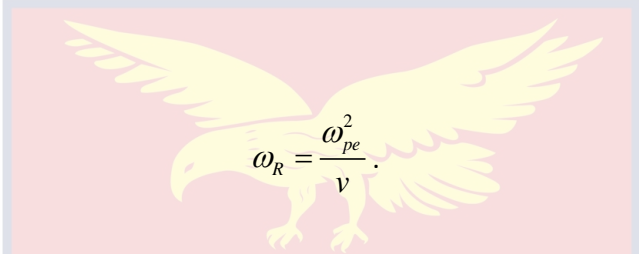
$$\left(\omega^2 - k^2 v_s^2\right)\left\{1 - \frac{1}{\left(\omega - kv_0\right)}\left[\frac{\omega_{pe}^2}{\omega - kv_0 - iv - \dfrac{Dvk^2}{\left(\omega - kv_0\right)}} + \frac{4\pi}{3}l\frac{\omega\omega_{pn}^2}{X}\right]\right\} = K^2 k^2 v_s^2 \quad \text{I12}$$

For collision dominated limit: $\omega \ll v$ and $kv_0 \ll v$

76

$$\left(\omega^2 - k^2 v_s^2\right)\left\{1 - \frac{1}{\left(\omega - kv_0\right)}\left[\frac{\omega_{pe}^2}{-iv - \dfrac{Dvk^2}{\left(\omega - kv_0\right)}} + \frac{4\pi}{3}l\frac{\omega\omega_{pn}^2}{X}\right]\right\} = K^2 k^2 v_s^2 \qquad \text{I13}$$

$$\left(\omega^2 - k^2 v_s^2\right)\left\{1 + \left[\frac{\omega_{pe}^2}{iv\left(\omega - kv_0 - iDk^2\right)vk^2} - \frac{4\pi}{3}l\frac{\omega\omega_{pn}^2}{X\left(\omega - kv_0\right)}\right]\right\} = K^2 k^2 v_s^2 \qquad \text{I14}$$
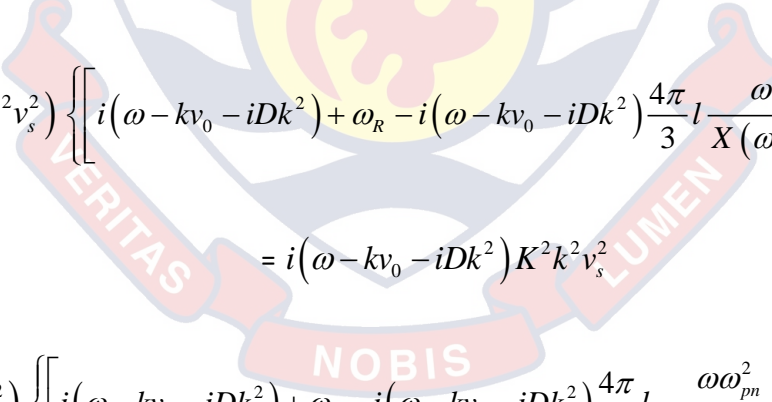
But

$$\omega_R = \frac{\omega_{pe}^2}{v}.$$

$$\left(\omega^2 - k^2 v_s^2\right)\left\{1 + \left[\frac{\omega_R}{i\left(\omega - kv_0 - iDk^2\right)} - \frac{4\pi}{3}l\frac{\omega\omega_{pn}^2}{X\left(\omega - kv_0\right)}\right]\right\} = K^2 k^2 v_s^2 \qquad \text{I15}$$

Multiplying through equation I15 by $i\left(\omega - kv_0 - iDk^2\right)$ gives

$$\left(\omega^2 - k^2 v_s^2\right)\left\{\left[i\left(\omega - kv_0 - iDk^2\right) + \omega_R - i\left(\omega - kv_0 - iDk^2\right)\frac{4\pi}{3}l\frac{\omega\omega_{pn}^2}{X\left(\omega - kv_0\right)}\right]\right\}$$

$$= i\left(\omega - kv_0 - iDk^2\right)K^2 k^2 v_s^2 \qquad \text{I16}$$

$$\left(\omega^2 - k^2 v_s^2\right)\left\{\left[i\left(\omega - kv_0 - iDk^2\right) + \omega_R - i\left(\omega - kv_0 - iDk^2\right)\frac{4\pi}{3}l\frac{\omega\omega_{pn}^2}{X\left(\omega - kv_0\right)}\right]\right\}$$

$$= i\left(\omega - kv_0 - iDk^2\right)K^2 k^2 v_s^2 \qquad \text{I17}$$

But

77

$$v_s = \frac{\omega}{k} \ .$$

This implies that,

$$\omega^2 = k^2 v_s^2$$

Hence equation I17 becomes:

$$\omega^2 \left(1 - \frac{k^2 v_s^2}{\omega^2}\right) \left\{\omega_R + i\left(\omega - kv_0 - iDk^2\right)\left[1 - \frac{4\pi}{3} l \frac{\omega\omega_{pn}^2}{X(\omega - kv_0)}\right]\right\} = i\left(\omega - kv_0 - iDk^2\right) K^2 k^2 v_s^2$$

I18

Dividing equation I18 by the second term in the left-hand side parenthesis gives

$$\left(1 - \frac{k^2 v_s^2}{\omega^2}\right) = \frac{i\left(\omega - kv_0 - iDk^2\right) K^2}{\left\{\omega_R + i\left(\omega - kv_0 - iDk^2\right)\left[1 - \frac{4\pi}{3} l \frac{\omega\omega_{pn}^2}{X(\omega - kv_0)}\right]\right\}}$$

I19

$$\frac{k^2 v_s^2}{\omega^2} = 1 + \frac{i\left(kv_0 - \omega + iDk^2\right) K^2}{\left\{\omega_R + i\left(\omega - kv_0 - iDk^2\right)\left[1 - \frac{4\pi}{3} l \frac{\omega\omega_{pn}^2}{X(\omega - kv_0)}\right]\right\}}$$

I20

From binomial expansion $(1 + x)^n = 1 + nx$ for x been very small

$$\frac{kv_s}{\omega} = 1 + \frac{\frac{1}{2} i\left(kv_0 - \omega + iDk^2\right) K^2}{\left\{\omega_R + i\left(\omega - kv_0 - iDk^2\right)\left[1 - \frac{4\pi}{3} l \frac{\omega\omega_{pn}^2}{X(\omega - kv_0)}\right]\right\}}$$

I21

But

$$\frac{kv_s}{\omega} = 1 + i\alpha .$$

$$1 + i\alpha = 1 + \frac{\frac{1}{2}i\left(kv_0 - \omega + iDk^2\right)K^2}{\left\{\omega_R + i\left(\omega - kv_0 - iDk^2\right)\left[1 - \frac{4\pi}{3}l\frac{\omega\omega_{pn}^2}{X\left(\omega - kv_0\right)}\right]\right\}} \qquad \text{I22}$$

$$\alpha = \frac{\frac{1}{2}\left(\frac{kv_0}{\omega} - 1 + \frac{iDk^2}{\omega}\right)K^2\omega}{\left\{\omega_R + i\left(\omega - kv_0 - iDk^2\right)\left[1 + \frac{4\pi}{3}l\frac{\omega_{pn}^2}{X\left(\frac{kv_0}{\omega} - 1\right)}\right]\right\}} \qquad \text{I23}$$

But

$$v_s = \frac{\omega}{k},$$

and

$$\gamma = \frac{v_0}{v_s} - 1 .$$
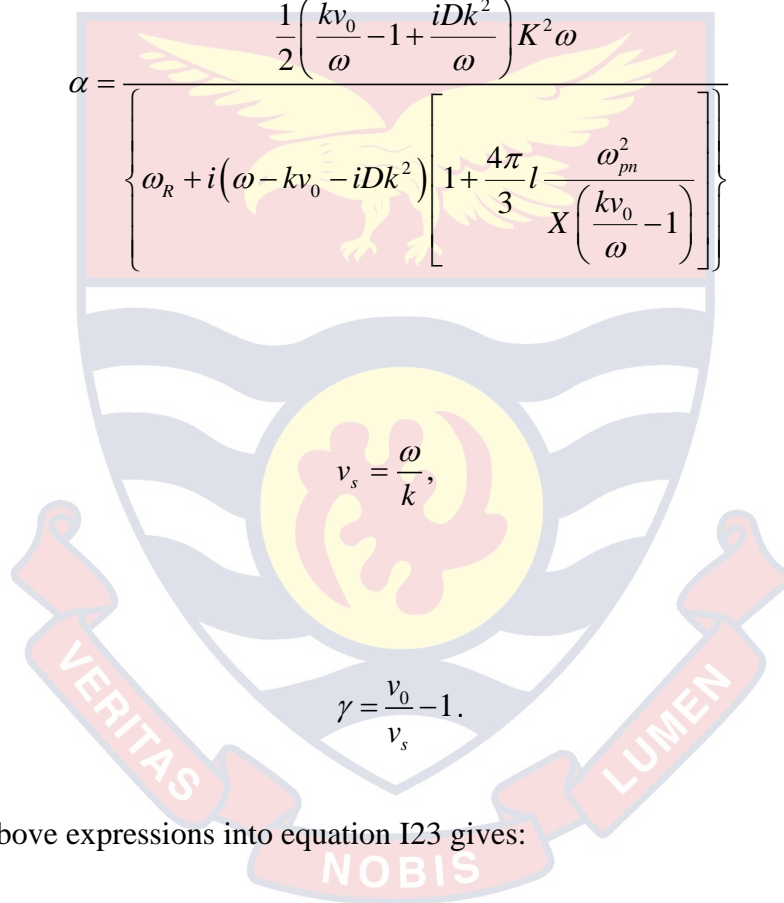
Substituting the above expressions into equation I23 gives:

$$\alpha = \frac{\frac{1}{2}\left(\gamma + \frac{iDk^2}{\omega}\right)K^2X}{\left(\frac{\omega_R}{\omega}\right)\left\{X + \frac{\omega^2}{\omega_R\omega_D}\left(X + \frac{4\pi}{3}l\frac{\omega_{pn}^2}{\gamma}\right)\right\} - i\left(\gamma X + \frac{4\pi}{3}l\omega_{pn}^2\right)} \qquad \text{I24}$$

Rationalizing the equation I24 and neglecting all real terms and considering only the coefficient of complex terms gives:

79

$$\alpha = \frac{\dfrac{1}{2}\left(\gamma + \dfrac{iDk^2}{\omega}\right)K^2 X\left[\left(\dfrac{\omega_R}{\omega}\right)\left\{X + \dfrac{\omega^2}{\omega_R\omega_D}\left(X + \dfrac{4\pi}{3}l\dfrac{\omega_{pn}^2}{\gamma}\right)\right\} + i\left(\gamma X + \dfrac{4\pi}{3}l\omega_{pn}^2\right)\right]}{\left[\left(\dfrac{\omega_R}{\omega}\right)\left\{X + \dfrac{\omega^2}{\omega_R\omega_D}\left(X + \dfrac{4\pi}{3}l\dfrac{\omega_{pn}^2}{\gamma}\right)\right\} - i\left(\gamma X + \dfrac{4\pi}{3}l\omega_{pn}^2\right)\right] \times}$$

$$\left[\left(\dfrac{\omega_R}{\omega}\right)\left\{X + \dfrac{\omega^2}{\omega_R\omega_D}\left(X + \dfrac{4\pi}{3}l\dfrac{\omega_{pn}^2}{\gamma}\right)\right\} + i\left(\gamma X + \dfrac{4\pi}{3}l\omega_{pn}^2\right)\right] \tag{I25}$$

$$\alpha = \frac{\dfrac{1}{2}K^2\gamma X^2\dfrac{\omega_R}{\omega}}{\left(\dfrac{\omega_R}{\omega}\right)^2\left[X + \dfrac{\omega^2}{\omega_R\omega_D}\left(X + \dfrac{4\pi}{3}l\dfrac{\omega_{pn}^2}{\gamma}\right)\right]^2 + \left[\gamma X + \dfrac{4\pi}{3}l\omega_{pn}^2\right]^2} \tag{I26}$$

80
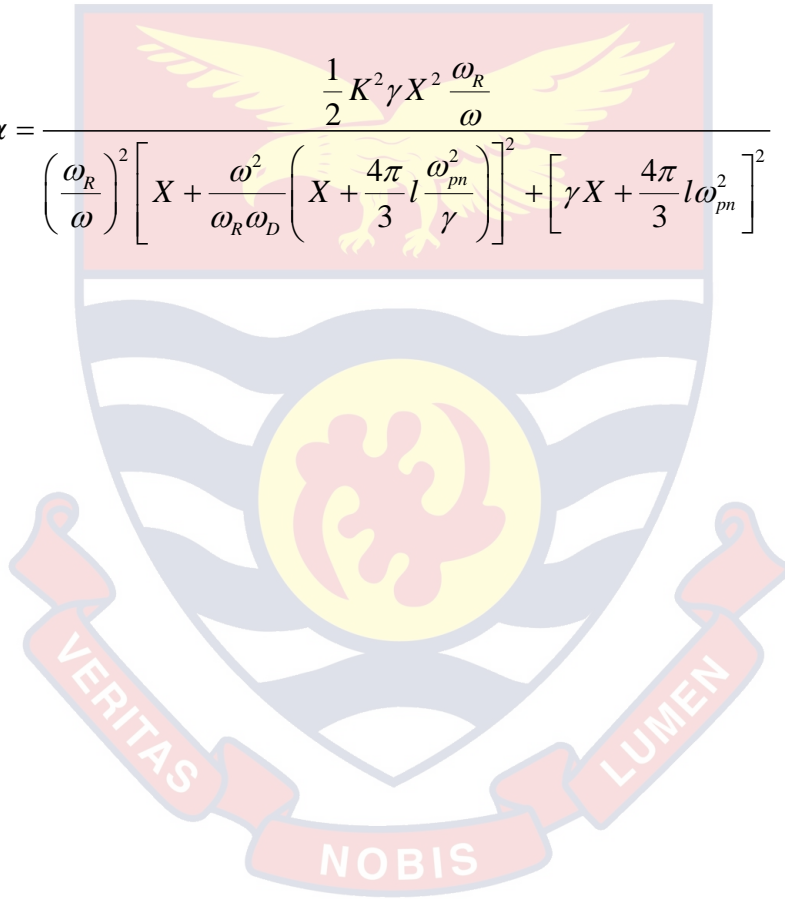
APPENDIX J

DERIVATION OF THE ACOUSTIC GAIN IN THE PRESENCE OF COMBINED DC-AC FIELDS

From equation I3:

$$\varepsilon \vec{E}_Z \left[1 + \frac{\beta^2 k^2}{\varepsilon \left(-\rho \omega^2 + Ck^2 \right)} \right] = \frac{\varepsilon \vec{E}_Z}{\left(\omega - kv_0 \right)} \left[\frac{\omega_{pe}^2}{F(\omega,k)} + \frac{4\pi}{3} l \frac{\omega \omega_{pn}^2}{X} \right] \qquad \text{J1}$$

But

$$E_Z = E_0 + E_1 \cos \omega t$$

Substituting the above expression into equation J1 and dividing through by ε gives

$$\left(E_0 + E_1 \cos \omega t \right) \left[1 + \frac{\beta^2 k^2}{\varepsilon \left(-\rho \omega^2 + Ck^2 \right)} \right] = \frac{\left(E_0 + E_1 \cos \omega t \right)}{\left(\omega - kv_0 \right)} \left[\frac{\omega_{pe}^2}{F(\omega,k)} + \frac{4\pi}{3} l \frac{\omega \omega_{pn}^2}{X} \right] \qquad \text{J2}$$

$$E_0 + \frac{E_0 \beta^2 k^2}{\varepsilon \left(-\rho \omega^2 + Ck^2 \right)} + E_1 \cos \omega t + \frac{E_1 \cos \omega t \beta^2 k^2}{\varepsilon \left(-\rho \omega^2 + Ck^2 \right)} = \frac{\omega_{pe}^2 \left(E_0 + E_1 \cos \omega t \right)}{\left(\omega - kv_0 \right) F(\omega,k)} + \frac{\left(E_0 + E_1 \cos \omega t \right)}{\left(\omega - kv_0 \right)} \frac{4\pi}{3} l \frac{\omega \omega_{pn}^2}{X}$$

$$\text{J3}$$

$$\left(E_0 + E_1 \cos \omega t \right) + \left(E_0 + E_1 \cos \omega t \right) \left[\frac{\beta^2 k^2}{\varepsilon \left(-\rho \omega^2 + Ck^2 \right)} \right] = \frac{\left(E_0 + E_1 \cos \omega t \right)}{\left(\omega - kv_0 \right)} \left[\frac{\omega_{pe}^2}{F(\omega,k)} + \frac{4\pi}{3} l \frac{\omega \omega_{pe}^2}{X} \right]$$

$$\text{J4}$$

$$\left[\left(E_0 + E_1 \cos \omega t \right) - \frac{\left(E_0 + E_1 \cos \omega t \right)}{\left(\omega - kv_0 \right)} \left\{ \frac{\omega_{pe}^2}{F(\omega,k)} + \frac{4\pi}{3} l \frac{\omega \omega_{pn}^2}{X} \right\} \right] = -\left(E_0 + E_1 \cos \omega t \right) \left[\frac{\beta^2 k^2}{\varepsilon \left(-\rho \omega^2 + Ck^2 \right)} \right]$$

$$\text{J5}$$

Multiplying through equation J5 by $\left(\omega^2 - k^2 v_s^2\right)$ gives

$$\left(\omega^2 - k^2 v_s^2\right)\left[E_0 + E_1 \cos\omega t - \frac{\left(E_0 + E_1 \cos\omega t\right)}{\left(\omega - kv_0\right)}\left\{\frac{\omega_{pe}^2}{F\left(\omega,k\right)} + \frac{4\pi}{3}\frac{\omega\omega_{pn}^2}{X}l\right\}\right] =$$

$$-\left(E_0 + E_1 \cos\omega t\right)\left[\frac{\beta^2 k^2}{\varepsilon\left(-\rho\omega^2 + Ck^2\right)}\right]\left(\omega^2 - k^2 v_s^2\right) \qquad \text{J6}$$

$$\left(\omega^2 - k^2 v_s^2\right)\left[E_0 + E_1 \cos\omega t - \frac{\left(E_0 + E_1 \cos\omega t\right)}{\left(\omega - kv_0\right)}\left\{\frac{\omega_{pe}^2}{F\left(\omega,k\right)} + \frac{4\pi}{3}l\frac{\omega\omega_{pn}^2}{X}\right\}\right] =$$

$$-\left(E_0 + E_1 \cos\omega t\right)\frac{\beta^2}{C\varepsilon}\left[\frac{k^2}{\left(-\dfrac{\rho}{C}\omega^2 + k^2\right)}\right]\left(\omega^2 - k^2 v_s^2\right) \qquad \text{J7}$$

$$\left(\omega^2 - k^2 v_s^2\right)\left[E_0 + E_1 \cos\omega t - \frac{\left(E_0 + E_1 \cos\omega t\right)}{\left(\omega - kv_0\right)}\left\{\frac{\omega_{pe}^2}{F\left(\omega,k\right)} + \frac{4\pi}{3}l\frac{\omega\omega_{pn}^2}{X}\right\}\right] =$$

$$-\left(E_0 + E_1 \cos\omega t\right)K^2\left[\frac{k^2}{\left(-\dfrac{1}{v_s^2}\omega^2 + k^2\right)}\right]\left(\omega^2 - k^2 v_s^2\right) \qquad \text{J8}$$

$$\left(\omega^2 - k^2 v_s^2\right)\left[E_0 + E_1 \cos\omega t - \frac{\left(E_0 + E_1 \cos\omega t\right)}{\left(\omega - kv_0\right)}\left\{\frac{\omega_{pe}^2}{F\left(\omega,k\right)} + \frac{4\pi}{3}l\frac{\omega\omega_{pn}^2}{X}\right\}\right] =$$

$$-\left(E_0 + E_1 \cos\omega t\right)K\left[\frac{k^2}{\dfrac{-1}{v_s^2}\left(\omega^2 - k^2 v_s^2\right)}\right]\left(\omega^2 - k^2 v_s^2\right) \qquad \text{J9}$$

82

$$\left(\omega^2 - k^2 v_s^2\right)\left[E_0 + E_1 \cos \omega t - \frac{\left(E_0 + E_1 \cos \omega t\right)}{\left(\omega - kv_0\right)}\left\{\frac{\omega_{pe}^2}{F\left(\omega,k\right)} + \frac{4\pi}{3} l \frac{\omega \omega_{pn}^2}{X}\right\}\right] = \left(E_0 + E_1 \cos \omega t\right) K^2 k^2 v_s^2$$

J10

For no piezoelectricity, $\beta = 0$, and $K = 0$.

$$\left(\omega^2 - k^2 v_s^2\right)\left[E_0 + E_1 \cos \omega t - \frac{\left(E_0 + E_1 \cos \omega t\right)}{\left(\omega - kv_0\right)}\left\{\frac{\omega_{pe}^2}{F\left(\omega,k\right)} + \frac{4\pi}{3} l \frac{\omega \omega_{pn}^2}{X}\right\}\right] = 0 \qquad \text{J11}$$

$$\left(\omega^2 - k^2 v_s^2\right) = 0 \qquad \text{J12}$$

and

$$\left[E_0 + E_1 \cos \omega t - \frac{\left(E_0 + E_1 \cos \omega t\right)}{\left(\omega - kv_0\right)}\left\{\frac{\omega_{pe}^2}{F\left(\omega,k\right)} + \frac{4\pi}{3} l \frac{\omega \omega_{pn}^2}{X}\right\}\right] = 0 \qquad \text{J13}$$

But

$$F\left(\omega,k\right) = \left[\omega - kv_0 - iv - \frac{Dvk^2}{\left(\omega - kv_0\right)}\right]$$

$$\left(\omega^2 - k^2 v_s^2\right)\left[\left(E_0 + E_1 \cos \omega t\right) - \frac{\left(E_0 + E_1 \cos \omega t\right)}{\left(\omega - kv_0\right)}\left\{\frac{\omega_{pe}^2}{\omega - kv_0 - iv - \dfrac{Dvk^2}{\left(\omega - kv_0\right)}} + \frac{4\pi}{3} l \frac{\omega \omega_{pn}^2}{X}\right\}\right]$$

$$= \left(E_0 + E_1 \cos \omega t\right) K^2 k^2 v_s^2 \qquad \text{J14}$$

For collision dominated limit: $\omega \ll v$ and $kv_0 \ll v$.

83

$$\left(\omega^2 - k^2 v_s^2\right)\left[\left(E_0 + E_1\cos\omega t\right) - \frac{\left(E_0 + E_1\cos\omega t\right)}{\left(\omega - kv_0\right)}\left\{\frac{\omega_{pe}^2}{\left[-iv - \frac{Dvk^2}{\left(\omega - kv_0\right)}\right]} + \frac{4\pi}{3}l\frac{\omega\omega_{pn}^2}{X}\right\}\right] = \left(E_0 + E_1\cos\omega t\right)K^2 k^2 v_s^2$$

$$\text{J15}$$

$$\left(\omega^2 - k^2 v_s^2\right)\left[\left(E_0 + E_1\cos\omega t\right) - \left(E_0 + E_1\cos\omega t\right)\left\{\frac{\omega_{pe}^2}{\left[-iv\left(\omega - kv_0\right) - Dvk^2\right]} + \frac{4\pi}{3}l\frac{\omega\omega_{pn}^2}{X\left(\omega - kv_0\right)}\right\}\right]$$

$$= \left(E_0 + E_1\cos\omega t\right)K^2 k^2 v_s^2 \qquad\qquad \text{J16}$$

$$\left(\omega^2 - k^2 v_s^2\right)\left[\left(E_0 + E_1\cos\omega t\right) + \left(E_0 + E_1\cos\omega t\right)\left\{\frac{\omega_{pe}^2}{\left[iv\left(\omega - kv_0 - iDk^2\right)\right]} - \frac{4\pi}{3}l\frac{\omega\omega_{pn}^2}{X\left(\omega - kv_0\right)}\right\}\right]$$

$$= \left(E_0 + E_1\cos\omega t\right)K^2 k^2 v_s^2 \qquad\qquad \text{J17}$$

But

$$\omega_R = \frac{\omega_{pe}^2}{v}$$

$$\left(\omega^2 - k^2 v_s^2\right)\left[\left(E_0 + E_1\cos\omega t\right) + \left(E_0 + E_1\cos\omega t\right)\left\{\frac{\omega_R}{i\left(\omega - kv_0 - iDk^2\right)} - \frac{4\pi}{3}l\frac{\omega\omega_{pn}^2}{X\left(\omega - kv_0\right)}\right\}\right]$$

$$= \left(E_0 + E_1\cos\omega t\right)K^2 k^2 v_s^2 \qquad\qquad \text{J18}$$

Multiplying through equation J18 by $i\left(\omega - kv_0 - iDk^2\right)$

$$\left(\omega^2 - k^2 v_s^2\right)\left[i\left(\omega - kv_0 - iDk^2\right)\left(E_0 + E_1\cos\omega t\right) + \left(E_0 + E_1\cos\omega t\right)\omega_R - \left(E_0 + E_1\cos\omega t\right)i\left(\omega - kv_0 - iDk^2\right)\frac{4\pi}{3}l\frac{\omega\omega_{pn}^2}{X\left(\omega - kv_0\right)}\right]$$

84

$$= i\left(\omega - kv_0 - iDk^2\right)\left(E_0 + E_1\cos\omega t\right)K^2k^2v_s^2 \qquad \text{J19}$$

But

$$v_s = \frac{\omega}{k},$$

and

$$\omega^2 = k^2v_s^2$$

Hence equation J19 becomes:

$$\omega^2\left(1 - \frac{k^2v_s^2}{\omega^2}\right)\left[\left(E_0 + E_1\cos\omega t\right)\omega_R + i\left(\omega - kv_0 - iDk^2\right)\left\{\left(E_0 + E_1\cos\omega t\right) - \left(E_0 + E_1\cos\omega t\right)\frac{4\pi}{3}l\frac{\omega\omega_{pn}^2}{X\left(\omega - kv_0\right)}\right\}\right]$$

$$= i\left(E_0 + E_1\cos\omega t\right)K^2k^2v_s^2\left(\omega - kv_0 - iDk^2\right) \qquad \text{J20}$$

Dividing J20 through by the term in the square bracket gives

$$\left(1 - \frac{k^2v_s^2}{\omega^2}\right) = \frac{i\left(E_0 + E_1\cos\omega t\right)K^2\left(\omega - kv_0 - iDk^2\right)}{\left[\left(E_0 + E_1\cos\omega t\right)\omega_R + i\left(\omega - kv_0 - iDk^2\right)\left\{\left(E_0 + E_1\cos\omega t\right) - \left(E_0 + E_1\cos\omega t\right)\frac{4\pi}{3}l\frac{\omega\omega_{pn}^2}{X\left(\omega - kv_0\right)}\right\}\right]}$$

$$\text{J21}$$

$$\frac{kv_s}{\omega} = 1 + \frac{\frac{1}{2}i\left(E_0 + E_1\cos\omega t\right)K^2\left(\omega - kv_0 - iDk^2\right)}{\left[\left(E_0 + E_1\cos\omega t\right)\omega_R + i\left(\omega - kv_0 - iDk^2\right)\left\{\left(E_0 + E_1\cos\omega t\right) - \left(E_0 + E_1\cos\omega t\right)\frac{4\pi}{3}l\frac{\omega\omega_{pn}^2}{X\left(\omega - kv_0\right)}\right\}\right]}$$

$$\text{J22}$$

85

$$1 + i\alpha = 1 + \frac{\frac{1}{2}i\left(E_0 + E_1 \cos \omega t\right) K^2 \left(kv_0 - \omega + iDk^2\right)}{\left[\left(E_0 + E_1 \cos \omega t\right)\omega_R + i\left(\omega - kv_0 - iDk^2\right)\left\{\left(E_0 + E_1 \cos \omega t\right) - \left(E_0 + E_1 \cos \omega t\right)\frac{4\pi}{3}l\frac{\omega\omega_{pn}^2}{X\left(\omega - kv_0\right)}\right\}\right]}$$

<div align="right">J23</div>

$$\alpha = \frac{\frac{1}{2}\left(E_0 + E_1 \cos \omega t\right) K^2 \omega \left(\frac{kv_0}{\omega} - 1 + \frac{iDk^2}{\omega}\right)}{\left[\left(E_0 + E_1 \cos \omega t\right)\omega_R + i\left(\omega - kv_0 - iDk^2\right)\left\{\left(E_0 + E_1 \cos \omega t\right) + \left(E_0 + E_1 \cos \omega t\right)\frac{4\pi}{3}l\frac{\omega_{pn}^2}{X\left(\frac{kv_0}{\omega} - 1\right)}\right\}\right]}$$

<div align="right">J24</div>

But

$$v_s = \frac{\omega}{k}$$

and

$$\gamma = \frac{v_0}{v_s} - 1$$
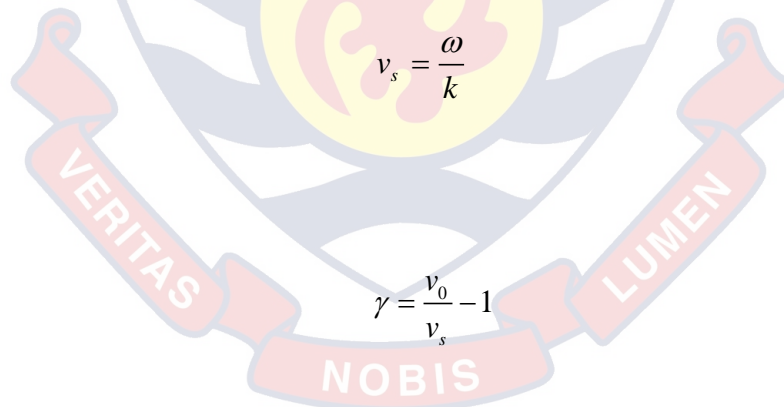
Substituting the above expressions into equation J24 gives

$$\alpha = \frac{\frac{1}{2}\left(E_0 + E_1 \cos \omega t\right) K^2 \omega \left(\gamma + \frac{iDk^2}{\omega}\right)}{\left[\left(E_0 + E_1 \cos \omega t\right)\omega_R + i\left(\omega - kv_0 - iDk^2\right)\left\{\left(E_0 + E_1 \cos \omega t\right) + \left(E_0 + E_1 \cos \omega t\right)\frac{4\pi}{3}l\frac{\omega_{pn}^2}{X\gamma}\right\}\right]}$$

<div align="right">J25</div>

<div align="center">86</div>

Further simplification of equation J25 produces

$$\alpha = \frac{\frac{1}{2}K^2 X \left(\gamma + \frac{iDk^2}{\omega} \right)\left(E_0 + E_1 \cos \omega t \right)}{\left(\frac{\omega_R}{\omega} \right)\left[\left(E_0 + E_1 \cos \omega t \right) X + \frac{\omega^2 \left(E_0 + E_1 \cos \omega t \right)}{\omega_R \omega_D} \left(X + \frac{4\pi}{3} l \frac{\omega_{pn}^2}{\gamma} \right) \right] - }$$

$$\overline{i \left[\left(\gamma \left(E_0 + E_1 \cos \omega t \right) X + \left(E_0 + E_1 \cos \omega t \right) \frac{4\pi}{3} l \omega_{pn}^2 \right) \right]} \qquad \text{J26}$$

Rationalizing the above equation and neglecting all real terms and considering only the coefficient of complex terms gives:

$$\alpha = \frac{\frac{1}{2}K^2 \gamma X^2 \frac{\omega_R}{\omega} \left(E_0 + E_1 \cos \omega t \right)}{\left(\frac{\omega_R}{\omega} \right)^2 \left[\left(E_0 + E_1 \cos \omega t \right) X + \frac{\omega^2 \left(E_0 + E_1 \cos \omega t \right)}{\omega_R \omega_D} \left(X + \frac{4\pi}{3} l \frac{\omega_{pn}^2}{\gamma} \right) \right]^2 + }$$

$$\overline{\left[\left(\gamma \left(E_0 + E_1 \cos \omega t \right) X + \left(E_0 + E_1 \cos \omega t \right) \frac{4\pi}{3} l \omega_{pn}^2 \right) \right]^2} \qquad \text{J27}$$

APPENDIX K

DERIVATION OF THE ACOUSTIC GAIN IN THE PRESENCE OF

COMMENSURATE FIELDS

From equation I3:

$$\varepsilon \vec{E}_Z \left[1 + \frac{\beta^2 k^2}{\varepsilon\left(-\rho\omega^2 + Ck^2\right)} \right] = \frac{\varepsilon \vec{E}_Z}{\left(\omega - kv_0\right)} \left[\frac{\omega_{pe}^2}{F\left(\omega,k\right)} + \frac{4\pi}{3} l \frac{\omega \omega_{pn}^2}{X} \right] \qquad \text{K1}$$

But

$$E_Z = E_1 \cos \omega_1 t + E_2 \cos\left(\omega_2 t + \theta\right)$$

Substituting the above expression into equation K1 and dividing through by ε gives:

$$\left(E_1 \cos \omega_1 t + E_2 \cos\left(\omega_2 t + \theta\right)\right)\left[1 + \frac{\beta^2 k^2}{\varepsilon\left(-\rho\omega^2 + Ck^2\right)} \right] =$$

$$\frac{\left(E_1 \cos \omega_1 t + E_2 \cos\left(\omega_2 t + \theta\right)\right)}{\left(\omega - kv_0\right)} \left[\frac{\omega_{pe}^2}{F\left(\omega,k\right)} + \frac{4\pi}{3} l \frac{\omega \omega_{pn}^2}{X} \right] \qquad \text{K2}$$

$$E_1 \cos \omega_1 t + \frac{E_1 \cos \omega_1 t \beta^2 k^2}{\varepsilon\left(-\rho\omega^2 + Ck^2\right)} + E_2 \cos\left(\omega_2 t + \theta\right) + \frac{E_2 \cos\left(\omega_2 t + \theta\right)\beta^2 k^2}{\varepsilon\left(-\rho\omega^2 + Ck^2\right)} = \frac{\omega_{pe}^2 \left(E_1 \cos \omega_1 t + E_2 \cos\left(\omega_2 t + \theta\right)\right)}{\left(\omega - kv_0\right)F\left(\omega,k\right)} +$$

$$\left(E_1 \cos \omega_1 t + E_2 \cos\left(\omega_2 t + \theta\right)\right)\frac{4\pi}{3} l \frac{\omega \omega_{pn}^2}{\left(\omega - kv_0\right)X} \qquad \text{K3}$$

$$\left(E_1 \cos \omega_1 t + E_2 \cos\left(\omega_2 t + \theta\right)\right) + \frac{\left(E_1 \cos \omega_1 t + E_2 \cos\left(\omega_2 t + \theta\right)\right)\beta^2 k^2}{\varepsilon\left(-\rho\omega^2 + Ck^2\right)} =$$

88

$$\frac{\left(E_1\cos\omega_1 t + E_2\cos\left(\omega_2 t+\theta\right)\right)}{\left(\omega-kv_0\right)}\left[\frac{\omega_{pe}^2}{F\left(\omega,k\right)}+\frac{4\pi}{3}l\frac{\omega\omega_{pn}^2}{X}\right] \qquad \text{K4}$$

$$\left(E_1\cos\omega_1 t + E_2\cos\left(\omega_2 t+\theta\right)\right) - \frac{\left(E_1\cos\omega_1 t + E_2\cos\left(\omega_2 t+\theta\right)\right)}{\left(\omega-kv_0\right)}\left[\frac{\omega_{pe}^2}{F\left(\omega,k\right)}+\frac{4\pi}{3}l\frac{\omega\omega_{pn}^2}{X}\right]=$$

$$-\frac{\left(E_1\cos\omega_1 t + E_2\cos\left(\omega_2 t+\theta\right)\right)\beta^2 k^2}{\varepsilon\left(-\rho\omega^2 + Ck^2\right)} \qquad \text{K5}$$

Multiplying through equation K5 by $\left(\omega^2 - k^2 v_s^2\right)$ gives

$$\left(\omega^2 - k^2 v_s^2\right)\left\{\left(E_1\cos\omega_1 t + E_2\cos\left(\omega_2 t+\theta\right)\right) - \frac{\left(E_1\cos\omega_1 t + E_2\cos\left(\omega_2 t+\theta\right)\right)}{\left(\omega-kv_0\right)}\left[\frac{\omega_{pe}^2}{F\left(\omega,k\right)}+\frac{4\pi}{3}l\frac{\omega\omega_{pn}^2}{X}\right]\right\}$$

$$= -\left(E_1\cos\omega_1 t + E_2\cos\left(\omega_2 t+\theta\right)\right)\left[\frac{\beta^2 k^2}{\varepsilon\left(-\rho\omega^2 + Ck^2\right)}\right]\left(\omega^2 - k^2 v_s^2\right) \qquad \text{K6}$$

$$\left(\omega^2 - k^2 v_s^2\right)\left\{\left(E_1\cos\omega_1 t + E_2\cos\left(\omega_2 t+\theta\right)\right) - \frac{\left(E_1\cos\omega_1 t + E_2\cos\left(\omega_2 t+\theta\right)\right)}{\left(\omega-kv_0\right)}\left[\frac{\omega_{pe}^2}{F\left(\omega,k\right)}+\frac{4\pi}{3}l\frac{\omega\omega_{pn}^2}{X}\right]\right\}=-$$

$$\left(E_1\cos\omega_1 t + E_2\cos\left(\omega_2 t+\theta\right)\right)\frac{\beta^2}{C\varepsilon}\left[\frac{k^2}{\left(\frac{-\rho}{C}\omega^2 + k^2\right)}\right]\left(\omega^2 - k^2 v_s^2\right) \qquad \text{K7}$$

$$\left(\omega^2 - k^2 v_s^2\right)\left\{\left(E_1\cos\omega_1 t + E_2\cos\left(\omega_2 t+\theta\right)\right) - \frac{\left(E_1\cos\omega_1 t + E_2\cos\left(\omega_2 t+\theta\right)\right)}{\left(\omega-kv_0\right)}\left[\frac{\omega_{pe}^2}{F\left(\omega,k\right)}+\frac{4\pi}{3}l\frac{\omega\omega_{pn}^2}{X}\right]\right\}=-$$

$$\left(E_1\cos\omega_1 t + E_2\cos\left(\omega_2 t+\theta\right)\right)K^2\left[\frac{k^2}{\left(\frac{-1}{v_s^2}\omega^2 + k^2\right)}\right]\left(\omega^2 - k^2 v_s^2\right) \qquad \text{K8}$$

$$\left(\omega^2 - k^2 v_s^2\right)\left\{\left(E_1 \cos \omega_1 t + E_2 \cos\left(\omega_2 t + \theta\right)\right) - \frac{\left(E_1 \cos \omega_1 t + E_2 \cos\left(\omega_2 t + \theta\right)\right)}{\left(\omega - kv_0\right)}\left[\frac{\omega_{pe}^2}{F\left(\omega,k\right)} + \frac{4\pi}{3} l \frac{\omega \omega_{pn}^2}{X}\right]\right\} = -$$

$$\left(E_1 \cos \omega_1 t + E_2 \cos\left(\omega_2 t + \theta\right)\right) K^2 \left[\frac{k^2}{\frac{-1}{v_s^2}\left(\omega^2 - k^2 v_s^2\right)}\right]\left(\omega^2 - k^2 v_s^2\right) \qquad \text{K9}$$

$$\left(\omega^2 - k^2 v_s^2\right)\left\{\left(E_1 \cos \omega_1 t + E_2 \cos\left(\omega_2 t + \theta\right)\right) - \frac{\left(E_1 \cos \omega_1 t + E_2 \cos\left(\omega_2 t + \theta\right)\right)}{\left(\omega - kv_0\right)}\left[\frac{\omega_{pe}^2}{F\left(\omega,k\right)} + \frac{4\pi}{3} l \frac{\omega \omega_{pn}^2}{X}\right]\right\} =$$

$$\left(E_1 \cos \omega_1 t + E_2 \cos\left(\omega_2 t + \theta\right)\right) K^2 k^2 v_s^2 \qquad \text{K10}$$

For no piezoelectricity, $\beta = 0$ and $K = 0$.

$$\left(\omega^2 - k^2 v_s^2\right)\left\{\left(E_1 \cos \omega_1 t + E_2 \cos\left(\omega_2 t + \theta\right)\right) - \frac{\left(E_1 \cos \omega_1 t + E_2 \cos\left(\omega_2 t + \theta\right)\right)}{\left(\omega - kv_0\right)}\left[\frac{\omega_{pe}^2}{F\left(\omega,k\right)} + \frac{4\pi}{3} l \frac{\omega \omega_{pn}^2}{X}\right]\right\} = 0$$

$$\text{K11}$$

$$\left(\omega^2 - k^2 v_s^2\right) = 0 \qquad \text{K12}$$

and

$$\left\{\left(E_1 \cos \omega_1 t + E_2 \cos\left(\omega_2 t + \theta\right)\right) - \frac{\left(E_1 \cos \omega_1 t + E_2 \cos\left(\omega_2 t + \theta\right)\right)}{\left(\omega - kv_0\right)}\left[\frac{\omega_{pe}^2}{F\left(\omega,k\right)} + \frac{4\pi}{3} l \frac{\omega \omega_{pn}^2}{X}\right]\right\} = 0$$

$$\text{K13}$$

But

90

$$F(\omega,k)=\left[\omega-kv_0-iv-\frac{Dvk^2}{(\omega-kv_0)}\right].$$

$$\left(\omega^2-k^2v_s^2\right)\left\{\left(E_1\cos\omega_1 t+E_2\cos(\omega_2 t+\theta)\right)-\frac{\left(E_1\cos\omega_1 t+E_2\cos(\omega_2 t+\theta)\right)}{(\omega-kv_0)}\right.$$

$$\left.\left[\frac{\omega_{pe}^2}{\left[\omega-kv_0-iv-\dfrac{Dvk^2}{(\omega-kv_0)}\right]}+\frac{4\pi}{3}l\frac{\omega\omega_{pn}^2}{X}\right]\right\}=\left(E_1\cos\omega_1 t+E_2\cos(\omega_2 t+\theta)\right)K^2k^2v_s^2 \qquad \text{K14}$$

For collision dominated limit: $\omega\ll v$ and $kv_0\ll v$

$$\left(\omega^2-k^2v_s^2\right)\left\{\left(E_1\cos\omega_1 t+E_2\cos(\omega_2 t+\theta)\right)-\frac{\left(E_1\cos\omega_1 t+E_2\cos(\omega_2 t+\theta)\right)}{(\omega-kv_0)}\left[\frac{\omega_{pe}^2}{\left[-iv-\dfrac{Dvk^2}{(\omega-kv_0)}\right]}+\frac{4\pi}{3}l\frac{\omega\omega_{pn}^2}{X}\right]\right\}$$

$$=\left(E_1\cos\omega_1 t+E_2\cos(\omega_2 t+\theta)\right)K^2k^2v_s^2 \qquad \text{K15}$$

$$\left(\omega^2-k^2v_s^2\right)\left\{\left(E_1\cos\omega_1 t+E_2\cos(\omega_2 t+\theta)\right)-\right.$$

$$\left(E_1\cos\omega_1 t+E_2\cos(\omega_2 t+\theta)\right)\left[\frac{\omega_{pe}^2}{\left[-iv(\omega-kv_0)-Dvk^2\right]}+\frac{4\pi}{3}l\frac{\omega\omega_{pn}^2}{X(\omega-kv_0)}\right]\right\}=$$

$$\left(E_1\cos\omega_1 t+E_2\cos(\omega_2 t+\theta)\right)K^2k^2v_s^2 \qquad \text{K16}$$
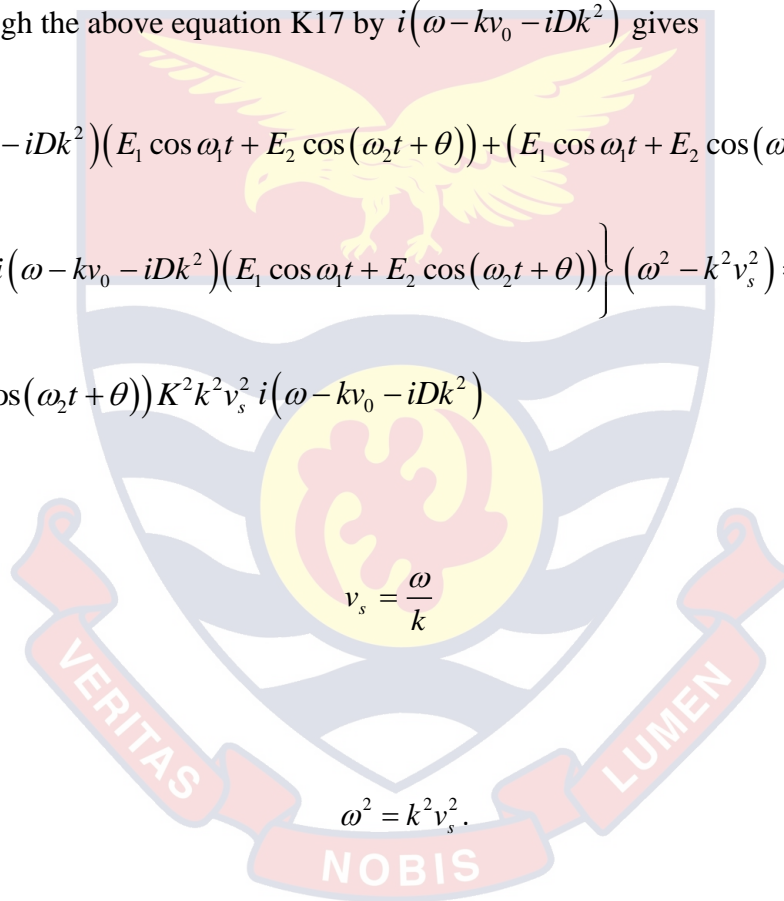
But

$$\omega_R=\frac{\omega_{pe}^2}{v}$$

91

$$\left(\omega^2 - k^2 v_s^2\right)\left\{\left(E_1\cos\omega_1 t + E_2\cos\left(\omega_2 t + \theta\right)\right)+\right.$$

$$\left(E_1\cos\omega_1 t + E_2\cos\left(\omega_2 t + \theta\right)\right)\left[\frac{\omega_R}{\left[i\left(\omega - kv_0 - iDk^2\right)-Dvk^2\right]}-\frac{4\pi}{3}l\frac{\omega\omega_{pn}^2}{X\left(\omega - kv_0\right)}\right]\right\}=$$

$$\left(E_1\cos\omega_1 t + E_2\cos\left(\omega_2 t + \theta\right)\right)K^2 k^2 v_s^2 \qquad\qquad \text{K17}$$

Multiplying through the above equation K17 by $i\left(\omega - kv_0 - iDk^2\right)$ gives

$$\left\{i\left(\omega - kv_0 - iDk^2\right)\left(E_1\cos\omega_1 t + E_2\cos\left(\omega_2 t + \theta\right)\right)+\left(E_1\cos\omega_1 t + E_2\cos\left(\omega_2 t + \theta\right)\right)\omega_R -\right.$$

$$\frac{4\pi}{3}l\frac{\omega\omega_{pn}^2}{X\left(\omega - kv_0\right)}i\left(\omega - kv_0 - iDk^2\right)\left(E_1\cos\omega_1 t + E_2\cos\left(\omega_2 t + \theta\right)\right)\right\}\left(\omega^2 - k^2 v_s^2\right)=$$

$$\left(E_1\cos\omega_1 t + E_2\cos\left(\omega_2 t + \theta\right)\right)K^2 k^2 v_s^2\, i\left(\omega - kv_0 - iDk^2\right) \qquad\qquad \text{K18}$$

But

$$v_s = \frac{\omega}{k}$$

and

$$\omega^2 = k^2 v_s^2.$$

$$\left\{\left(E_1\cos\omega_1 t + E_2\cos\left(\omega_2 t + \theta\right)\right)\omega_R + i\left(\omega - kv_0 - iDk^2\right)\left[\left(E_1\cos\omega_1 t + E_2\cos\left(\omega_2 t + \theta\right)\right)\right.\right.$$

$$\left.\left.-\left(E_1\cos\omega_1 t + E_2\cos\left(\omega_2 t + \theta\right)\right)\frac{4\pi}{3}l\frac{\omega\omega_{pn}^2}{X\left(\omega - kv_0\right)}\right]\right\}\omega^2\left(1 - \frac{k^2 v_s^2}{\omega^2}\right)=$$

$$\left(E_1\cos\omega_1 t + E_2\cos\left(\omega_2 t + \theta\right)\right)K^2 k^2 v_s^2\, i\left(\omega - kv_0 - iDk^2\right) \qquad\qquad \text{K19}$$

Dividing K19 by the first term in the left-hand side parenthesis gives

92

$$\left(1-\frac{k^2 v_s^2}{\omega^2}\right) = \frac{\left(E_1 \cos \omega_1 t + E_2 \cos(\omega_2 t + \theta)\right) iK^2 \left(\omega - kv_0 - iDk^2\right)}{\left\{\left(E_1 \cos \omega_1 t + E_2 \cos(\omega_2 t + \theta)\right)\omega_R + i\left(\omega - kv_0 - iDk^2\right)\times}$$

$$\overline{\left[\left(E_1 \cos \omega_1 t + E_2 \cos(\omega_2 t + \theta)\right) - \left(E_1 \cos \omega_1 t + E_2 \cos(\omega_2 t + \theta)\right)\frac{4\pi}{3}l\frac{\omega \omega_{pn}^2}{X(\omega - kv_0)}\right]\right\}} \qquad \text{K20}$$

$$\frac{kv_s}{\omega} = 1 + \frac{\frac{1}{2}\left(E_1 \cos \omega_1 t + E_2 \cos(\omega_2 t + \theta)\right) iK^2 \left(kv_0 - \omega + iDk^2\right)}{\left\{\left(E_1 \cos \omega_1 t + E_2 \cos(\omega_2 t + \theta)\right)\omega_R + i\left(\omega - kv_0 - iDk^2\right)\times}$$

$$\overline{\left[\left(E_1 \cos \omega_1 t + E_2 \cos(\omega_2 t + \theta)\right) - \left(E_1 \cos \omega_1 t + E_2 \cos(\omega_2 t + \theta)\right)\frac{4\pi}{3}l\frac{\omega \omega_{pn}^2}{X(\omega - kv_0)}\right]\right\}} \qquad \text{K21}$$

But

$$\frac{kv_s}{\omega} = 1 + i\alpha \, .$$

$$1 + i\alpha = 1 + \frac{\frac{1}{2}\left(E_1 \cos \omega_1 t + E_2 \cos(\omega_2 t + \theta)\right) iK^2 \left(kv_0 - \omega + iDk^2\right)}{\left\{\left(E_1 \cos \omega_1 t + E_2 \cos(\omega_2 t + \theta)\right)\omega_R + i\left(\omega - kv_0 - iDk^2\right)\times}$$

$$\overline{\left[\left(E_1 \cos \omega_1 t + E_2 \cos(\omega_2 t + \theta)\right) - \left(E_1 \cos \omega_1 t + E_2 \cos(\omega_2 t + \theta)\right)\frac{4\pi}{3}l\frac{\omega \omega_{pn}^2}{X(\omega - kv_0)}\right]\right\}} \qquad \text{K22}$$

$$i\alpha = \frac{\frac{1}{2}\left(E_1 \cos \omega_1 t + E_2 \cos(\omega_2 t + \theta)\right) iK^2 \left(kv_0 - \omega + iDk^2\right)}{\left\{\left(E_1 \cos \omega_1 t + E_2 \cos(\omega_2 t + \theta)\right)\omega_R + i\left(\omega - kv_0 - iDk^2\right)\times}$$

$$\overline{\left[\left(E_1 \cos \omega_1 t + E_2 \cos(\omega_2 t + \theta)\right) + \left(E_1 \cos \omega_1 t + E_2 \cos(\omega_2 t + \theta)\right)\frac{4\pi}{3}l\frac{\omega_{pn}^2}{X\left(\frac{kv_0}{\omega} - 1\right)}\right]\right\}} \qquad \text{K23}$$

93

But

$$v_s = \frac{\omega}{k}$$

and

$$\gamma = \frac{v_0}{v_s} - 1.$$

$$\alpha = \frac{\frac{1}{2}\left(E_1 \cos \omega_1 t + E_2 \cos(\omega_2 t + \theta)\right) K^2 \omega \left(\frac{kv_0}{\omega} - 1 + \frac{iDk^2}{\omega}\right)}{\left\{\left(E_1 \cos \omega_1 t + E_2 \cos(\omega_2 t + \theta)\right)\omega_R + i\left(\omega - kv_0 - iDk^2\right)\times \right.}$$

$$\overline{\left[\left(E_1 \cos \omega_1 t + E_2 \cos(\omega_2 t + \theta)\right) + \left(E_1 \cos \omega_1 t + E_2 \cos(\omega_2 t + \theta)\right)\frac{4\pi}{3}l\frac{\omega_{pn}^2}{X\gamma}\right]\right\}} \qquad \text{K24}$$

Further simplification of equation K24 produces

$$\alpha = \frac{\frac{1}{2}\left(E_1 \cos \omega_1 t + E_2 \cos(\omega_2 t + \theta)\right) K^2 X \left(\gamma + \frac{iDk^2}{\omega}\right)}{\left(\frac{\omega_R}{\omega}\right)\left\{\left(E_1 \cos \omega_1 t + E_2 \cos(\omega_2 t + \theta)\right)X + \frac{\omega^2\left(E_1 \cos \omega_1 t + E_2 \cos(\omega_2 t + \theta)\right)}{\omega_R \omega_D}\left(X + \frac{4\pi}{3}l\frac{\omega_{pn}^2}{\gamma}\right)\right\} - }$$

$$\overline{\left\{i\left[\left(E_1 \cos \omega_1 t + E_2 \cos(\omega_2 t + \theta)\right)\frac{4\pi}{3}l\omega_{pn}^2 + \gamma\left(E_1 \cos \omega_1 t + E_2 \cos(\omega_2 t + \theta)\right)X\right]\right\}}$$

K25

Rationalizing the above equation and neglecting all real terms and considering only the coefficient of complex terms gives:

$$\alpha = \cfrac{\dfrac{1}{2}K^2\gamma X^2 \dfrac{\omega_R}{\omega}\left(E_1\cos\omega_1 t + E_2\cos(\omega_2 t + \theta)\right)}{\left(\dfrac{\omega_R}{\omega}\right)^2\left[\left(E_1\cos\omega_1 t + E_2\cos(\omega_2 t + \theta)\right)X + \dfrac{\omega^2\left(E_1\cos\omega_1 t + E_2\cos(\omega_2 t + \theta)\right)}{\omega_R\omega_D}\left(X + \dfrac{4\pi}{3}l\dfrac{\omega_{pn}^2}{\gamma}\right)\right]^2 \times}$$

$$\overline{\left[\left(E_1\cos\omega_1 t + E_2\cos(\omega_2 t + \theta)\right)\dfrac{4\pi}{3}l\omega_{pn}^2 + \gamma\left(E_1\cos\omega_1 t + E_2\cos(\omega_2 t + \theta)\right)X\right]^2}$$

K26

95

APPENDIX L

CODES FOR FIGURES

1. Interaction in the presence of combined dc-ac fields

The following are the MATLAB codes for CdS.The same codes were also used for MoS$_2$ but with different physical parameters(density=p,piezoelectric constant=B,effective mass=m,electron mobility=n)and field constants(amplitude of a dc field=s1, amplitude of an ac field=s2)as p=5060,B=0.0156,m=0.16185*9.11e-31,n=0.041,s1=1 and s2=0.5.

(i) Variation of acoustic gain with velocity ratio

```
close all
x=0.5:0.5:3.0; % x represents velocity ratio
T=300;          % T represents absolute temperature
e=9.35*8.85e-12;% e represents relative permitivity
ec=1.602e-19;   % ec is the electric charge
KB=1.38e-23;    % KB is the boltzman constant
m=0.17*9.11e-31; % m is the effective mass of the piezoelectric material
p=4820;         % p is the density
B=0.21;         % B is the piezoelectric constant
n=0.035;        % n is the electron mobility
l=0.000;   % l is the dimensionless physical parameter of nanoparticle
cluster
s1=1;           % s1 is the amplitude of the dc field
s2=0.5;         % s2 is the amplitude of the ac field
w1=3e12;        % w1 is the wave frequency of the ac field
t=2;            % t is the time
w=5e12;         % w is the wave frequency
C=24.1e9;       % C is the elastic stiffness constant
Vs=sqrt(C./p);  % Vs is the velocity of sound
K=sqrt((B.^2)./(C.*e)); % K is the non-dimensional electromechanical
coupling coefficient
Noe=1e26;           % Noe is the carrier density
Non=1e26;           % Non is the electron density
Wpe=sqrt((Noe.*(ec).^2)./(m.*e)); % Wpe is the electron plasma frequency
Wpn=sqrt((Non*(ec).^2)./(m.*e));   % Wpe is the electron plasma frequency
X=((w.^2)-((Wpn.^2)./3));          % X represents the effect of a
nanoparticle on acoustic gain as it contains the plasma frequency of
electron cloud of nanoparticle.
D=(n.*KB.*T)./ec;               % D is the diffusion coefficient
f=ec./(m*n);                    % f is the momentum transfer collision
frequency
wD=(Vs.^2)./D;                  % WD is the diffusion frequency
wR=(Wpe.^2)./f;                 % WR is the relaxation frequency
%y1=0.5.*(K^2).*(x-1).*(X.^2).*(wR./w).*(s1+s2.*cos(w1.*t));
%y2=((wR./w).^2);
%y3=((w.^2).*(s1+s2.*cos(w1.*t))./(wD.*wR));
%y4=(X+(4.*pi.*l.*(Wpn.^2))./(3.*(x-1)));
%y5=(y3).*(y4);
%y6=((s1+s2.*cos(w1.*t)).*X)+(y5);
%y7=(y2).*((y6).^2);
```

96

```matlab
%y8=(X.*(s1+s2.*cos(w1.*t))).*(x-
1))+((s1+s2.*cos(w1.*t)).*4.*pi.*l.*(Wpn.^2)./3).^2;
%y9=(y7)+(y8);
y=(y1)./(y9);
plot(x,(y.*10^6),'g');
hold on
hold on
x=0.5:0.5:3.0;
T=300;
e=9.35.*8.85e-12;
ec=1.602e-19;
KB=1.38e-23;
m=0.17*9.11e-31;
p=4820;
B=0.21;
n=0.035;
s1=1;
s2=0.5;
w1=3e12;
t=2;
l=0.001;
w=5e12;
C=24.1e9;
Vs=sqrt(C./p);
K=sqrt((B.^2)./(C.*e));
Non=1e26;
Noe=1e26;
Wpe=sqrt((Noe.*(ec).^2)./(m.*e));
Wpn=sqrt((Non*(ec).^2)./(m.*e));
X=((w.^2)-((Wpn.^2)./3));
D=(n.*KB.*T)./ec;
f=ec./(m*n);
wD=(Vs.^2)./D;
wR=(Wpe.^2)./f;
%y1=0.5.*(K^2).*(x-1).*(X.^2).*(wR./w).*(s1+s2.*cos(w1.*t));
%y2=((wR./w).^2);
%y3=((w.^2).*(s1+s2.*cos(w1.*t))./(wD.*wR));
%y4=(X+(4.*pi.*l.*(Wpn.^2))./(3.*(x-1)));
%y5=(y3).*(y4);
%y6=((s1+s2.*cos(w1.*t)).*X)+(y5);
%y7=(y2).*((y6).^2);
%y8=(X.*(s1+s2.*cos(w1.*t))).*(x-
1))+((s1+s2.*cos(w1.*t)).*4.*pi.*l.*(Wpn.^2)./3).^2;
%y9=(y7)+(y8);
y=(y1)./(y9);
plot(x,(y.*10^6),'--b');
hold on
x=0.5:0.5:3.0;
T=300;
e=9.35.*8.85e-12;
ec=1.602e-19;
KB=1.38e-23;
m=0.17*9.11e-31;
p=4820;
B=0.21;
n=0.035;
s1=1;
```

97

```
s2=0.5;
w1=3e12;
t=2;
l=0.008;
w=5e12;
C=24.1e9;
Vs=sqrt(C./p);
K=sqrt((B.^2)./(C.*e));
Non=1e26;
Noe=1e26;
Wpe=sqrt((Noe.*(ec).^2)./(m.*e));
Wpn=sqrt((Non*(ec).^2)./(m.*e));
X=((w.^2)-((Wpn.^2)./3));
D=(n.*KB.*T)./ec;
f=ec./(m*n);
wD=(Vs.^2)./D;
wR=(Wpe.^2)./f;
%y1=0.5.*(K^2).*(x-1).*(X.^2).*(wR./w).*(s1+s2.*cos(w1.*t));
%y2=((wR./w).^2);
%y3=((w.^2)./(wD.*wR));
%y4=(X+(4.*pi.*l.*(Wpn.^2))./(3.*(x-1)));
%y5=(y3).*(y4);
%y6=X+(y5);
%y7=(y2).*((y6).^2);
%y8=(X.*(s1+s2.*cos(w1.*t)).*(x-
1))+((s1+s2.*cos(w1.*t)).*4.*pi.*l.*(Wpn.^2)./3).^2;
%y9=(y7)+(y8);
y=(y1)./(y9);
plot(x,(y.*10^6),'-.r');
set(findall(gca, 'Type', 'Line'),'LineWidth',1.5);
legend('0.000','0.001','0.008');
grid on
xlabel('Vo/Vs');
ylabel('\alpha(10^{-6})');
```

(ii) Variation of acoustic gain per unit length with wave frequency

```
close all
x=0e12:0.5e12:40e12;
T=300;
e=9.35.*8.85e-12;
ec=1.602e-19;
KB=1.38e-23;
m=0.17*9.11e-31;
p=4820;
B=0.21;
n=0.035;
s1=1;
s2=0.5;
w1=3e12;
t=2;
l=0.000;
C=24.1e9;
j=0.25; % j is a term expressed interms of velocity ratio
Vs=sqrt(C/p);
K=sqrt((B.^2)./(C.*e));
```

98

```
Non=1e26;
Noe=1e26;
Wpe=sqrt((Noe.*(ec).^2)./(m.*e));
Wpn=sqrt((Non*(ec).^2)./(m.*e));
X=((x.^2)-((Wpn.^2)./3));
D=(n.*KB.*T)./ec;
f=ec./(m*n);
wD=(Vs.^2)./D;
wR=(Wpe.^2)./f;
%y1=(0.5.*(K^2).*(j).*(X.^2).*(wR./x).*(s1+s2.*cos(w1.*t)));
%y2=((wR./x).^2);
%y3=((x.^2).*(s1+s2.*cos(w1.*t))./(wD.*wR));
%y4=(X+(4.*pi.*l.*(Wpn.^2))./(3.*(j)));
%y5=(y3).*(y4);
%y6=((s1+s2.*cos(w1.*t)).*X)+(y5);
%y7=(y2).*((y6).^2);
%y8=(X.*(s1+s2.*cos(w1.*t)).*j)+((s1+s2.*cos(w1.*t)).*4.*pi.*l.*(Wpn.^2)./
3).^2;
%y9=(y7)+(y8);
%y10=(y1)./(y9);
y=((y10.*x)./Vs);
plot((x.*10.^-12),(y.*10.^-3),'g');
hold on
x=0e12:0.5e12:40e12;
T=300;
E=9.35.*8.85e-12;
e=1.602e-19;
k=1.38e-23;
m=0.17*9.11e-31;
p=4820;
B=0.21;
n=0.035;
s1=1;
s2=0.5;
w1=3e12;
t=2;
l=0.001;
C=24.1e9;
Vs=sqrt(C./p);
j=0.25;
K=sqrt((B.^2)./(C.*E));
Non=1e26;
Noe=1e26;
Wpe=sqrt((Noe*(e).^2)/(m.*E));
Wpn=sqrt((Non*(e).^2)/(m.*E));
X=((x.^2)-((Wpn.^2)/3));
D=(n*k*T)/e;
f=e/(m*n);
wD=(Vs^2)/D;
wR=(Wpe^2)/f;
%y1=(0.5*(K^2)*(j)*(X.^2).*(wR./x).*(s1+s2.*cos(w1.*t)));
%y2=((wR./x).^2);
%y3=((x.^2).*(s1+s2.*cos(w1.*t))./(wD.*wR));
%y4=(X+(4*pi*l*(Wpn^2))/(3*(j)));
%y5=(y3).*(y4);
%y6=((s1+s2.*cos(w1.*t)).*X)+(y5);
%y7=(y2).*((y6).^2);
```

99

```
%y8=(X.*(s1+s2.*cos(w1.*t)).*j)+((s1+s2.*cos(w1.*t)).*4.*pi.*l.*(Wpn.^2)./
3).^2;
%y9=(y7)+(y8);
%y10=(y1)./(y9);
y=((y10.*x)./Vs);
plot((x.*10.^-12),(y.*10.^-3),'--b');
hold on
x=0e12:0.5e12:40e12;
T=300;
e=9.35.*8.85e-12;
ec=1.602e-19;
KB=1.38e-23;
m=0.17*9.11e-31;
p=4820;
B=0.21;
n=0.035;
s1=1;
s2=0.5;
w1=3e12;
t=2;
l=0.008;
C=24.1e9;
j=0.25;
Vs=sqrt(C/p);
K=sqrt((B.^2)./(C.*e));
Non=1e26;
Noe=1e26;
Wpe=sqrt((Noe.*(ec).^2)./(m.*e));
Wpn=sqrt((Non*(ec).^2)./(m.*e));
X=((x.^2)-((Wpn.^2)./3));
D=(n.*KB.*T)./ec;
f=ec./(m*n);
wD=(Vs.^2)./D;
wR=(Wpe.^2)./f;
%y1=(0.5.*(K^2).*(j).*(X.^2).*(wR./x).*(s1+s2.*cos(w1.*t)));
%y2=((wR./x).^2);
%y3=((x.^2).*(s1+s2.*cos(w1.*t))./(wD.*wR));
%y4=(X+(4.*pi.*l.*(Wpn.^2))./(3.*(j)));
%y5=(y3).*(y4);
%y6=((s1+s2.*cos(w1.*t)).*X)+(y5);
%y7=(y2).*((y6).^2);
%y8=(X.*(s1+s2.*cos(w1.*t)).*j)+((s1+s2.*cos(w1.*t)).*4.*pi.*l.*(Wpn.^2)./
3).^2;
%y9=(y7)+(y8);
%y10=(y1)./(y9);
y=((y10.*x)./Vs);
plot((x.*10.^-12),(y.*10.^-3),'-.r');
set(findall(gca, 'Type', 'Line'),'LineWidth',1.5);
legend('0.000','0.001','0.008');
xlabel('\omega(10^{12}s^{-1})')
ylabel('\alpha\omega/v_s(10^{3})')
```

(iii) Variation of acoustic gain with carrier density

```
clc, clear all, close all
x=0e25:0.05e25:40e25;
T=300;
```

```
e=9.35.*8.85e-12;
ec=1.602e-19;
KB=1.38e-23;
m=0.17*9.11e-31;
p=4820;
B=0.21;
n=0.035;
s1=1;
s2=0.5;
w1=3e12;
t=2;
l=0.000;
w=5e12;
C=24.1e9;
Vs=sqrt(C./p);
j=0.25;
K=sqrt((B.^2)./(C.*e));
Non=1e26;
Wpe=sqrt((x.*(ec).^2)./(m.*e));
Wpn=sqrt((Non*(ec).^2)./(m.*e));
X=((w.^2)-((Wpn.^2)./3));
D=(n.*KB.*T)./ec;
f=ec./(m*n);
wD=(Vs.^2)./D;
wR=(Wpe.^2)./f;
%y1=(0.5.*(K^2).*(j).*(X.^2).*(wR./w).*(s1+s2.*cos(w1.*t)));
%y2=((wR./w).^2);
%y3=((w.^2).*(s1+s2.*cos(w1.*t))./(wD.*wR));
%y4=(X+(4.*pi.*l.*(Wpn.^2))./(3.*(j)));
%y5=(y3).*(y4);
%y6=((s1+s2.*cos(w1.*t)).*X)+(y5);
%y7=(y2).*((y6).^2);
%y8=(X.*(s1+s2.*cos(w1.*t)).*j)+((s1+s2.*cos(w1.*t)).*4.*pi.*l.*(Wpn.^2)./
3).^2;
%y9=(y7)+(y8);
y=(y1)./(y9);
plot((x.*10^-25),(y*10^6),'g');
hold on
x=0e25:0.05e25:40e25;
T=300;
e=9.35.*8.85e-12;
ec=1.602e-19;
KB=1.38e-23;
m=0.17*9.11e-31;
p=4820;
B=0.21;
n=0.035;
s1=1;
s2=0.5;
w1=3e12;
t=2;
l=0.001;
w=5e12;
C=24.1e9;
Vs=sqrt(C./p);
j=0.25;
K=sqrt((B.^2)./(C.*e));
```

101

```
Non=1e26;
Wpe=sqrt((x.*(ec).^2)./(m.*e));
Wpn=sqrt((Non*(ec).^2)./(m.*e));
X=((w.^2)-((Wpn.^2)./3));
D=(n.*KB.*T)./ec;
f=ec./(m*n);
wD=(Vs.^2)./D;
wR=(Wpe.^2)./f;
%y1=(0.5.*(K^2).*(j).*(X.^2).*(wR./w).*(s1+s2.*cos(w1.*t)));
%y2=((wR./w).^2);
%y3=((w.^2).*(s1+s2.*cos(w1.*t))./(wD.*wR));
%y4=(X+(4.*pi.*l.*(Wpn.^2))./(3.*(j)));
%y5=(y3).*(y4);
%y6=((s1+s2.*cos(w1.*t)).*X)+(y5);
%y7=(y2).*((y6).^2);
%y8=(X.*(s1+s2.*cos(w1.*t)).*j)+((s1+s2.*cos(w1.*t)).*4.*pi.*l.*(Wpn.^2)./
3).^2;
%y9=(y7)+(y8);
y=(y1)./(y9);
plot((x.*10^-25),(y*10^6),'--b');
hold on
x=0e25:0.05e25:40e25;
T=300;
e=9.35.*8.85e-12;
ec=1.602e-19;
KB=1.38e-23;
m=0.17*9.11e-31;
p=4820;
B=0.21;
n=0.035;
s1=1;
s2=0.5;
w1=3e12;
t=2;
l=0.008;
w=5e12;
C=24.1e9;
Vs=sqrt(C./p);
j=0.25;
K=sqrt((B.^2)./(C.*e));
Non=1e26;
Wpe=sqrt((x.*(ec).^2)./(m.*e));
Wpn=sqrt((Non*(ec).^2)./(m.*e));
X=((w.^2)-((Wpn.^2)./3));
D=(n.*KB.*T)./ec;
f=ec./(m*n);
wD=(Vs.^2)./D;
wR=(Wpe.^2)./f;
%y1=(0.5.*(K^2).*(j).*(X.^2).*(wR./w).*(s1+s2.*cos(w1.*t)));
%y2=((wR./w).^2);
%y3=((w.^2).*(s1+s2.*cos(w1.*t))./(wD.*wR));
%y4=(X+(4.*pi.*l.*(Wpn.^2))./(3.*(j)));
%y5=(y3).*(y4);
%y6=((s1+s2.*cos(w1.*t)).*X)+(y5);
%y7=(y2).*((y6).^2);
%y8=(X.*(s1+s2.*cos(w1.*t)).*j)+((s1+s2.*cos(w1.*t)).*4.*pi.*l.*(Wpn.^2)./
3).^2;
```

```
%y9=(y7)+(y8);
y=(y1)./(y9);
plot((x.*10^-25),(y*10^6),'-.r');
set(findall(gca, 'Type', 'Line'),'LineWidth',1.5);
legend('0.000','0.001','0.008');
grid on
xlabel('n_{0e}(10^{25}m^{-3})');
ylabel('\alpha(10^{-6})');
```

2. Interaction in the presence of commensurate fields

```
The following are the MATLAB codes for CdS.The same codes were also used
for MoS2 but with different physical parameters(density=p,piezoelectric
constant=B,effective mass=m,electron mobility=n)and field constants(
amplitude of a dc field=s1, amplitude of an ac field=s2)as
p=5060,B=0.0156,m=0.16185*9.11e-31,n=0.041,s1=1 and s2=1.
```

(i) Variation of acoustic gain with velocity ratio
```
close all
x=0.5:0.5:3.0;
T=300;
e=9.35*8.85e-12;
ec=1.602e-19;
KB=1.38e-23;
m=0.17*9.11e-31;
p=4820;
B=0.21;
n=0.035;
s1=1;
s2=1;
w1=3e12;  % w1 is a commensurate frequency
w2=6e12;  % w2 is also a commensurate frequency
l=0.000;
d=2;
t=2;
w=5e12;
C=24.1e9;
Vs=sqrt(C./p);
K=sqrt((B.^2)./(C.*e));
Noe=1e26;
Non=1e26;
Wpe=sqrt((Noe.*(ec).^2)./(m.*e));
Wpn=sqrt((Non*(ec).^2)./(m.*e));
X=((w.^2)-((Wpn.^2)./3));
D=(n.*KB.*T)./ec;
f=ec./(m*n);
wD=(Vs.^2)./D;
wR=(Wpe.^2)./f;
%y1=(0.5.*(K^2).*(x-
1).*(X.^2).*(wR./w).*(s1.*cos(w1.*t)+s2.*cos(w2.*t+d)));
%y2=((wR./w).^2);
%y3=((w.^2).*(s1.*cos(w1.*t)+s2.*cos(w2.*t+d))./(wD.*wR));
%y4=(X+(4.*pi.*l.*(Wpn.^2))./(3.*(x-1)));
%y5=(y3).*(y4);
```

103

```
%y6=((s1.*cos(w1.*t)+s2.*cos(w2.*t+d)).*X)+(y5);
%y7=(y2).*((y6).^2);
%y8=(X.*(s1.*cos(w1.*t)+s2.*cos(w2.*t+d)).*(x-
1))+((s1.*cos(w1.*t)+s2.*cos(w2.*t+d)).*4.*pi.*l.*(Wpn.^2)./3).^2;
%y9=(y7)+(y8);
y=(y1)./(y9);
plot(x,(y*10^7),'g');
hold on
hold on
x=0.5:0.5:3.0;
T=300;
e=9.35.*8.85e-12;
ec=1.602e-19;
KB=1.38e-23;
m=0.17*9.11e-31;
p=4820;
B=0.21;
n=0.035;
s1=1;   % s1 represents the amplitude of first commensurate field
s2=1;   % s2 represents the amplitude of the second commensurate field
w1=3e12;
w2=6e12;
d=2;
t=2;
l=0.001;
w=5e12;
C=24.1e9;
Vs=sqrt(C./p);
K=sqrt((B.^2)./(C.*e));
Non=1e26;
Noe=1e26;
Wpe=sqrt((Noe.*(ec).^2)./(m.*e));
Wpn=sqrt((Non*(ec).^2)./(m.*e));
X=((w.^2)-((Wpn.^2)./3));
D=(n.*KB.*T)./ec;
f=ec./(m*n);
wD=(Vs.^2)./D;
wR=(Wpe.^2)./f;
%y1=(0.5.*(K^2).*(x-
1).*(X.^2).*(wR./w).*(s1.*cos(w1.*t)+s2.*cos(w2.*t+d)));
%y2=((wR./w).^2);
%y3=((w.^2).*(s1.*cos(w1.*t)+s2.*cos(w2.*t+d))./(wD.*wR));
%y4=(X+(4.*pi.*l.*(Wpn.^2))./(3.*(x-1)));
%y5=(y3).*(y4);
%y6=((s1.*cos(w1.*t)+s2.*cos(w2.*t+d)).*X)+(y5);
%y7=(y2).*((y6).^2);
%y8=(X.*(s1.*cos(w1.*t)+s2.*cos(w2.*t+d)).*(x-
1))+((s1.*cos(w1.*t)+s2.*cos(w2.*t+d)).*4.*pi.*l.*(Wpn.^2)./3).^2;
%y9=(y7)+(y8);
y=(y1)./(y9);
plot(x,(y*10^7),'--b');
hold on
x=0.5:0.5:3.0;
T=300;
e=9.35.*8.85e-12;
ec=1.602e-19;
KB=1.38e-23;
```

```
m=0.17*9.11e-31;
p=4820;
B=0.21;
n=0.035;
s1=1;
s2=1;
w1=3e12;
w2=6e12;
d=2;
t=2;
l=0.008;
w=5e12;
C=24.1e9;
Vs=sqrt(C./p);
K=sqrt((B.^2)./(C.*e));
Non=1e26;
Noe=1e26;
Wpe=sqrt((Noe.*(ec).^2)./(m.*e));
Wpn=sqrt((Non*(ec).^2)./(m.*e));
X=((w.^2)-((Wpn.^2)./3));
D=(n.*KB.*T)./ec;
f=ec./(m*n);
wD=(Vs.^2)./D;
wR=(Wpe.^2)./f;
%y1=(0.5.*(K^2).*(x-
1).*(X.^2).*(wR./w).*(s1.*cos(w1.*t)+s2.*cos(w2.*t+d)));
%y2=((wR./w).^2);
%y3=((w.^2).*(s1.*cos(w1.*t)+s2.*cos(w2.*t+d))./(wD.*wR));
%y4=(X+(4.*pi.*l.*(Wpn.^2))./(3.*(x-1)));
%y5=(y3).*(y4);
%y6=((s1.*cos(w1.*t)+s2.*cos(w2.*t+d)).*X)+(y5);
%y7=(y2).*((y6).^2);
%y8=(X.*(s1.*cos(w1.*t)+s2.*cos(w2.*t+d)).*(x-
1))+((s1.*cos(w1.*t)+s2.*cos(w2.*t+d)).*4.*pi.*l.*(Wpn.^2)./3).^2;
%y9=(y7)+(y8);
y=(y1)./(y9);
plot(x,(y*10^7),'-.r');
set(findall(gca, 'Type', 'Line'),'LineWidth',1.5);
legend('0.000','0.001','0.008');
grid on
xlabel('Vo/Vs');
ylabel('\alpha');
```

(ii) Variation of acoustic gain per unit length with wave frequency

```
close all
x=0e12:0.05e12:40e12;
T=300;
e=9.35.*8.85e-12;
ec=1.602e-19;
KB=1.38e-23;
m=0.17*9.11e-31;
p=4820;
B=0.21;
n=0.035;
s1=1;
```

105

```
s2=1;
w1=3e12;
w2=6e12;
d=2;
t=2;
l=0.000;
C=24.1e9;
j=0.25;
Vs=sqrt(C/p);
K=sqrt((B.^2)./(C.*e));
Non=1e26;
Noe=1e26;
Wpe=sqrt((Noe.*(ec).^2)./(m.*e));
Wpn=sqrt((Non*(ec).^2)./(m.*e));
X=((x.^2)-((Wpn.^2)./3));
D=(n.*KB.*T)./ec;
f=ec./(m*n);
wD=(Vs.^2)./D;
wR=(Wpe.^2)./f;
%y1=(0.5.*(K^2).*(j).*(X.^2).*(wR./x).*(s1.*cos(w2.*t+d)));
%y2=((wR./x).^2);
%y3=((x.^2).*(s1.*cos(w1.*t)+s2.*cos(w2.*t+d))./(wD.*wR));
%y4=(X+(4.*pi.*l.*(Wpn.^2))./(3.*(j)));
%y5=(y3).*(y4);
%y6=((s1.*cos(w1.*t)+s2.*cos(w2.*t+d)).*X)+(y5);
%y7=(y2).*((y6).^2);
%y8=(X.*(s1.*cos(w1.*t)+s2.*cos(w2.*t+d)).*j)+((s1.*cos(w1.*t)+s2.*cos(w2.
*t+d)).*4.*pi.*l.*(Wpn.^2)./3).^2;
%y9=(y7)+(y8);
%y10=(y1)./(y9);
y=((y10.*x)./Vs);
plot((x.*10.^-12),(y*10^-4),'g');
hold on
x=0e12:0.05e12:40e12;
T=300;
E=9.35*8.85e-12;
e=1.602e-19;
kB=1.38e-23;
m=0.17*9.11e-31;
p=4820;
B=0.21;
n=0.035;
s1=1;
s2=1;
w1=3e12;
w2=6e12;
d=2;
t=2;
l=0.001;
C=24.1e9;
Vs=sqrt(C./p);
j=0.25;
K=sqrt((B.^2)./(C.*E));
Non=1e26;
Noe=1e26;
Wpe=sqrt((Noe*(e).^2)/(m.*E));
Wpn=sqrt((Non*(e).^2)/(m.*E));
```

106

```
X=((x.^2)-((Wpn.^2)/3));
D=(n*k*T)/e;
f=e/(m*n);
wD=(Vs^2)/D;
wR=(Wpe^2)/f;
%y1=(0.5.*(K^2).*(j).*(X.^2).*(wR./x).*(s1.*cos(w2.*t+d)));
%y2=((wR./x).^2);
%y3=((x.^2).*(s1.*cos(w1.*t)+s2.*cos(w2.*t+d))./(wD.*wR));
%y4=(X+(4*pi*l*(Wpn^2))/(3*(j)));
%y5=(y3).*(y4);
%y6=((s1.*cos(w1.*t)+s2.*cos(w2.*t+d)).*X)+(y5);
y7=(y2).*((y6).^2);
y8=(X.*(s1.*cos(w1.*t)+s2.*cos(w2.*t+d)).*j)+((s1.*cos(w1.*t)+s2.*cos(w2.*
t+d)).*4.*pi.*l.*(Wpn.^2)./3).^2;
y9=(y7)+(y8);
y10=(y1)./(y9);
y=((y10.*x)./Vs);
plot((x.*10.^-12),(y*10^-4),'--b');
hold on
x=0e12:0.05e12:40e12;
T=300;
e=9.35.*8.85e-12;
ec=1.602e-19;
KB=1.38e-23;
m=0.17*9.11e-31;
p=4820;
B=0.21;
n=0.035;
s1=1;
s2=1;
w1=3e12;
w2=6e12;
d=2;
t=2;
l=0.008;
C=24.1e9;
j=0.25;
Vs=sqrt(C/p);
K=sqrt((B.^2)./(C.*e));
Non=1e26;
Noe=1e26;
Wpe=sqrt((Noe.*(ec).^2)./(m.*e));
Wpn=sqrt((Non.*(ec).^2)./(m.*e));
X=((x.^2)-((Wpn.^2)./3));
D=(n.*KB.*T)./ec;
f=ec./(m*n);
wD=(Vs.^2)./D;
wR=(Wpe.^2)./f;
%y1=(0.5.*(K^2).*(j).*(X.^2).*(wR./x).*(s1.*cos(w2.*t+d)));
%y2=((wR./x).^2);
%y3=((x.^2).*(s1.*cos(w1.*t)+s2.*cos(w2.*t+d))./(wD.*wR));
%y4=(X+(4.*pi.*l.*(Wpn.^2))./(3.*(j)));
%y5=(y3).*(y4);
%y6=((s1.*cos(w1.*t)+s2.*cos(w2.*t+d)).*X)+(y5);
%y7=(y2).*((y6).^2);
%y8=(X.*(s1.*cos(w1.*t)+s2.*cos(w2.*t+d)).*j)+((s1.*cos(w1.*t)+s2.*cos(w2.
*t+d)).*4.*pi.*l.*(Wpn.^2)./3).^2;
```

107
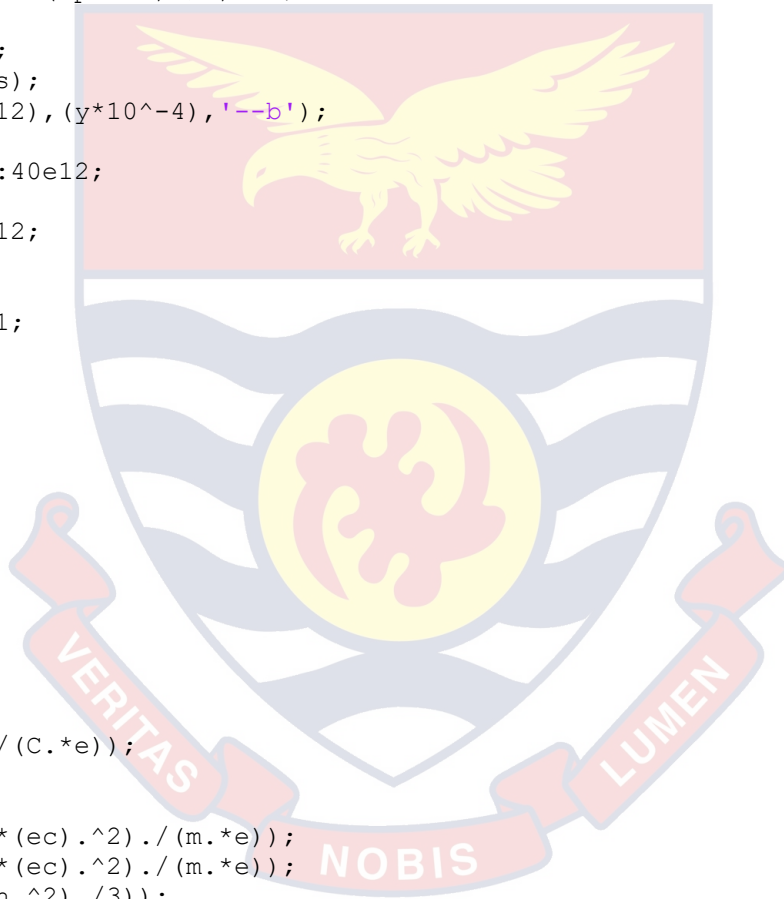
```
%y9=(y7)+(y8);
%y10=(y1)./(y9);
y=((y10.*x)./Vs);
plot((x.*10.^-12),(y*10^-4),'-.r');
set(findall(gca, 'Type', 'Line'),'LineWidth',1.5);
legend('0.000','0.001','0.008');
xlabel('\omega(10^{12}s^{-1})')
ylabel('\alpha\omega/v_s(10^{-4})')
```

(iii) Variation of acoustic gain with carrier density
```
close all
x=0e25:0.05e25:40e25;
T=300;
e=9.35.*8.85e-12;
ec=1.602e-19;
KB=1.38e-23;
m=0.17*9.11e-31;
p=4820;
B=0.21;
n=0.035;
s1=1;
s2=1;
w1=3e12;
w2=6e12;
d=2;
t=2;
l=0.000;
w=5e12;
C=24.1e9;
Vs=sqrt(C./p);
j=0.25;
K=sqrt((B.^2)./(C.*e));
Non=1e26;
Wpe=sqrt((x.*(ec).^2)./(m.*e));
Wpn=sqrt((Non*(ec).^2)./(m.*e));
X=((w.^2)-((Wpn.^2)./3));
D=(n.*KB.*T)./ec;
f=ec./(m*n);
wD=(Vs.^2)./D;
wR=(Wpe.^2)./f;
y1=(0.5.*(K^2).*(x-
1).*(X.^2).*(wR./w).*(s1.*cos(w1.*t)+s2.*cos(w2.*t+d)));
y2=((wR./w).^2);
y3=((w.^2).*(s1.*cos(w1.*t)+s2.*cos(w2.*t+d))./(wD.*wR));
y4=(X+(4.*pi.*l.*(Wpn.^2))./(3.*(j)));
y5=(y3).*(y4);
y6=((s1.*cos(w1.*t)+s2.*cos(w2.*t+d)).*X)+(y5);
y7=(y2).*((y6).^2);
y8=(X.*(s1.*cos(w1.*t)+s2.*cos(w2.*t+d)).*j)+((s1.*cos(w1.*t)+s2.*cos(w2.*
t+d)).*4.*pi.*l.*(Wpn.^2)./3).^2;
y9=(y7)+(y8);
y=(y1)./(y9);
plot((x.*10^-25),(y*10^-18),'g');
hold on
x=0e25:0.05e25:40e25;
```

108

```
T=300;
e=9.35.*8.85e-12;
ec=1.602e-19;
KB=1.38e-23;
m=0.17*9.11e-31;
p=4820;
B=0.21;
n=0.035;
s1=1;
s2=1;
w1=3e12;
w2=6e12;
d=2;
t=2;
l=0.001;
w=5e12;
C=24.1e9;
Vs=sqrt(C./p);
j=0.25;
K=sqrt((B.^2)./(C.*e));
Non=1e26;
Wpe=sqrt((x.*(ec).^2)./(m.*e));
Wpn=sqrt((Non*(ec).^2)./(m.*e));
X=((w.^2)-((Wpn.^2)./3));
D=(n.*KB.*T)./ec;
f=ec./(m*n);
wD=(Vs.^2)./D;
wR=(Wpe.^2)./f;
%y1=(0.5.*(K^2).*(x-1).*(X.^2).*(wR./w).*(s1.*cos(w1.*t)+s2.*cos(w2.*t+d)));
%y2=((wR./w).^2);
%y3=((w.^2).*(s1.*cos(w1.*t)+s2.*cos(w2.*t+d)).*(wD.*wR));
%y4=(X+(4.*pi.*l.*(Wpn.^2)).*(3.*(j)));
%y5=(y3).*(y4);
%y6=((s1.*cos(w1.*t)+s2.*cos(w2.*t+d)).*X)+(y5);
%y7=(y2).*((y6).^2);
%y8=(X.*(s1.*cos(w1.*t)+s2.*cos(w2.*t+d)).*j)+((s1.*cos(w1.*t)+s2.*cos(w2.*t+d)).*4.*pi.*l.*(Wpn.^2)./3).^2;
%y9=(y7)+(y8);
y=(y1)./(y9);
plot((x.*10^-25),(y*10^-18),'--b');
hold on
x=0e25:0.05e25:40e25;
T=300;
e=9.35.*8.85e-12;
ec=1.602e-19;
KB=1.38e-23;
m=0.17*9.11e-31;
p=4820;
B=0.21;
n=0.035;
s1=1;
s2=1;
w1=3e12;
w2=6e12;
d=2;
t=2;
```

```matlab
l=0.008;
w=5e12;
C=24.1e9;
Vs=sqrt(C./p);
j=0.25;
K=sqrt((B.^2)./(C.*e));
Non=1e26;
Wpe=sqrt((x.*(ec).^2)./(m.*e));
Wpn=sqrt((Non*(ec).^2)./(m.*e));
X=((w.^2)-((Wpn.^2)./3));
D=(n.*KB.*T)./ec;
f=ec./(m*n);
wD=(Vs.^2)./D;
wR=(Wpe.^2)./f;
%y1=(0.5.*(K^2).*(x-
1).*(X.^2).*(wR./w).*(s1.*cos(w1.*t)+s2.*cos(w2.*t+d)));
%y2=((wR./w).^2);
%y3=((w.^2).*(s1.*cos(w1.*t)+s2.*cos(w2.*t+d))./(wD.*wR));
%y4=(X+(4.*pi.*l.*(Wpn.^2))./(3.*(j)));
%y5=(y3).*(y4);
%y6=((s1.*cos(w1.*t)+s2.*cos(w2.*t+d)).*X)+(y5);
%y7=(y2).*((y6).^2);
%y8=(X.*(s1.*cos(w1.*t)+s2.*cos(w2.*t+d)).*j)+((s1.*cos(w1.*t)+s2.*cos(w2.
*t+d)).*4.*pi.*l.*(Wpn.^2)./3).^2;
%y9=(y7)+(y8);
y=(y1)./(y9);
plot((x.*10^-25),(y*10^-18),'-.r');
set(findall(gca, 'Type', 'Line'),'LineWidth',1.5);
legend('0.000','0.001','0.008');
grid on
xlabel('n_{0e}(10^{25}m^{-3})');
ylabel('\alpha(10^{-18})');
```

110